AN IN-DEPTH ANALYSIS OF

IRON AND PATHOGENICITY REGULATORY PATHWAYS

IN *Pseudomonas syringae* pv. *syringae* B728A

A Dissertation

by

JESSICA WILLIAMS GREENWALD

Submitted to the Office of Graduate Studies of
Texas A&M University
in partial fulfillment of the requirements for the degree of

DOCTOR OF PHILOSOPHY

August 2011

Major Subject: Plant Pathology

An In-Depth Analysis of Iron and Pathogenicity Regulatory Pathways

in *Pseudomonas syringae* pv. *syringae* B728a

AN IN-DEPTH ANALYSIS OF

IRON AND PATHOGENICITY REGULATORY NETWORKS

IN *Pseudomonas syringae* pv. *syringae* B728A

A Dissertation

by

JESSICA WILLIAMS GREENWALD

Submitted to the Office of Graduate Studies of
Texas A&M University
in partial fulfillment of the requirements for the degree of

DOCTOR OF PHILOSOPHY

Approved by:

Chair of Committee,	Dennis C. Gross
Committee Members,	Carlos F. Gonzalez
	Paul de Figueiredo
	Helene Andrews-Polymenis
Head of Department,	Leland S. Pierson III

August 2011

Major Subject: Plant Pathology

ABSTRACT

An In-Depth Analysis of Iron and Pathogenicity Regulatory Pathways in *Pseudomonas syringae* pv. *syringae* B728a. (August 2011)

Jessica Williams Greenwald, B.S., The College of William & Mary

Chair of Advisory Committee: Dr. Dennis C. Gross

Pseudomonas syringae pv. *syringae* strain B728a (*P.s.s.* B728a) is an economically significant plant pathogen that is capable of successful epiphytic colonization of leaf surfaces. Although the virulence factors associated with this pathogen's ability to cause disease have been well studied, the transition from epiphyte to pathogen is not well understood. The research described in this dissertation utilizes high throughput sequencing transcriptome analyses to define an iron regulatory network that is predicted to be utilized during the epiphytic portion of the *P.s.s.* B728a lifecycle. This dissertation also describes a collaborative microarray analysis that analyzes the *P.s.s.* B728a transcriptome at a global level.

An iron associated sigma factor, AcsS, encoded within a peptide synthesis rich region of the *P.s.s.* B728a genome is shown to regulate the citrate siderophore achromobactin. RNA-seq transcriptome analysis reveals that this sigma factor regulates expression of genes predicted to be involved in functions that are important during the epiphytic stage of *P.s.s.* B728a, including genes involved in iron response, secretion, extracellular polysaccharide production, and cell motility.

As part of a collaboration, the transcriptomes of the *P.s.s.* B728a genome and nine deletion mutants in regulatory genes were analyzed by microarray analayses using seven treatment conditions, including epiphytic and in planta conditions. As part of these microarray analyses, results are described for the global regulator, GacS, and a downstream transcription factor, SalA. This study confirms the role of GacS and SalA in the regulation of major virulence components of *P.s.s.* B728a such as phytotoxin production and Type III secretion. This study also elucidates a role for GacS and SalA regulation of genes important for epiphytic survival and function, including the Type VI secretion system, iron acquisition, and EPS production.

I dedicate this work to my mother and father,

who instilled in me the desire to achieve greatness and

an appreciation for the greatness of others.

And to my loving husband, who complements my mutations.

ACKNOWLEDGEMENTS

I would like to express my sincere gratitiude to my major advisor, Dr. Dennis Gross. As my advisor you have granted me the freedom to express myself and grow, as an individual and a scientist. Thank you for your guidance, support, and patience.

I would like to thank my committee members Dr. Carlos Gonzalez, Dr. Paul de Figueiredo, and Dr. Helene Andrews-Polymenis for their constructive criticisms and support of my scientific research.

I would like to thank my collaborators: Dr. Tadhg Begley (Texas A&M University), Dr. Benjamin Philmus (Texas A&M University), Dr. Gwyn Beattie (Iowa State University), Dr. Steven Lindow (University of California Berkley), Dr. Daniel Nettleton (Iowa State University), Steven P. Lund (Iowa State University; Russell A. Scott (University of California, Berkley), and Xilan Yu (Iowa State University). I offer a special thanks to Dr. Benjamin Philmus for his perseverance and words of encouragement.

I offer my sincerest gratitude to the present and former members of my research laboratory, who have offered scientific and moral support. I offer my thanks to Dr. Brenda Schroeder, Dr. Shien Lu, Dr. Nian Wang, Dr. Angela Records, Amber Lorge, Poulami Basu Thakur, Dr. Aravind Ravindran, and Vanessa Vaughn. Special thanks are given to my undergraduate research assistant and friend, Ryan Cieker.

I would like to acknowledge those members of the Texas A&M community who have offered special assistance with or suggestions about my research. These include:

Dr. Larry Dangott, Dr. Herman Scholthof, Dr. Veria Alvarado, Dr. Joshua Yuan, Dr. Weibing Shi, Dr. Kevin Ong, Dr. Mehdi Kabbage, Dr. Jim Starr, Dr. Daniel Ebbole, Dr. Heather Wilkinson, and Dr. Won Bo Shim.

I would like to thank Patsy Bolch, Dora Lee-Haberstroh, Karen Hodges, Chris Court, and Tracy Hurych for their assistance, compassion, and friendship. While I appreciate all of the technical skills that these individuals provided to my research, I am most grateful for their kind words, encouragement, and friendship.

I would like to thank the two Karens in my life for being my mentors, my soul sisters, and my friends.

I offer my love and gratitude to my husband, Charles, for his scientific knowledge, expertise, love, support, and especially for his sense of humor.

I would like to thank Mom, Dad, Granny, and Grandma for their endless support and love.

Thank you to my friend Sara, for listening to my endless rants and pointing out the silver lining in every rain cloud. For keeping me grounded, I thank my friend Angela. For stirring the pot and encouraging my fiery nature, I thank Dustin. For providing sound scientific advice and delicious Kosher-friendly meals, I would like to thank Samir. I offer thanks to my dear friend Gabby, whose wicked humor makes me smile.

Finally I offer thanks to four little people that I love unconditionally, Sam, Jack, Olivia, and Carter. Thank you for encouraging me to enjoy life and to smile more.

TABLE OF CONTENTS

Page

LIST OF FIGURES

LIST OF TABLES

TABLE Page

CHAPTER I

INTRODUCTION

Pseudomonas syringae was first described over a century ago when it was isolated from a diseased lilac (*Syringa vulgaris*) (42). Since then *P. syringae* has been isolated from a broad host range of both monocot and dicot plant species. At present *P. syringae* strains have been divided into approximately 50 pathovars based upon the identified host range of each (26). For instance *P. syringae* pv. *syringae* B728a (*P.s.s.* B728a) causes brown spot on beans (*Phaseolis vulgaris* L.), a disease characterized by water-soaked and necrotic lesions on the leaves and pods (58). While the related strain *P. syringae* pv. *syringae* B301D (*P.s.s.* B301D), which is known to have similar virulence mechanisms, causes necrosis and cankers on cherry and other stone fruits. Host range variability serves as a useful systematic tool; however, many questions remain concerning the biology responsible for these differences.

Recent technological shifts permitting the affordable and efficient sequencing of microbial genomes has propelled the scientific community into a new era. This new era provides scientists with an immense opportunity to understand microbes at their most basic level by not only identifying the function of genes and proteins, but by discovering the mechanisms by which these genes are properly expressed and regulated to allow

---

This dissertation follows the style of Journal of Bacteriology.

appropriate microbial functioning. Numerous *Pseudomonas* genomes have been partially or completely sequenced and are publicly available; including five published *P. syringae* strains: *P.s.s.* B728a, *P. syringae* pv. *tomato* DC3000 (*P.s.t.* DC3000), *P. syringae* pv. *tomato* T1 (*P.s.t.* T1), *P. syringae* pv. *phaseolicola* 1448a (*P.s.p.* 1448a), and *P. syringae* pv. *oryzae* 1-6 (*P.s.o.* 1-6) (45). These genomic sequences have substantially accelerated the progress of scientific research by providing scientists with easily accessible bioinformatics data for formulating hypotheses that can be experimentally tested. The sequencing and publication of the *P.s.s.* B728a genome has provided an invaluable resource for further investigation of the regulatory networks involved in pathogenicity and disease (26).

Most members of the pathovar *syringae*, including *P.s.s.* B728a have the ability to function both as a plant pathogen and as an epiphyte. Epiphytic populations of *P.s.s.* B728a can reach populations > 10^7 colony forming units (CFU) per gram of plant tissue; thereby serving as an efficient source of inoculum under the appropriate environmental circumstances (26). Upon entering the host plant cells, via a wound or through the stomata, the bacteria colonize the apoplastic spaces and extensively express pathogenicity and virulence related genes. The *hrp* gene cluster encodes the Type III secretion system apparatus and effector proteins which are essential for pathogenicity (6). Additionally numerous genes encode extracellular polysaccharides, phytotoxins, cell wall-degrading enzymes, and other gene products that contribute to the virulence of phytopathogenic pseudomonads.

P.s.s. strains, including *P.s.s.* B728a and *P.s.s.* B301D, serve as significant plant pathogens on numerous monocot and dicot species (53). Regardless of the plant host, the predominant symptom associated with diseases caused by *P.s.s.* strains is cell necrosis, a direct outcome of the pathogen's ability to produce the potent phytotoxins syringomycin and syringopeptin (53, 94). These nonribosomally synthesized lipodepsinonapeptides are major virulence factors, with *P.s.s.* B301D insertional mutant strains for syringomycin and syringopeptin exhibiting a 26% and 59% respective reduction in virulence (103). Both syringomycin and syringopeptin are composed of a cyclic-polar peptide head attached to an amino acid chain and a 3-hydroxydodecanoic acid tail (6, 53). The amphipathic nature of these peptides results in the formation of cation-permeable transmembrane pores in host cell plasma membranes, which leads to disrupted cell membrane potential and host cell lysis (6, 53). The significance of these phytotoxins to plant disease has made them the focus of extensive research. Specific laboratory conditions under which syringomycin and syringopeptin are synthesized were defined in 1985 by D.C. Gross and include a minimum of 2 μmol/L available iron and less than 1 mmol/L phosphate (36). Despite known laboratory conditions necessary for the production of syringomycin and syringopeptin, iron is a limited resource in both the epiphytic and apoplastic environments where *P.s.s.* B728a dwells. Thus, a broader knowledge of the acquisition, utilization, and regulation of iron and iron-influenced molecules will also enhance our understanding of plant disease.

One method *P.s.s.* B728a utilizes to acquire sufficient iron from the environment is the biosynthesis of siderophores, low-molecular weight, chelating molecules that bind

and solubilize Fe^{3+} in iron-depleted environments (37). This study focuses on the regulatory network involved in the biosynthesis and secretion of the citrate siderophore, achromobactin. An extracytoplasmic function RNA-polymerase σ-factor gene, named *acsS*, encoded within the cluster of genes responsible for the biosynthesis and secretion of achromobactin was hypothesized to contribute to achromobactin regulation. Illumina RNA-Seq transcriptome analysis, and peptide purification and mass spectrometry were utilized to demonstrate that AcsS positively regulates the gene cluster responsible for achromobactin biosynthesis and secretion. Additionally, other AcsS regulated genes were identified in the RNA-seq analysis by differential gene expression analysis that led to the hypothesis that AcsS and achromobactin are involved in the epiphytic survival and function of *P.s.s.* B728a.

This study also introduces a major collaborative effort, wherein the gene expression of *P.s.s.*B728a and nine regulatory mutant strains were evaluated across seven experimental conditions using microarray analysis. This project was funded by NIFA NRI/AFRI Microbial Biology Program and Microbial Functional Genomics Program and is a collaboration between Dr. Gwyn Beattie (Iowa State University), Dr. Steven Lindow (University of California, Berkley), Dr. Dennis Gross (Texas A&M University), and Dr. Dan Nettleton (Iowa State University).

This dissertation focuses on the implications of the microarray analysis specifically regarding the *P.s.s.* B728a regulatory networks of the sensor-kinase, GacS, and the transcription factor, SalA. Prior to this study a substantial amount of research had been performed on the GacS/GacA two-component system of *P.s.s.* B728a, due to

the substantial decrease in virulence seen when this system is mutated. *P.s.s.* B728a strains with *gacS/gacA* mutations are unable to cause necrotic lesions due to decreased biosynthesis of the phytotoxins, syringomycin and syringopeptin (58). The transcription factor SalA is known to work downstream of GacS/GacA in the activation of genes involved in the biosynthesis and secretion of syringomycin and syringopeptin (119). Although GacS/GacA are also known to be involved in numerous biologically important systems of *P.s.s.* B728a including secondary metabolite biosynthesis, quorum sensing, and exopolysaccharides, the role of SalA in these systems has only been evaluated in a few circumstances. One objective of this study was to analyze and evaluate the role of SalA to determine whether it functions downstream of GacS/GacA in all circumstances or if SalA has a smaller and/or unique set of genes in its regulon.

The analysis of this microarray study reveals that the GacS/SalA regulons are extensively interlaced and regulate numerous aspects of the *P.s.s.* B728a genome involved with both pathogenicity and the epiphytic lifestyle. These findings confirm previous analyses of the GacS/SalA regulon and provide evidence for a multisensory regulatory system that may serve as the regulatory switch between epiphytic survival and plant disease.

CHAPTER II

AN IRON RESPONSIVE SIGMA FACTOR, AcsS, REGULATES ACHROMOBACTIN BIOSYNTHESIS IN *Pseudomonas syringae* pv. *syringae* B728a

Overview

Iron is an essential micronutrient for *P.s.s.* B728a and many other microorganisms; therefore, it has evolved methods of iron acquirement including the use of iron-chelating siderophores. The citrate siderophore achromobactin is encoded in a peptide rich region of the *P.s.s.* B728a genome that appears to be more prone to genetic recombination events. In this study a sigma factor, AcsS, encoded within the achromobactin gene cluster is shown to be a major regulator of the biosynthesis and secretion of this siderophore. However, analysis of the metabolite achromobactin revealed that deletion of the sigma factor reduced achromobactin production by half, implying that other regulators may be involved. RNA-seq analysis shows that 287 genes are differentially expressed between the AcsS deletion mutant and the wild type strain. These genes are involved in iron response, secretion, extracellular polysaccharide production, and cell motility. Thus, the transcriptome analysis supports a role for AcsS in the regulation of achromobactin production and the activity of both AcsS and achromobactin in the epiphytic stage of the *P.s.s.* B728a lifecycle.

Introduction and Literature Review

Iron is the fourth most common element in the Earth's crust and, as such, has played an important role in microbial metabolism for millions of years (122). Some scientists hypothesize that Fe^{2+} was freely available in the anaerobic Precambrian environment and that microbes were able to oxidize the molecules as one of earliest forms of respiration (122). This hypothesis has been supported by findings of both Archaea and bacteria which utilize biological iron apportionment as their primary metabolic system; furthermore, this metabolic process has been postulated as a potential method for microbial metabolism on other planets (122). The ability to acquire and utilize iron is essential to the proper metabolism and basic cellular functioning of most macro and microorganisms, including *P.s.s.* B728a (82). In addition to functioning as a co-factor for many metabolic enzymes, iron plays a predominant role in the electron transfer chain, as well as, the catalysis of numerous cellular redox reactions (82).

Iron availability

In low pH environments Fe^{2+} is increasingly stable with the molecule existing in a soluble state below pH 4, thus making the iron molecules easily accessible for microbial use (122). Microbial uptake systems for iron in its reduced state, Fe^{2+}, have been identified and extensively studied in both bacterial and yeast systems. However, many microorganisms of scientific interest dwell in aerobic, aqueous conditions which are also oxidizing environments (51). In environments with physiological pH and oxygen tension the oxidized ferric iron (Fe^{3+}) forms stable, insoluble ferric oxide hydrate

complexes that cannot be readily utilized by microorganisms (59, 82). The formation of these stable complexes leaves an environment with a free iron content of only 10^{-9} to 10^{-18} M, well below the 10^{-6} to 10^{-8} M required by most microorganisms (51, 82).

Iron limitation in the rhizosphere

For microorganisms that dwell in and around the plant rhizosphere acquiring the iron necessary for basic cellular functioning is further hindered by competition with both the plant and other microorganisms (112). Two strategies have been described for the uptake of iron by plant roots; one found in dicotyledonous and nongraminaceous monocotyledonous plants and the other found in graminaceous plants (12, 22). Dicotyledenous plants and nongraminaceous, monocotyledonous plants lower soil pH by the excretion of protons by the activation of H^+-ATPases in the root epidermal cells (22, 112). One study has found soil pH levels reduced to values below 3, which is sufficient for considerable reduction of Fe^{3+} to soluble Fe^{2+} (38). This strategy can be combined with the further reduction of ferric iron complexes (Fe^{3+}) by plant secreted NADPH-ferric chelate reductase, followed by plant uptake of the Fe^{2+} by cellular transporters (22, 112). Alternatively, graminaceous plants synthesize and secrete iron-binding molecules, called phytosiderophores, into the rhizosphere (22). These phytosiderophores, composed of a family of mugineic acids, are able to chelate and solubilize Fe^{3+} (22). The iron-bound phytosiderophore can then be transported across the plant cell membrane by a specific cellular transporter (22). The use of phytosiderophores is more efficient at acquiring iron from the rhizospheric environment than the reduction strategy of

dicotyledenous and nongraminaceous monocotyledonous plants; therefore, graminaceous plants are more adept at surviving in extreme iron-deficient soil conditions (22).

In the rhizosphere plant pathogenic microbes have to compete for iron not only with the plant, but also with other rhizospheric microbes, both symbiotic and pathogenic bacteria and fungi dwelling in the thin soil layer surrounding the plant roots. Competition for iron in the rhizosphere is a major factor involved in determining the constituents of the rhizospheric microbial community (126). Exudates secreted by the plant roots are also a major influence on the composition of the rhizospheric microbial community, as these exudates alter the soil chemistry and provide substrates for microbial metabolism. For instance, plant root exudates in the zone of elongation, the region behind the root tips, consist primarily of simple sugars and organic acids which provide the appropriate nutrition for primary root colonizing microbes (126). Rhizospheric microbes are under severe evolutionary pressure to adapt to an environment where nutrient competition is fierce. Some rhizospheric bacteria have evolved mechanisms for the uptake and utilization of phytosiderophores (126). Given that in extreme iron stress conditions phytosiderophores can compose up to 50% of the plant root exudates, the ability to plunder plant chelating molecules for individual gain serves as an exceptional advantage to these bacteria (126). Thus the iron limited environment plays a significant role in the composition and evolutionary adaptation of the rhizospheric microbial community.

Iron limitation in the phyllosphere

Since many microorganisms that are important plant pathogens and biocontrol agents spend at least a portion of their life cycle on the leaf surface, it is also important to consider the role that the environment plays in shaping the genetic adaptations and microbial community composition of the phyllosphere. Although the leaf surface may appear relatively smooth from a human perspective, when examined from the microbe vantage, often only a few microns in length, the topography of the leaf surface is more like that of our planet, with mountains, valleys, and plains (43). These topographical variations can have a major impact on the conditions that the microbes in that particular region of the leaf surface have to face. For instance, just as people at higher elevations are exposed to increased ultraviolet exposure from the sun, microbes on raised surfaces of the leaf will encounter more ultraviolet waves than their counterparts in a leaf crevasse. In addition to the leaf surface being a series of microclimates, the leaf surface overall is exposed to vast fluctuations in conditions on a daily basis, which are either accentuated or mitigated by the precise topographical location on the surface. During the day leaf temperatures are elevated with intense ultraviolet light exposure, followed by decreasing temperatures at night with aqueous conditions where dew gathers (43). Thus microbes in a fixed location on the leaf surface can be exposed to extreme fluctuations in temperature and water availability during a single 24 hour period. For these reasons, in order for microbes to survive in the phylloplane, they must be capable of adapting to the rapid changes in their microclimate. Additionally, nutrient availability on the leaf surface is limited, with sufficient nutrition for growth and replication being

available in a few phyllospheric "oases" resulting from plant cell leakage from trichomes, hydathodes, or injury sites (67). Surprisingly, available iron (Fe^{3+}) is sporadically dispersed across the phylloplane environment, with many locations consisting of sufficient Fe^{3+} quantities for microbial functioning (51). However, when considering the situation from the perspective of the microbe, although these iron limited regions of the vast phylloplane are less geographically expansive than anticipated, if brought to a human scale they would still amount to tracts of land equivalent to whole counties, states or countries. The microbes unfortunate enough to land in these nutritionally void areas must adapt to survive.

Despite the extreme nature of the environmental conditions on leaf surfaces, they are inhabited by a diverse collection of yeast, bacteria, fungi, and bacteriophages, with each leaf being potentially occupied by millions of individual microbes (43). Leaf surfaces provide microbes with a large area of real estate to select from, with the estimated inhabitable surface area of terrestrial leaves being 6.4×10^8 km^2 (67). This is over four times the area of all land on Earth. Combine this knowledge with the vast number of leaf surfaces available and one could estimate a worldwide phyllosphere microbial population of one hundred septillion (10^{26}) microbes (67). This number amounts to fourteen quadrillion, seven hundred trillion times the world's human population.

Iron limitation in the apoplast

Within plant tissues iron is present in ample quantities; however, it is predominantly sequestered by molecular components such as iron proteins, phenolic compounds, heme, citrate, and malate (17, 25, 83). After being acquired from the soil, available iron is bound to citrate or malate and transported from root tissues to aerial tissues via the xylem vessels (25). Iron is also transported through the phloem by binding to the unusual amino acid, nicotianamine (12, 108). Nicotianamine is ubiquitously found amongst plants and plays a role in the transport of iron to growing tissues via the phloem (12, 108). However, the transport of iron through the phloem is less extensively studied and many of the details regarding this process remain unknown (12). Intracellularly iron is found in several organelles including vacuoles, mitochondria, and chloroplasts. Within the leaves, the majority of iron is located in the chloroplasts where it is stored in plastids as iron-ferritin complexes (12). Ferritins are high molecular weight proteins utilized for iron storage that have been evolutionarily conserved in animals, plants, and microorganisms; however, they play specialized roles in each system (111). In addition to the inaccessibility of iron within plant tissues and cells due to a complex transport and storage system, phytobacteria such as *P.s.s.* B728a are largely limited to the apoplastic space, an iron depleted environment containing only 1.6 to 6 μM Fe^{3+} (50).

Very little quantifiable data is available regarding the precise nutritional composition of the rhizosphere, phyllosphere, and apoplast. In addition, it is becoming increasingly clear that these environments are not stagnant, but are in a state of constant

flux. The majority of our understanding of these environments is based upon the physiological and genetic responses of the microorganisms that dwell in these environments. Therefore, further knowledge of the biological systems utilized by microbes in these environments will lend valuable knowledge to our understanding of both the conditions present in these environments and the organismal responses to these conditions.

Iron acquisition by bacterial siderophores

To compensate for the low level of available iron and the heavy competition by plant tissues and other microbes, many microorganisms have evolved systems for scavenging iron from their environment. Much like the phytosiderophores produced by plant and excreted into the rhizosphere, a common method of iron acquisition by bacteria is through the utilization of siderophores. Siderophores, meaning 'iron carriers' in Greek, are low-molecular weight, chelating molecules synthesized and secreted by many bacteria to acquire and solubilize Fe^{3+} from an iron-depleted environment (37). Iron starvation conditions (when the cellular iron concentration is too low to sustain bacterial growth) trigger the synthesis and secretion of siderophores (82). After binding to Fe^{3+} in the environment, the iron-laden siderophore binds to ferric-chelate-specific transporters in the bacterial membrane. The TonB-dependent outer membrane receptors are large gated porins composed of 22 β-strands forming a β-barrel (19). The *P.s.s.* B728a genome contains 19 TonB-dependent receptor genes, 13 of which are also conserved in *Pseudomonas syringae* pv. *tomato* DC3000 (*P.s.t.* DC3000) and

Pseudomonas syringae pv. *phaseolicola* 1448a (*P.s.p.* 1448a) (20). Within the bacterial cell, the ferric iron is reduced and utilized. If iron starvation conditions continue the siderophore is recycled, otherwise the iron-chelating molecules are degraded.

Bacterial siderophores are classified in three groups based on the predominant chemical groups involved in their chelation of iron (86). This classification system of dividing siderophores into catecholates, hydroxamates, and carboxylates is not all-inclusive, as several mixed-type siderophores have been characterized (82). Although all three classes of siderophores have a high affinity for iron, the formation constants of these classes listed from lowest to highest are carboxylates, hydroxamates, and catecholates (86). This variation in affinity may play a role in bacterial systems containing more than one siderophore system. Different classes of siderophore systems may have evolved for adaptation to different environmental conditions or niches.

Pyoverdine

With several hundred species being members of the bacterial genus *Pseudomonas,* there are multiple characteristics that can be used to divide and group these bacteria. The presence or absence of the yellow-green fluorescent siderophores, pyoverdines, is one commonly used method of division (86). Pyoverdines consist of a fluorescent dihydroxyquinoline chromophore with a small dicarboxylic acid at the NH_2– group, and a variable peptide moiety, six to twelve amino acids in length (86, 116). They are classified as mixed-type siderophores due to their composition of both catecholate and hydroxamate groups (114). The chromophore portion of the molecule is

highly conserved; however, variability of amino acids within the peptide chain differentiates the three types of pyoverdines (PvdI to PvdIII) (65). Peptide variability leads to high levels of structural differences between pyoverdines, such that different strains of the same *Pseudomonas* species often have structurally diverse pyoverdine molecules (114).

Pyoverdines, like many siderophores and secondary metabolites, are assembled by nonribosomal peptide synthetases (NRPSs). NRPSs are characterized by their modular construct, consisting of adenylation, condensation, thiolation, and thioesterase domains, which function as independent points in the catalysis of peptide synthesis (76). Each module encodes the appropriate catalytic enzymes for the incorporation of a single amino acid into the peptide chain. The pyoverdine NRPS genes vary amongst pseudomonads, giving rise to the variable peptide regions. However, the *pvdL* gene is highly conserved and is predicted to synthesize the chromophore portion of the pyoverdine molecule (114). Pyoverdine biosynthesis in *P.s.s.* B728a consists of an 18-gene cluster (*Psyr_1944-1961*) that also contains genes necessary for pyoverdine regulation and cellular uptake (26).

Regulation of iron acquisition

Due to the importance of iron for cellular growth and function, iron-related genes are highly regulated. However, a delicate regulatory balance must occur in order to maintain cellular iron levels within the bacteria in a physiologically appropriate range. Insufficient iron availability will cripple normal cellular functioning, as many of the

enzymes that require iron as a cofactor are essential to cellular metabolism and respiration. Moreover, an overabundance of Fe^{2+} in the presence of oxygen can increase the production of highly reactive hydroxyl radicals by the Fenton reaction, thereby causing excessive damage to the microbial cell (80). In iron replete environments, siderophore biosynthesis and uptake genes are repressed by the negative regulator Fur (ferric uptake regulator) (86). When Fur is in the presence of its cofactor, Fe^{2+}, it is able to dimerize and bind to the promoter regions of iron-regulated genes, thereby blocking transcription (115). When iron is limited the apo-Fur molecule is unable to dimerize or bind to DNA; thus, transcription of iron acquisition genes may proceed. The synthesis and uptake of siderophores is a cellularly expensive process; therefore, the negative regulation of these molecules by Fur is exceptionally important.

Likewise, when iron is scarce it is essential that the bacteria are able to quickly adapt and produce iron-scavenging molecules. The expression of iron-related genes, including siderophore biosynthesis and transport genes, requires RNA-polymerase σ-factors from the extracytoplasmic function (ECF) subfamily of the σ^{70} family, which typically respond to environmental signals (86). The 187-residue ECF sigma factor regulating pyoverdine biosynthesis, PvdS, was first identified in *Pseudomonas aeruginosa* PAO1 (115). Homologues of *pvdS* have been identified in many other fluorescent pseudomonads, including *P.s.s. B728a* (89). PvdS-regulated genes can be identified by the iron starvation (IS) box, a conserved sequence in their promoter region, approximately 33 base pairs upstream from the transcriptional start-point (114). In *P. aeruginosa,* PvdS initiates, through complex signaling networks, the transcription of

several virulence factors including exotoxin A and PrpL protease (114). Genome-wide promoter screens of the plant pathogenic bacterium *P.s.t.* DC3000 did not reveal any virulence associated regulation by the PvdS homolog (109). Thus, the PvdS sigma factor may have evolved differing regulatory networks within the various fluorescent pseudomonads.

In addition to the various regulatory roles that PvdS has in different fluorescent pseudomonads, pyoverdine itself appears to play varying roles in the life cycles of these organisms. Pyoverdine production has been associated with an increased ability of *P. aeruginosa* to infect and sustain disease in several mammalian model systems (60). In these systems, the production of pyoverdine plays a vital role in the bacterial formation of biofilms, a critical component of disease sustainability in a mammalian host (114). Without the acquirement and delivery of iron to the innermost layers of the biofilm, the bacterial cells reinstitute a motile lifestyle and are more susceptible to the host immune response. The role of pyoverdine in the disease cycle of plant pathogenic pseudomonads is less well-defined.

In 1987, Cody and Gross reported that the biosynthesis and uptake of pyoverdine was not essential to the pathogenicity or virulence of *P.s.s.* B301D (18). The sequenced genome of the closely related species *P.s.s.* B728a and experimental data from other plant pathogenic pseudomonads suggest that further investigation of the role of pyoverdine in pathogenesis is necessary. The various fluorescent pseudomonads produce similar pyoverdine molecules, which can be taken up and utilized by other pyoverdine-producing species and strains. This is a competitive advantage for

fluorescent pseudomonads in environments such as the rhizosphere and phyllosphere (112). In these environments, fluorescent pseudomonads can effectively compete with other species by sequestering iron from the environment in such a manner that the iron can only be utilized by themselves. In planta, this level of microbial competition does not exist; therefore, it is feasible that the utilization of pyoverdine as an iron acquisition strategy is limited to the rhizospheric and/or phyllospheric stages of the pseudomonad life cycle. Additionally, as suggested by Jones et. al, another high-affinity siderophore could have compensatory action for the loss of pyoverdine (50). Investigation of the *P.s.s.* B728a genome reveals a second siderophore cluster that may be capable of such compensatory action (26).

A second siderophore: achromobactin

In addition to the previously characterized gene cluster responsible for the biosynthesis and transport of pyoverdine, a second siderophore gene cluster in *P.s.s.* B728a was identified based on sequence analysis (26). The 14-gene cluster was noted for containing six biosynthetic genes with high sequence similarity to those genes responsible for synthesizing the citrate siderophore achromobactin in *Dickeya dadantii* and *Pectobacterium carotovorum* subsp. *atrosepticum* (26). The presence of both pyoverdine and achromobactin siderophores has also been reported in the biocontrol strain, *Pseudomonas syringae* pv. *syringae* 22d/93 (*P.s.s.* 22d/93), and the soybean pathogen, *Pseudomonas syringae* pv. *glycinea* 1a/96 (123).

Dickeya dadantii strain 3937 is a necrotrophic plant pathogen on a variety of hosts including African violets (*Saintpaulia ionantha*) (28, 127). In addition to pectic enzymes which degrade host cell walls, the siderophore chrysobactin is considered a major virulence factor for this pathogen due to its necessity for the establishment of systemic plant infection (28, 127). However, *Dickeya dadantii* strain 3937 also produces a second siderophore, the citrate derivative achromobactin (28).

Although most polypeptide-based siderophores, including pyoverdine and chrysobactin, are synthesized by NRPSs, in recent years a new class of non-polypeptide based siderophores have been identified and intensely researched, including achromobactin (16, 81). These non-polypeptide based siderophores are biosynthesized via an NRPS-independent siderophore (NIS) pathway, an assembly process that is both enzymatically and mechanistically different from the NRPS system (8, 81). Similarly to the NRPS mechanism of enzymatically incorporating amino acids into a peptide chain, the NIS pathways involve an equivalent concept in linking and modifying carboxylic acid substrates (8). The NIS system was first characterized in *Escherichia coli* with the biosynthesis of the siderophore aerobactin (16). In aerobactin biosynthesis the amide linkages of the iron-chelating functional groups, dicarboxylic acid and diamine units, are catalyzed by the siderophore synthetase enzymes, IucA and IucC (16). Additional studies and bioinformatic analysis have identified predicted NIS synthesized siderophore

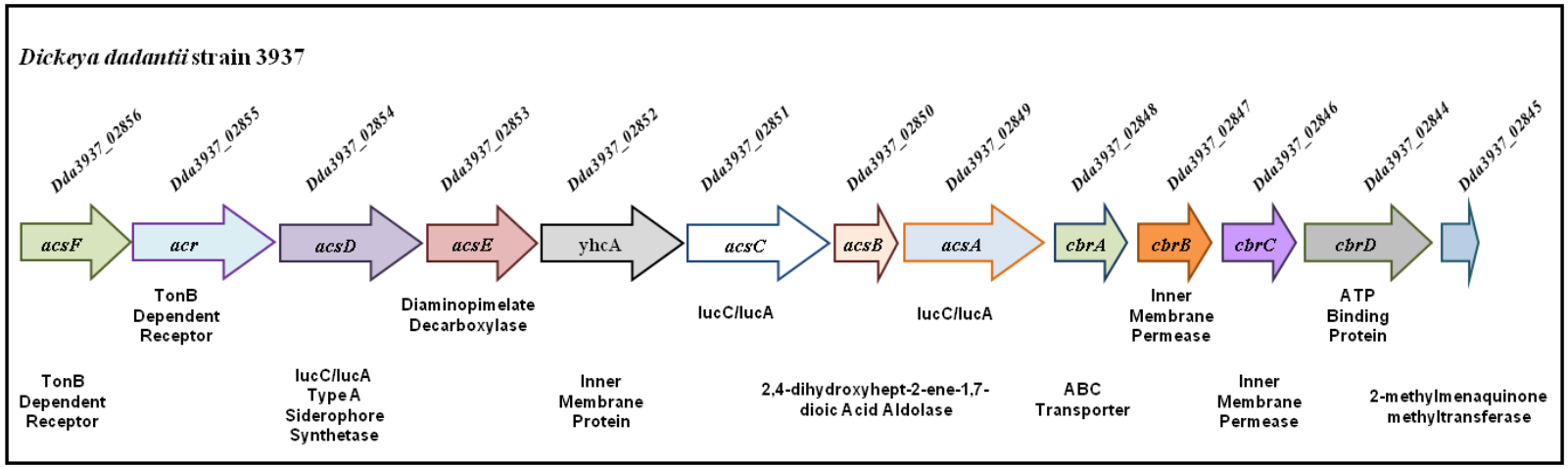

FIG. 1. Genomic region of *Dickeya dadantii* strain 3937 containing the NIS synthetase genes responsible for the biosynthesis of the siderophore achromobactin.

systems in over 40 bacterial species, with no less than eight known siderophore constructs (16).

Within the *Dickeya dadantii* strain 3937 genome, the biosynthesis of achromobactin is encoded in a gene cluster that is directly regulated by the ferric uptake regulator, Fur (28). Several genes within this cluster have high sequence similarity to the NIS synthetase genes, *iucC* and *iucA,* and are essential for the production of achromobactin (31, 81) (Fig. 1). Although the complete biosynthesis pathway of achromobactin in *Dickeya dadantii* strain 3937 has not been elucidated, a proposed schematic for synthesis of this citrate siderophore in *P.s.s.* B728a has been published and biochemically confirmed (8) (Fig. 2). As seen in Figure 2, Berti and Thomas propose that citrate[1] is converted to *O*-citryl-serine[2] by the NIS synthetase, AcsD. *O*-citryl-serine[2] is decarboxylated by AcsE, a diaminopimelate decarboxylase, to form *O*-citryl-ethanolamine[3], which is then converted to diaminobutyryl-citryl-ethanolamine[4] by the NIS synthetase, AcsC. In the final biosynthetic step, AcsA, another NIS synthetase, catalyzes the addition of α-ketoglutarate moieties thereby generating achromobactin (8). Cross-feeding assays have confirmed that the achromobactin siderophore produced by *P.s.s.* B728a, *P.s.s.* 22d/93 and *Pseudomonas syringae* pv. *glycinea* 1a/96 can be detected, imported, and utilized by *Dickeya dadantii* strain 3937, thereby showing that the chemical construct of the achromobactin produced by these strains is highly similar (123). Therefore, it is likely that the achromobactin biosynthesis pathway in *Dickeya dadantii* strain 3937 is comparable to that outlined by Berti and Thomas in *P.s.s.* B728a (8).

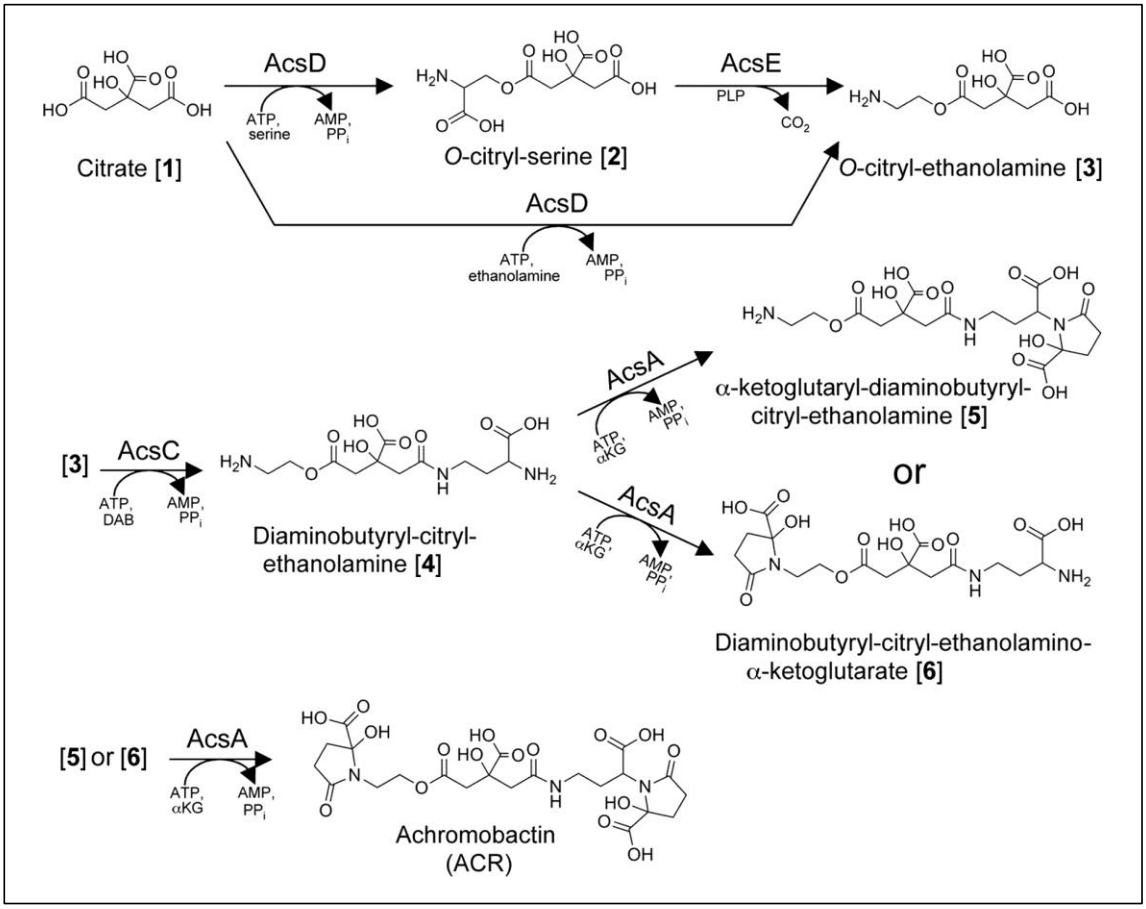

FIG. 2. Proposed scheme for the biosynthesis of achromobactin. The following abbreviations are used: DAB, 2-4-diaminobutyrate; αKG, α-ketoglutarate; PLP, pyridoxal phosphate. Reprinted with permission from "Analysis of Achromobactin Biosynthesis by *Pseudomonas syringae* pv. *syringae* B728a" by Andrew D. Berti and Michael G. Thomas, 2009. *J. Bacteriol.* 191, 4594-4604, Copyright 2009 by American Society for Microbiology.

The biological function of achromobactin in the lifecycle of *P.s.s.* B728a has not been determined and is one of the aims of this study. Because achromobactin is a biochemically simpler molecule and the citrate backbone is readily available from the citric acid cycle, it is assumed that achromobactin is a biologically cheaper molecule to synthesize than pyoverdine (87). In *Dickeya dadantii* strain 3937 achromobactin is necessary for the establishment of bacterial growth in planta, as it is produced at less

stringent iron limitation levels than the siderophore chrysobactin (28, 123). As the in planta bacterial population rises the available iron becomes increasingly depleted and the *Dickeya dadantii* strain 3937 population gradually increases its production of chrysobactin, which has a higher binding affinity for iron (28, 123). Hence in *Dickeya dadantii* strain 3937, the two siderophore systems are utilized concurrently as a method of adapting to changing iron availability in the plant environment. Additionally, the epiphytic fitness of *P.s.s.* 22d/93 was significantly impaired by disruption of either pyoverdine or achromobactin biosynthesis; thereby implicating that a similar compensatory siderophore may be involved in this system (123).

After analyzing the achromobactin gene cluster and the surrounding genomic region for gene homology, an extracytoplasmic function (ECF) sigma factor, *acsS,* predicted to regulate achromobactin biosynthesis was identified. The objective of this study was to determine if AcsS serves as a regulator of achromobactin biosynthesis and secretion, and to identify other gene targets within the AcsS regulon. By identifying gene targets regulated concurrently with achromobactin biosynthesis and secretion, I hoped to gain further understanding about the portions of the *P.s.s.* B728a lifecycle in which achromobactin is utilized. In this study it is demonstrated that AcsS regulates the biosynthesis and secretion of achromobactin, as well as other *P.s.s.* B728a genes that may be involved in epiphytic competition and survival.

Materials and Methods

Bioinformatic analysis

Genome database searches were performed with the Basic Local Alignment Search Tool (BLAST) at NCBI (http://blast.ncbi.nlm.nih.gov/Blast.cgi). Operon prediction was performed by Steven Lund and Dr. Daniel S. Nettleton at Iowa State University as part of the NIFA NRI/AFRI Microbial Biology Program and Microbial Functional Genomics Program entitled "Functional genomics of the epiphytic and pathogenic lifestyles of the bacterial plant pathogen *Pseudomonas syringae"*(NIFA Award Number: 2008-35600-18766). This project is described in Chapter III of this dissertation. Adjacent genes in the *P.s.s.* B728a genome, transcribed in the same direction, were analyzed to determine whether they were in common operons. To classify potential operon pairs in *P.s.s.* B728a the differences between assumed operon pairs (Ops) and assumed non-operon pairs (NOPs) in the distributions of distance and correlation of expression data was considered to classify a potential operon pair as either an OP or a NOP. The previously annotated genome of *Pseudomonas aeruginosa* strain PAO1 was used to provide OP probabilities for assumed OPs and NOPs. Gene pairs with OP probabilities above 0.9 were assumed to be OPs and gene pairs with OP probabilities below 0.1 were assumed to be NOPs.

Bacterial strains, plasmids, and growth conditions

The bacterial strains and plasmids used in this study are listed in Table A-1 located in the Appendix A. For general cloning *Escherichia coli* DH10B was cultured in

Luria-Bertani (LB) liquid or agar medium at 37°C (100, 101). For topoisomerase reactions One Shot® TOP10 *Escherichia coli* or Mach 1 T1™ *Escherichia coli* cells were used in accordance with the manufacturer's protocol (Invitrogen, Carlsbad, CA). *P.s.s.* B728a strains were grown at 26°C with shaking at 200 rotations per minute (rpm). King's B (56) and LB served as media for general growth of *P.s.s.* B728a. For iron limited conditions hrp-inducing minimal media (HMM) [0.2 M KH_2PO_4, 1.2 M K_2HPO_4, 1.3 M $(NH_4)_2SO_4$, 5.9 M $MgCl_2$, 5.8 M NaCl, 0.2% fructose] was used (47). Water for use in iron limited media was treated to remove free iron using 10 grams of Chelex®100 (Bio-Rad) per 100 milliliters of ultrapure water (Barnstead E-Pure D4642-33). Antibiotics were added as needed at the following concentrations ($\mu g\ ml^{-1}$): rifampicin 100, kanamycin 75, tetracycline 20, chloramphenicol 20, gentamycin 5, and spectinomycin 100.

For iron limited conditions, glassware was treated to remove exogenous iron as described by Kadurugamuwa, J.L. et al. (52). Glassware was soaked in 5% Extran MA01 (EMD Chemicals, Germany) for 6 hours followed by soaking in 0.01% EDTA (J.T. Baker, Phillipsburg, NJ) for 12 hours. Glassware was rinsed in 1% HCl, followed by extensive rinsing in ultrapure water (Barnstead E-Pure D4642-33). Glassware was dried in a 160°C oven for 3 hours, followed by autoclaving.

Construction of markerless deletion mutations in P.s.s. B728a

Targeted deletion mutants in *P.s.s.* B728a were made utilizing a modified version of the phage lambda Red recombinase system developed by Datsenko and Wanner (24,

99). With this strategy, the gene of interest (GOI) along with 3 to 4 kb of flanking DNA on each side was PCR amplified using Phusion® high fidelity, long-range proofreading polymerase (ThermoScientific F-553S) (flank-GOI-flank). The primers for this PCR reaction, Prr2580F and Prr2580R, were designed to add a TOPO cloning tag onto the 5' end of the PCR product (Table A-2). The purified PCR product was then transferred into the Gateway entry vector pENTR/D-TOPO (Invitrogen pENTR/D-TOPO cloning kit catalog #45-0218) and transformed into chemically competent *E. coli* Mach 1 cells (pENTR: flank-GOI-flank). The gene of interest with its flanking regions were recombined into the *Pseudomonas* suicide vector, pLVC-D, using a Gateway reaction (Invitrogen LR Clonase II catalog #11791-020). Site specific recombination proteins from the bacteriophage lambda are utilized to recombine the gene of interest and flanking region from the pENTR vector into the pLVC-D destination vector (pLVC-D: flank-GOI-flank).

The pLVC-D: flank-GOI-flank destination vector was then transformed into the recombineering (recombination-mediated genetic engineering) strain *E. coli* SW105 (http://recombineering.ncifcrf.gov/). The genome of this strain contains a defective lambda prophage containing the Red recombinase genes. These genes are regulated by a temperature sensitive repressor, *cI857*, which is active at 32°C thereby preventing any recombination proteins from being produced. A 15 minute heat-shock at 42°C inactivates the *cI857* repressor and allows transcription of the Red recombinase proteins. The Red recombinase proteins allow the insertion of linear DNA directly into the target DNA molecule, pLVC-D: flank-GOI-flank. The linear DNA is a PCR product

containing 36 bp of DNA flanking each side of the gene of interest and a kanamycin (Km) resistance cassette amplified from the vector pKD13 using primers Prr2580KmF and Prr2580KmR (Table A-2). The pKD13 vector was used to amplify the FRT (FLP recognition target) sites that are utilized to remove the Km cassette. The linear DNA is recombined into the destination plasmid by electroporation of heat-shocked *E.coli* SW105: pLVC-D: flank-GOI-flank with the linear DNA product. The resulting *E.coli* SW105: pLVC-D: flank-Km-flank is utilized for triparental mating to introduce the Km cassette in place of the gene of interest. The Km cassette was removed using FLP recombinase. Colony PCR and Southern blot analysis were utilized to confirm all double recombination mating events.

General DNA manipulations

Restriction enzymes, Calf Intestinal Phosphatase (CIP), and T4 DNA ligase were purchased from New England Biolabs (Beverly, Mass.) and used according to the manufacturers' protocols. Thermo Scientific Phusion High-Fidelity DNA polymerase was purchased from Fisher Scientific. Cloning strategies involved the amplification of target genes via PCR and utilization of Gateway technology to insert the PCR product into the pENTR/D-TOPO vector were done in accordance with manufacturers' protocols (Invitrogen) (61). Recombination between pENTR constructs and Gateway destination vectors were performed in accordance with the manufacturers' instructions provided for LR clonase (Invitrogen). Plasmids were incorporated into *E.coli* via chemical transformation or electroporation (101). Tri-parental mating with the helper plasmid

pRK2073 was utilized for the incorporation of plasmids in *P.s.s.* B728a for recombination events (63). Complementation of *P.s.s.* B728a was accomplished by electroporation of the complement construct. Primer sequences are listed in Table A-2 and standard PCR cycling conditions were used.

Construction of complementing plasmids

An intact copy of the *acsS* gene including the predicted promoter region was amplified from the *P.s.s.* B728a genome with *Eco* RI restriction enzymes sites on each end of the PCR product using primers P-*acsS*compF and P-*acsS*compR (Table A-2). The PCR product was digested with *Eco* RI at 37°C for 1 hour and the restriction enzyme was heat inactivated at 65°C for 20 minutes. The broad-host-range promoter-probe vector, pPROBE-KT' was digested with *Eco* RI at 37°C for 1 hour and CIP treated at 37°C for 1 hour (84). The digested vector was purified using the Wizard® SV Gel and PCR Clean-Up System (Promega). Both digestion products were quantified using micro-spectrophotometry (Nano-Drop Technologies, Inc.). Ligation of the vector and insert was performed using T4 DNA ligase (New England Biolabs) and the complement construct was transformed into *E.coli* Mach 1 T1™ cells (Invitrogen) for construct confirmation. The pPROBE-KT':*acsS* construct was introduced into *P.s.s.* B728a *ΔacsS* by electroporation.

Quantitative real time PCR

Quantitative real time reverse-transcription PCR (qRT-PCR) was utilized to determine if the sigma factor *acsS* is responsive to low iron environmental conditions. Experimental design and controls are based on the guidelines outlined by Bustin et al. (15). Total RNA was extracted from *P.s.s.* B728a that had been grown to late logarithmic phase (OD_{600} of 0.6) at 26°C in iron limited HMM media, HMM media plus 10 μM iron, and HMM media plus 100 μM iron. Three biological replicates of *P.s.s.* B728a for each media condition were extracted on separate days with separate batches of media. The cultures were fixed using RNA protect™ Bacterial Reagent (Qiagen), in a ratio of 2 mL of reagent per 1 mL of bacterial culture. Centrifugation was used to pellet the cells (5000 rpm, 4°C, 20 min) and the supernatant was discarded. Cell lysis was performed using 7 mg/mL lysozyme (M.P. Biomedicals) in TE buffer (10mM TrisCl, 1 mM EDTA, pH 8.0) with frequent vortexing for 7 min at room temperature. Samples were extracted from the *P.s.s.* B728a using an RNeasy® Mini Kit (Qiagen) and eluted in RNase/DNase free water. RNA samples were treated with TURBO™ DNase (Ambion®) using the manufacturer's protocol. The RNA was tested for DNA contamination using qRT-PCR in which the RNA is utilized as the template and reverse transcription reaction is not performed. The RNA quality was measured by Regina M. Hokanson at the Texas AgriLife Genomics and Bioinformatics Services using an Agilent 2100 Bioanalyzer (Agilent Technologies, Inc.) and only RNA samples with an RNA Integrity Number (RIN) above 8.0 were selected (49). Total RNA samples were quantified using micro-spectrophotometry (Nano-Drop Technologies, Inc.).

Total RNA (150 ng per biological sample) was converted to double stranded cDNA by reverse transcription using Super Script Vilo™ cDNA Synthesis kit (Invitrogen™). Reverse transcription was conducted with the following temperature cycle: 10 min at 25°C, 60 min at 42°C, 5 min at 85°C. The double stranded cDNA was quantified using micro-spectrophotometry (Nano-Drop Technologies, Inc.) and samples were diluted to 10 ng/µL.

qRT-PCR was performed using an Applied Biosystems 7500 Fast Real-Time PCR System with the SYBR® GreenER™ Reagent System (Invitrogen™). For each 20 µL reaction the following was used: 10 µL SYBR® GreenER™ qPCR SuperMix Universal, 8.16 µL nuclease free water, 0.04 µL ROX reference dye, 0.4 µL forward primer (200 nM final), 0.4 µL reverse primer (200 nM final), 1 µL template DNA (10 ng/µL). Primers used for these reactions are listed in Table A-2, with the primers qRTrecAF/qRTrecAR and qRT16SF/qRT16SR being utilized for normalization (74). A dissociation curve was utilized to ensure that a single product is amplified; this cycle consisted of 95°C for 15 sec, 60°C for 1 min, 95°C for 15 sec. All primer pairs utilized amplified a single product in the conditions tested. The linearity of detection was confirmed for each primer pair by measuring a five-fold dilution curve for cDNA synthesized from total RNA in the conditions tested in this study. The correlation coefficient for this dilution curve was evaluated and confirmed to be at least 0.98 ($r^2 > 0.98$). The efficiency of the primers was calculated using the slope of the line from the five-fold dilution curve using the following equation: Efficiency = $10^{(-1/\text{slope})}$ -1. Only primers with efficiencies between 90% and 110% were utilized.

Data was analyzed using the comparative C_t method, wherein the C_t values of the samples of interest are compared to the C_t values of a control. All the C_t values are normalized to endogenously expressed genes, in this case the *recA* housekeeping gene and a 16S ribosomal RNA gene (74). The ΔC_t is calculated as: $C_{t\ sample} - C_{t\ housekeeping}$. The $\Delta\Delta C_t$ is the fold change between the control sample and the sample of interest and is calculated as: $\Delta C_{t\ sample\ of\ interest} - \Delta C_{t\ control\ sample}$.

Preparation of RNA samples for transcriptome analysis

RNA sample preparation and cDNA library generation was performed according to procedures outlined by Croucher et al., 2009 and Perkins et al., 2009 with slight modifications (21, 92). RNA samples were extracted from *P.s.s.* B728a and *P.s.s.* B728a Δ*acsS* which had been grown to late logarithmic phase (OD_{600} of 0.6) in iron limited HMM media at 26°C. The three biological replicates of each strain were extracted on separate days with separate batches of media. The cultures were fixed using RNA protect™ Bacterial Reagent (Qiagen), in a ratio of 2 mL of reagent per 1 mL of bacterial culture. Centrifugation was used to pellet the cells (5000 rpm, 4°C, 20 min) and the supernatant was discarded. Cell lysis was performed using 7 mg/mL lysozyme (M.P. Biomedicals) in TE buffer (10mM TrisCl, 1 mM EDTA, pH 8.0) with frequent vortexing for 7 min at room temperature. Samples were extracted from the *P.s.s.* B728a and *P.s.s.* B728a Δ*acsS* strains using RNeasy® Mini Kit (Qiagen) and eluted in RNase/DNase free water. RNA samples were treated with TURBO™ DNase (Ambion®) using the manufacturer's protocol. The RNA was tested for DNA

contamination using quantitative Real-Time reverse-transcription PCR (qRT-PCR) in which the RNA is utilized as the template and reverse transcription reaction is not performed. The RNA quality was measured by Regina M. Hokanson at the Texas AgriLife Genomics and Bioinformatics Services using an Agilent 2100 Bioanalyzer (Agilent Technologies, Inc.) and only RNA samples with an RNA Integrity Number (RIN) above 8.0 were selected (49). Total RNA samples were quantified using micro-spectrophotometry (Nano-Drop Technologies, Inc.) and the Quant-iT™ RiboGreen® RNA assay kit (Invitrogen).

RNA sample processing and reverse transcription

Complementary oligonucleotide hybridization was utilized to remove the 16S and 23S rRNA using the MICROBExpress™ bacterial mRNA enrichment kit (Ambion®) with *Pseudomonas* specific hybridization sequences provided by the manufacturer. Denaturing gel electrophoresis was used to ensure the removal of rRNA, a 2% Low Range UltraPure™ agarose denaturing gel was prepared with Tris-acetate-EDTA (TAE). Samples were prepared in a denaturing loading dye with a final concentration of 20mM EDTA and were denatured at 95°C for 10 min prior to being loaded on the gel. The gel electrophoresis was performed using 4 × TAE buffer and run at 60V. Enriched mRNA samples were quantified using micro-spectrophotometry (Nano-Drop Technologies, Inc.) and equal quantities of three biological samples were pooled to form a single mRNA sample for both *P.s.s.* B728a and *P.s.s.* B728a Δ*acsS* with a total concentration of 1.8 µg for each sample (54, 91). The pooled mRNA

samples were denatured at 65°C for 5 min with 50 ng μL^{-1} random hexamer primers (Invitrogen™) and 10mM dNTPs and placed on ice for 5 min. SuperScript III (Invitrogen™) reverse transcriptase was used to synthesize single stranded cDNA using the manufacturer's protocol, the synthesis cycle was 10 min at 25°C, 180 min at 45°C, 15 min at 70°C, 5 min at 85°C. *E. coli* RNase H (Invitrogen™) was used to remove complementary RNA. The single stranded cDNA was purified using the Wizard® SV Gel and PCR Clean-Up System (Promega) and quantified using micro-spectrophotometry (Nano-Drop Technologies, Inc.).

Library construction

Sequencing libraries for the Illumina GAIIX platform were constructed as follows. 5 µg of each single stranded cDNA sample was diluted in TE buffer to a total volume of 120 µL for cDNA shearing. Regina M. Hokanson at the Texas AgriLife Genomics and Bioinformatics Services performed the cDNA shearing using the Covaris S2 Adaptive Focused Acoustic Disruptor with a 200 base pair fragmentation cycle (Run at 10%, Intensity: 5, 200 cycles per burst, 4 cycles of 60 sec each). The sheared cDNA was purified using the QIAquick PCR Purification Kit (Qiagen) and eluted in 30 µL Buffer EB (10 mM TrisCl, pH 8.5) (Qiagen). Illumina DNA library construction was performed using the Illumina Paired-End Sequencing method (Cat. No. PE-102-1001) in accordance with the manufacturer's recommended protocol and with the assistance of Dr. Weibing Shi of Texas A&M University. After the ligation of Illumina adaptors, the samples were run on a denaturing gel (described above) and the band correlating to 200-

250 base pairs on the denatured DNA ladder was selected. The selected DNA constructs were amplified by 18 cycles of PCR using the Phusion® high-fidelity DNA polymerase and primers PE 1.0 and PE 2.0 provided in the Illumina library kit. The amplified constructs were purified using the Wizard® SV Gel and PCR Clean-Up System (Promega) and quantified using micro-spectrophotometry (Nano-Drop Technologies, Inc.).

Illumina library sequencing

Library quality and quantity was confirmed by Dr. Pieter Faber at the Genomics Core of the Lerner Research Institute of the Cleveland Clinic, Cleveland, OH using an Agilent 2100 Bioanalyzer (Agilent Technologies, Inc.). Sequencing of the libraries was also performed by Dr. Pieter Faber using an Illumina GAIIX. Each library was loaded onto a single lane of an Illumina GAIIX flow cell and single-end, 36-cycle sequencing was performed with all cluster formation, primer hybridization, and sequencing reactions in accordance with the manufacturer's recommended protocol.

Read mapping to reference genome

Sequencing reads were mapped to the reference genome, *Pseudomonas syringae* pv. *syringae* B728a (Genbank CP000075.1) which was downloaded from http://www.ncbi.nih.gov/genomes. The removal of sequence adapters, mapping to reference genome, and the normalization of gene expression was performed using CLC Genomics Workbench (V4.5, CLC Bio.). The normalization of gene expression by

Reads per Kilobase per Million Mapped Reads (RPKM) was calculated using the methods described by Mortazavi et al., 2008 (85). This analysis was performed by Dr. Charles J. Greenwald.

Differential gene expression analysis

The differential gene expression of the pooled samples from each condition was analyzed using the R sequence package DEGseq, under the random sampling model using the RPKM values obtained from the previous step (117). This analysis was performed by Dr. Charles J. Greenwald.

Purification of achromobactin from P.s.s. B728a

Achromobactin was purified from *P.s.s.* B728a, *P.s.s.* B728a ADB1005 (PVD-), *P.s.s.* B728a Δ*acsS,* and *P.s.s.* B728a Δ*acsS* pProbe-KT':*acsS.* The purification procedure is modified from Berti and Thomas (8). Cultures of the *Pseudomonas* strains were grown to late logarithmic phase (OD_{600} of 0.6). 1 mL of the culture was pelleted and washed three times in iron limited HMM media. Cell pellets were re-suspended in 1 mL of iron limited HMM media and used to inoculate 2800 mL flasks containing 1 L of iron limited HMM media with 1.7 mM sodium citrate. These cultures were grown at 26°C, shaking at 250 rotations per minute (rpm) for 4 days. Cells were removed by centrifugation at 5000 rpm for 30 minutes. Rotary evaporation was used to concentrate the supernatant to 10 mL. The supernatant was then brought to a 90% methanol concentration and filtered through 125 mm Whatman paper followed by a 0.2 μm

diameter pore size filter. The filtered supernatant was diluted 1:1 with ethyl acetate. Column chromatography was performed using a column of silica resin (SiliaFlash F60 40-63 μm, 230-400 mesh, SiliCycle, Quebec City, Canada). The column was washed with two column volumes of 10:9:1 solution ethyl acetate/methanol/water, and eluted in 1 L of 9:1 methanol/water. The eluted achromobactin was rotary evaporated to a final volume of 3 mL.

Mass spectrometry of achromobactin

Mass spectrometry analysis was performed by Dr. Benjamin Philmus with the support of Dr. Tadhg Begley at Texas A&M University. Siderophore analysis was accomplished by liquid chromatography-electro spray ionization-time of flight- mass spectrometry (LC-ESI TOF MS) analysis using an Agilent 1260 HPLC equipped with a binary pump, thermostated autosampler, heated column compartment and diode array detector in line with a MicroToF-QII MSD (Bruker Daltonics, Billerica, MA) equipped with an ESI source operating in negative ionization mode monitoring from *m/z* 50 – 2500. The crude media preparation from above was separated using a Poroshell 120 EC-C18 HPLC column (3.0 x 100 mm, 2.7 μm, Agilent Technologies, Santa Clara CA) held at 30 ^{o}C with the following program using a flow rate of 0.5 mL/min, where bottle A was 10 mM *N*,*N*-dimethylhexylamine, 10 mM ammonium acetate, pH 7.1 and bottle B was 75% methanol/25% water. The column was pre-equilibrated in 100% A for 2 min prior to injection. The mobile phase was held at 100 % A for 5 min and then changed to 100 % B over the following 15 min using a linear gradient, at which time the mobile

phase was held at 100 % B for 5 additional minutes followed by recycling the mobile phase to 100% A over 2 min and the column was held at 100% A for 2 min to equilibrate the column prior to the next injection. The MSD had the following settings: Capillary, 3000 V; End plate offset, -500 V; Nebulizer gas, 3.0 bar; Drying gas, 10 L/min; Drying gas temperature, 200^{o}C; Funnel 1 RF, 300 Vpp; Funnel 2 RF, 300 Vpp; ISCID energy, 0.0 eV; Hexapole RF, 300 Vpp; Quadrapole Ion energy, 5 eV; Low mass filter, 300 *m/z*; Collision cell RF, 300 Vpp; Collison energy, 8.0 eV, Transfer time, 100.0 μsec; Prepulse storage, 10.0 μsec. The MSD was calibrated using ESI tune mix-low solution (Agilent Technologies) prior to running a set of samples and each run contained an internal standard derived from an automatic injection of 20 μL sodium acetate (0.4 mg/mL). Data was processed using DataAnalysis 4.0 software (Bruker Daltonics, Billerica, MA).

N,N-dimethylhexylamine, sodium acetate, ammonium acetate were purchased from Sigma-Aldrich and used without purification. All solvents used during LC-MS analysis were of LC-MS grade.

Plant pathogenicity assays

In order to test the ability of *P.s.s.* B728a *ΔacsS* to multiply in planta and cause disease, vacuum infiltration of two week old Blue Lake 274 (Burpee Seeds, Warminster, PA) bean plants (*Phaseolis vulgaris* L.) and four week old *Nicotiana benthamiana* was performed. *P.s.s.* B728a was utilized as a positive control for this experiment and *P.s.s.* B728a *ΔgacS* served as our negative control. The bacterial strains were cultured overnight from an isolated colony in 5 mL of LB liquid media at 26°C with shaking at

200 rpm. The overnight cultures were used to inoculate flasks of 100 mL LB liquid, which were grown at 26°C with shaking at 200 rpm to an OD_{600} of 0.6. Cultures were pelleted at 5000 rpm for 10 min at room temperature. Cell pellets were washed in sterile distilled water. After washing cell pellets were resuspended to an OD_{600} of 0.3, which is equivalent to 5×10^8 colony forming units (CFU) per mL. Bacterial suspensions of 5×10^6 CFU/mL were made in sterile distilled water with 1% Silwet L-77 (Vac-In- Stuff) surfactant (Lehle Seeds, Round Rock, TX). Plants were suspended in the inocula and a vacuum was established. The vacuum was held at 20 in. Hg. for 1 min and slowly released. Plants were rinsed with distilled water and allowed to air dry. The plants were maintained at 25°C in a growth chamber for 72 hours. Each strain was analyzed on no less than three plants of each species, and the experiment was independently replicated three times.

To evaluate the ability of the bacterial strains to replicate in planta population analyses were performed for *P.s.s.* B728a, *P.s.s.* B728a *ΔacsS,* and *P.s.s.* B728a *ΔgacS* on Day 0, Day 2, and Day 4 after vacuum infiltration. A trifoliate leaf was selected and detached from each infiltrated plant and infiltrated tissue was removed using the bottom of a sterile 2 mL screw-cap microcentrifuge tube (Bio Plas Inc., San Francisco, CA). 20 leaf discs were removed per leaf and rinsed in sterile distilled water. Leaf discs were ground using a mortar and pestle with Silwet Phosphate Magnesium Buffer (SPM, 0.7% K_2HPO_4, 0.4% KH_2PO_4, 0.025% $MgSO_4{\cdot}7\ H_20$, 0.004% Silwet L-77). Serial dilutions were made and plated on KB agar plates followed by incubation at 26°C for 48 hours. Colonies were counted and populations were calculated.

Results and Discussion

Bioinformatic analysis: a peptide synthetase rich region

Analysis of the 6.1 Mb *P.s.s.* B728a genome revealed a peptide synthetase rich region of over 186 kb, including the syringomycin/syringopeptin (*syr/syp)* toxin clusters, the achromobactin siderophore cluster (*Psyr_2580-Psyr_2595*), and an eight module NRPS (*Psyr_2576-2577*) predicted to encode the lipopeptide syringafactin (9). By examining sequence similarities to other sequenced *Pseudomonas syringae* species at both the nucleotide and protein level, it is evident that the peptides encoded in this region were probably inherited from different microbial ancestors (Fig. 3). The syringafactin cluster (*Psyr_2576-2577)* has > 80% similarity, at the nucleotide level, to a group of genes in the *P.s.t.* DC3000 genome. However, the 14-gene cluster that is predicted to encode the citrate siderophore achromobactin is absent from the *P.s.t.* DC3000 genome, but has > 80% sequence similarity to a gene cluster in *P.s.p.* 1448a. Additionally, the *syr/syp* toxin clusters are found in neither *P.s.t.* DC3000 nor *P.s.p.* 1448a. Thus, this region of the *P.s.s.* B728a genome seems to have independently inherited three separate peptide clusters. Interestingly, this region accounts for over 3% of the *P.s.s.* B728a genome and appears to be more susceptible to genetic recombination events. Given the pattern of this genomic region with apparent blocks of genes that were

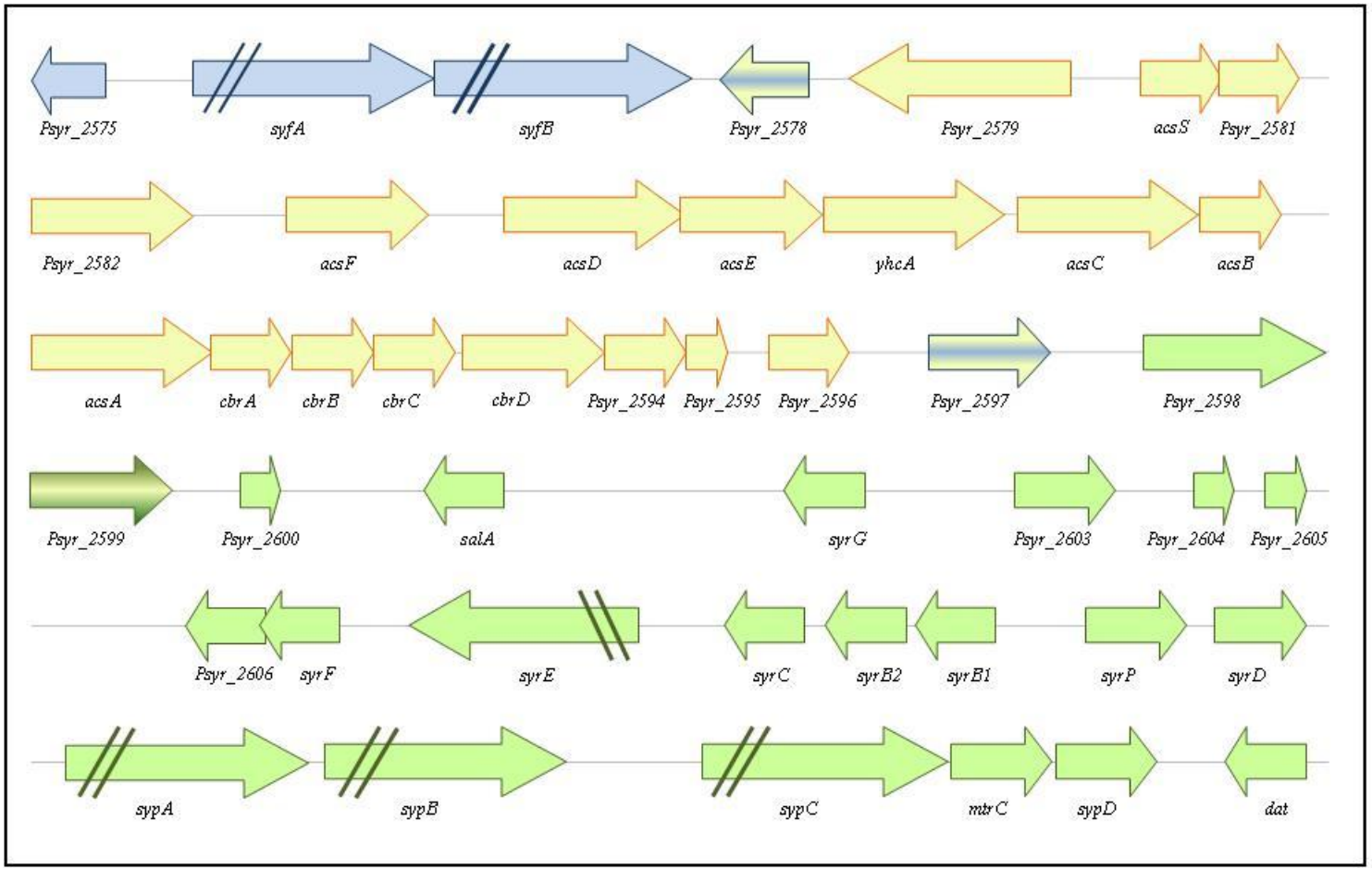

FIG. 3. A peptide synthesis region of the *P.s.s.* B728a genome. The color coding is based on nucleotide sequence similarity of > 80% in the *Pseudomonas* species listed below. *P.s.t.* DC3000 (blue), *P.s.p.* 1448a (yellow), and *P.s.s.* B728a only (green). Those genes with > 80% similarity in multiple genomes are striped with the colors of both genomes.

independently inherited, it is likely that the regulatory genes located within these peptide clusters are associated with the regulation of that specific peptide. Accordingly, I hypothesized that the ECF σ^{70} factor encoded on gene *Psyr*_2580, is directly involved in the regulation of the achromobactin gene cluster in response to iron limited conditions. This gene has been designated as the achromobactin sigma factor, *acsS.*

The 19.9 kb achromobactin gene cluster (*Psyr_2580-Psyr_2595*) of *P.s.s.* B728a has a homologous gene cluster in *P.s.p.*1448a with 88% similarity at the nucleotide level. This homologous gene cluster in *P.s.p.* 1448a includes a gene, *PSPPH_2747*, with 93% similarity at the nucleotide level to the ECF sigma factor gene *acsS* (Fig. 4). Furthermore, the achromobactin clusters in *P.s.s.* B728a (*Psyr_2580-Psyr_2595*) and *P.s.p.* 1448a (*PSPPH_2747-PSPPH_2762*) maintain sequence homology above 80% at the nucleotide level for each of the 16 genes in the cluster, as well as, gene order and directionality.

The achromobactin biosynthesis cluster from *Dickeya dadantii* strain 3937 is 20.6 kb in length and is 86% similar at the nucleotide level to the cluster found in *Dickeya zeae* strain Ech1591. When the entire achromobactin biosynthesis and secretion regions are compared, very little sequence similarity is seen between these *Dickeya* strains and the fluorescent pseudomonads. However, when analyzed for individual gene homology, 12 out of the 16 genes in the *P.s.s.* B728a achromobactin cluster have over 70% sequence similarity at the nucleotide level to the *Dickeya* strains. These genes include those necessary for achromobactin biosynthesis, *acsD*, *acsE*, *acsC*, and *acsA*, as well as the ABC transporter system encoded by genes *cbrABCD.* The sequence

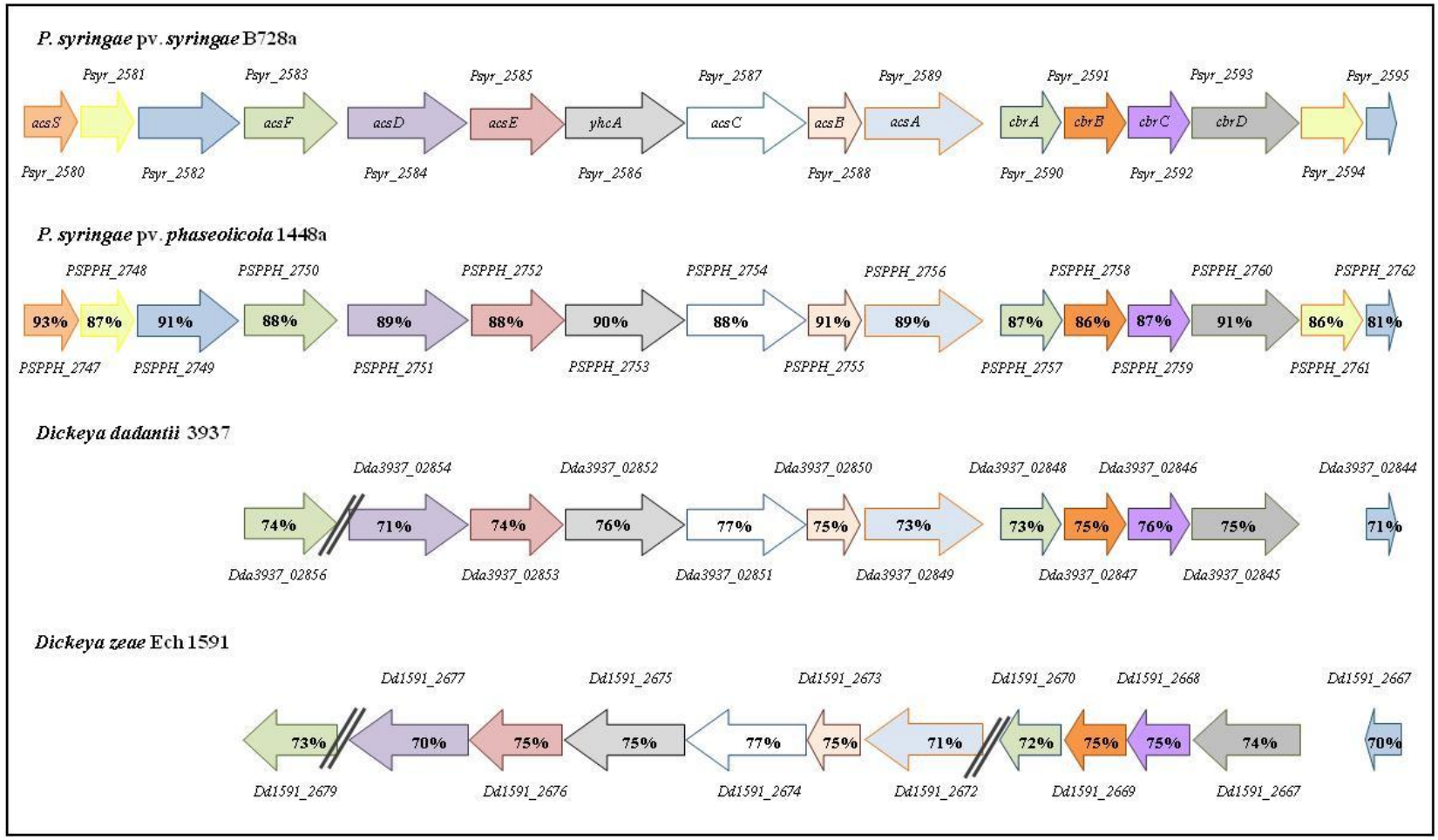

FIG. 4. Sequence homology of the achromobactin gene clusters in *P.s.s.* B728a, *P.s.p.* 1448a, *Dickeya dadantii* strain 3937, and *Dickeya zeae* strain Ech1591. Sequence homology shown as a percentage and is in reference to the *P.s.s.* B728a genome with homologous genes being shown in the same color. Parallel lines reflect a gap in the genome, wherein the genome shown has nucleotides and/or genes that are not found in that location in *P.s.s.* B728a.

similarity of these gene clusters, as well as previous research indicating that the achromobactin synthesized by *P.s.s.* B728a can be recognized and utilized by *Dickeya dadantii* strain 3937, supports that these genes are homologs to the achromobactin biosynthesis and secretion genes identified in *Dickeya dadantii* strain 3937 (123). Interestingly, the *Dickeya* strains do not contain homologs to the extracytoplasmic function (ECF) sigma factor *acsS;* therefore, it is likely that achromobactin biosynthesis is regulated differently in *P.s.s.* B728a than in the *Dickeya* strains.

Targeted mutagenesis of acsS

In order to test the hypothesis that the ECF σ^{70} factor encoded within the achromobactin gene cluster is directly involved in the regulation of achromobactin biosynthesis and secretion, a deletion mutant, *P.s.s.* B728a Δ*acsS*, was created using a modified Red Recombinase strategy as described in detail in the Materials and Methods. The resultant mutant strain was confirmed as harboring the expected genomic deletion by Southern blot analysis and colony PCR.

The *P.s.s.* B728a Δ*acsS* strain was complemented with the broad-host-range promoter-probe vector, pPROBE-KT', containing an intact *acsS* gene including its predicted native promoter region (84). The pPROBE-KT' was selected for the complement construct due to its stability, presence of a multicloning site, and because it does not interfere with the biosynthesis of bacterial phytotoxins.

Plant pathogenicity assays

To investigate the role of the AcsS sigma factor in planta, 2 week old bean plants (*Phaseolis vulgaris* L.) and 4 week old *Nicotiana benthamiana* were vacuum infiltrated with bacterial cultures. Wild type *P.s.s.* B728a, as well as, regulatory mutants *P.s.s.* B728a Δ*acsS*, and *P.s.s.* B728a Δ*gacS* were utilized for this study. The plants were infiltrated with 5×10^6 colony forming units (CFU) per mL of inoculum and placed in a growth chamber at 25°C. The infiltrated plants were visually inspected at day 0, day 2, and day 4 for disease symptoms and in planta colonization was analyzed on each of these days by population counts. The *P.s.s.* B728a *ΔacsS* infiltrated strains displayed disease symptoms equivalent to those seen with the wild type strain, *P.s.s.* B728a. Those plants inoculated with the negative control strain, *P.s.s.* B728a Δ*gacS,* did not exhibit any disease symptoms. The *P.s.s.* B728a *ΔacsS* and *P.s.s.* B728a strains had equivalent populations in the leaf tissue as determined by CFU per area of infected leaf tissue. Based on these analyses, it appears that AcsS is not necessary for the establishment and development of plant disease. However, since these experiments utilized vacuum infiltration, it is possible that AcsS plays a role in the bacterial entry into the apoplast or for bacterial survival and competition on the leaf surface. Since there is no apparent disease phenotype, expression analysis was utilized to further pursue the characterization of AcsS.

Quantitative real time reverse transcription PCR

Prior to intensive expression analysis studies the iron responsiveness of *acsS* was verified using quantitative real time reverse transcription PCR (qRT-PCR). *P.s.s.* B728a was cultured to late logarithmic phase (OD_{600} of 0.6) in HMM media with limited iron, 10 μM iron added, and 100 μM iron added. Total RNA was extracted and analyzed using qRT-PCR with primers for the housekeeping gene *recA* and a 16S ribosomal RNA gene serving as normalization controls (74). Expression analysis showed that *acsS* is highly expressed in low iron conditions and that expression decreased dramatically in both the 10 μM iron added and 100 μM iron added conditions. Expression of *acsS* was approximately 10 fold higher in the HMM with limited iron than in either of the conditions containing larger concentrations of iron (data not shown). The increased expression of *acsS* in low iron conditions supported the postulation that *acsS* is the sigma factor responsible for the regulation of the achromobactin gene cluster; therefore, further expression analyses was performed using a whole genome transcriptome analysis.

Transcriptome analysis

The cellular transcriptome is the complete set of mRNA, non-coding RNA, and small RNA transcripts present in a cell at a particular time in a specific condition (121). Analysis of the transcriptome can provide invaluable information about the cellular processes and regulatory events occurring in the conditions and cellular growth phase.

Hybridization technologies such as microarrays have often been used for this purpose; however, these technologies are riddled with irregularities and limitations. Since microarrays rely on DNA oligonucleotide probes, some major limitations are design bias, limited sensitivity, high levels of background fluorescence, and the inability of microarrays to detect transcripts that are not part of known genomic sequences (21, 121). However, with the advancement of deep-sequencing technologies, RNA-seq transcriptome analysis allows researchers to detect transcripts that do not align with known genomic sequence, thereby making this technology especially beneficial for studying organisms that have not been sequenced (121). Furthermore, transcriptome data gathered via RNA-seq technologies is highly reproducible across technical and biological replicates (27, 79). Despite the listed advantages associated with RNA-seq, hybridization based transcriptome analysis provides its own unique advantages to certain studies, and should be considered a complementary technology to sequencing based approaches (68).

Initially high-throughput sequencing technologies for RNA-seq, such as Roche 454 GS FLX, Illumina Genome Analyzer, and Life Technologies ABI SOLid were primarily limited to eukaryotic organisms, due to the ease of enriching mRNA from these organisms (27, 107). Less than 5% of the cellular RNA is mRNA (107); therefore, performing transcriptome analysis with total RNA would result in an abundance of sequencing results for the ribosomal RNA and tRNA with very few reads mapping to mRNA targets. The absence of a 3'-end poly(A) tail in prokaryotes presents a challenge for enriching mRNA in these systems; however, recent technological advancements have

made it possible to eliminate a large percentage of the ribosomal RNA in many Gram positive and Gram negative prokaryotic systems (107). The Ambion MicrobExpress™ system removes 16S and 23S ribosomal RNA from prokaryotic total RNA samples by hybridization to magnetic beads and was utilized in this study (21, 27, 92).

In an RNA-seq study, after gathering total RNA and removing ribosomal RNA, the enriched mRNA is converted into a cDNA. Traditionally double stranded cDNA has been used for these analyses; however, several recent studies have utilized single stranded cDNA in order to capture transcript directionality and isolate transcript signal strength by DNA strand (21, 27, 92). In this study the impact of the *acsS* mutation on the *P.s.s.* B728a transcriptome was analyzed using RNA-seq analysis of single stranded cDNA libraries on an Illumina Genome Analyzer platform. In order to investigate the regulatory role of the AcsS sigma factor on iron responsive genes, including the achromobactin cluster, *P.s.s.* B728a and *P.s.s.* B728a *ΔacsS* were grown in iron limited HMM media and total RNA was extracted. Due to the nature of RNA-seq analysis, in which contaminating DNA could lead to vastly misleading results, and the rapid degradation of prokaryotic mRNA, total RNA quality was strictly monitored. Samples were DNase treated and tested for DNA contamination using qRT-PCR in which the RNA is utilized as the template and reverse transcription reaction is not performed. An Agilent 2100 Bioanalyzer (Agilent Technologies, Inc.) analysis was performed for each biological replicate and only RNA samples with an RNA Integrity Number (RIN) above 8.0 were selected (49). The biological samples of each strain were independently mRNA enriched using the commercially available Ambion MicrobExpress™ kit with

species-specific primers for *Pseudomonas* 16S and 23S ribosomal RNA. Pooling of biological samples for hybridization based transcriptome analyses has been shown to increase the efficiency and cost-effectiveness of these analyses while continuing to provide equivalent statistical power (91). Similarly, RNA-seq using the Illumina sequencing platform was analyzed for technical reproducibility and the researchers concluded that a single mRNA sample run once in a single flow cell would provide sufficient data in many experimental design circumstances (79). Taking these analyses into consideration, this study used a pooled sample of three biological replicates for each strain. The samples were pooled as enriched mRNA, prior to first strand cDNA synthesis.

Sequencing libraries were constructed from the single stranded cDNA samples and subjected to sequencing on the Illumina GAIIX platform. A total of 21,295,605 reads were acquired for the *P.s.s.* B728a *ΔacsS* sample. After trimming, there were 20,936,474 million reads with an average length of 39.82 base pairs. The *P.s.s.* B728a sample resulted in a total of 9,813,229 reads. After trimming, there were 9,651,997 million reads with an average length of 39.82 base pairs. Alignments to the *P.s.s.* B728a genome were generated using CLC Genomics Workbench (V4.5, CLC Bio.). The *P.s.s.* B728a sample resulted in a total of 5,987,236 mapped reads (2,285,461 uniquely and 3,701,775 non-specific) and a total of 3,664,761 unmapped reads. The *P.s.s.* B728a *ΔacsS* sample resulted in a total of 13,220,583 mapped reads (4,480,571 unique and 8,740,012 non-specific) and a total of 7,715,891 unmapped reads. Many of the unmapped reads were further analyzed and BLASTed to poorly annotated regions of the

P.s.s. B728a genome, such as bacteriophage elements. Reads that mapped uniquely to the *P.s.s.* B728a genome were used to calculate the normalized gene expression as Reads per Kilobase per Million Mapped Reads (RPKM) (85).

The differential gene expression of the pooled samples from each condition was analyzed using the R sequence package DEGseq, which models the RNA-seq data as a random sampling process and utilizes the assumption that a binomial distribution can be used for the number of reads resulting from a gene (117). Using this statistical method the data from the two samples was normalized despite the variation in the number of uniquely mapped reads. The efficiency of this statistical approach is supported by the fact that known *P.s.s.* B728a reference genes, such as the *recA* housekeeping gene, are not differentially expressed between the wild type and mutant samples. Using a stringent p-value of less than 0.001, 287 genes were identified that were differentially expressed between *P.s.s.* B728a and *P.s.s. ΔacsS* (Table A-3). Ribosomal RNA genes were retracted from this dataset.

The sigma factor AcsS regulates achromobactin biosynthesis and transport. The Illumina RNA-seq analysis of *P.s.s.* B728a and *P.s.s. ΔacsS* in limited iron conditions provided secondary confirmation of the effective deletion of *acsS*, as the wild type strain had 923 fold higher expression of this gene than the *P.s.s. ΔacsS* strain (Table 1). Transcriptome analysis lends support to the hypothesis that the sigma factor AcsS is a regulator of achromobactin biosynthesis and transport. As seen in Table 1, 12 of the 15 genes in the achromobactin gene cluster had decreased gene expression in the *P.s.s. ΔacsS* strain. Additionally, the fold change associated with the achromobactin

TABLE 1. RNA-seq analysis of the achromobactin gene cluster.

Gene	Locus Tag	Operon	Functional Category	Gene Product	Fold Change[a]	P-value
acsS	*Psyr_2580*	508	Transcription	sigma 70 DNA-dependent RNA polymerase subunits	923.1559	1.20E-24
	Psyr_2581	508		FecR-like		
	Psyr_2582		Inorganic ion transport and metabolism	Ton-B dependent siderophore receptor	18.368	4.04E-75
acsF	*Psyr_2583*		Amino acid transport and metabolism	diaminobutyrate--2-oxoglutarate aminotransferase	25.581	1.92E-281
acsD	*Psyr_2584*	509	Secondary metabolites biosynthesis, transport and catabolism	IucA/IucC, Achromobactin synthesis	40.0539	1.12E-188
acsE	*Psyr_2585*	509	Amino acid transport and metabolism	Orn/DAP/Arg decarboxylase 2:Orn/DAP/Arg decarboxylase 2	32.2687	3.74E-153
yhcA	*Psyr_2586*	509	Carbohydrate transport and metabolism	EmrB/QacA family drug resistance transporter	41.1603	1.62E-60
acsC	*Psyr_2587*	510	Secondary metabolites biosynthesis, transport and catabolism	IucA/IucC	30.1028	3.31E-87
acsB	*Psyr_2588*	510	Carbohydrate transport and metabolism	HpcH/HpaI aldolase	39.6891	2.61E-64
acsA	*Psyr_2589*	510	Secondary metabolites biosynthesis, transport and catabolism	IucA/IucC	14.9494	4.98E-80
cbrA	*Psyr_2590*	510	Inorganic ion transport and metabolism	periplasmic binding protein	4.5983	1.24E-16
cbrB	*Psyr_2591*	510	Inorganic ion transport and metabolism	transport system permease protein	3.2514	3.30E-05
cbrC	*Psyr_2592*	510	Secondary metabolites biosynthesis, transport and catabolism	transport system permease protein		
cbrD	*Psyr_2593*	511	Secondary metabolites biosynthesis, transport and catabolism	ABC transporter		
	Psyr_2594	511		hypothetical	2.241	0.000336643
	Psyr_2595	511	Coenzyme transport and metabolism	Menaquinone biosynthesis	2.6833	1.52E-05

[a] Fold change is reflected as *P.s.s.* B728a in comparison to the *ΔacsS* deletion mutant; therefore, a positive fold change reflects a decreased level of gene expression in *P.s.s.* B728a *ΔacsS*.

TABLE 2. Iron associated genes identified in the RNA-seq analysis as having differential gene expression.

Gene	Locus Tag	Op.	Functional Category	Gene Product	Fold Change[a]	P-value
tonB-1	*Psyr_0203*	41	Transport	Tripartite ferric-siderophore uptake complex; TonB, C-terminal	1.4059	6.70E-05
exbD-1	Psyr_0204	41	Transport	Tripartite ferric-siderophore uptake complex; biopolymer transport protein ExbD		
exbB-1	*Psyr_0205*	41	Intracellular trafficking and secretion	MotA/TolQ/ExbB proton channel; TonB-system energizer ExbD	1.5438	3.35E-10
fpr	*Psyr_1387*		Energy production and conversion	ferredoxin--NADP(+) reductase	2.0798	4.33E-05
	Psyr_2141		Inorganic ion transport and metabolism	ferric uptake regulator family	1.4662	9.84E-09
	Psyr_3243		Inorganic ion transport and metabolism	Ton-B dependent siderophore receptor	2.0984	0.0001132
	Psyr_3345		Inorganic ion transport and metabolism	TonB-dependent siderophore receptor	1.8837	2.76E-08
	Psyr_3367	648	Transport	Iron permease FTR1	1.721	3.55E-08
	Psyr_3368	648		hypothetical protein	2.515	1.81E-12
	Psyr_3369	648	Secretion	Twin-arginine translocation pathway signal:Tat-translocated enzyme:Dyp-type peroxidase	2.516	5.74E-26
	Psyr_3370	648		hypothetical protein	2.242	4.21E-34
	Psyr_4730	927	Multifunctional	FecR protein, Fe dicitrate sensor, membrane component	1.9918	3.44E-07
	Psyr_4731	927	Transcription	RNA polymerase sigma factor	2.0258	1.14E-07
	Psyr_1375		Energy production and conversion	4Fe-4S ferredoxin, iron-sulfur binding	-1.79	0.0004046
	Psyr_4031		Energy production and conversion	Fe-S type hydro-lyase tartrate/fumarate alpha region:Fe-S type hydro-lyase tartrate/fumarate beta region; TCA cycle	-2.2236	0.000243

[a] Fold change is reflected as *P.s.s.* B728a in comparison to the *ΔacsS* deletion mutant; therefore, a positive fold change reflects a decreased level of gene expression in *P.s.s.* B728a *ΔacsS*

TABLE 3. RNA-seq analysis of the pyoverdine gene cluster.

Gene	Locus Tag	Op.	Functional Category	Gene Product	Fold Change[a]	P-value
pvdS	*Psyr_1943*		Transcription	extracytoplasmic-function sigma-70 factor; regulation of pyoverdine	1.5773	2.16E-09
	Psyr_1944		Secondary metabolites biosynthesis, transport and catabolism	thioesterase; pyoverdine synthetase	1.5347	1.01E-20
	Psyr_1945		Secondary metabolites biosynthesis, transport and catabolism	peptide synthase	1.6254	9.15E-22
dat	*Psyr_1946*		Amino acid transport and metabolism	diaminobutyrate--2-oxoglutarate aminotransferase; arginine biosynthesis	1.5394	1.13E-33
	Psyr_1947			MbtH-like protein		
	Psyr_1948	383	Transport	ABC transporter, periplasmic substrate-binding protein, putative		
	Psyr_1949	383		hypothetical		
	Psyr_1950	383	Inorganic ion transport and metabolism	ABC transporter	2.494	3.46E-05
	Psyr_1951	383	Transport	Periplasmic solute binding protein		
	Psyr_1952	383		hypothetical	2.0373	6.10E-07
	Psyr_1953	383		hypothetical	1.952	2.71E-06
	Psyr_1954	383		hypothetical		
	Psyr_1955	383		peptidase		
	Psyr_1956		Secondary metabolites biosynthesis, transport and catabolism	pyoverdine biosynthesis regulatory protein	1.5869	3.40E-95
	Psyr_1957	384	Secondary metabolites biosynthesis, transport and catabolism	amino acid adenylation; pyoverdine sidechain peptide synthetase I, epsilon-Lys module	1.4158	2.22E-14
	Psyr_1958	384	Secondary metabolites biosynthesis, transport and catabolism	non-ribosomal peptide synthase:amino acid adenylation; pyoverdine sidechain peptide synthetase II, D-Asp-L-Thr component	1.3759	5.45E-09
	Psyr_1959	384	Secondary metabolites biosynthesis, transport and catabolism	amino acid adenylation; pyoverdine sidechain peptide synthetase III, L-Thr-L-Ser component	1.3656	6.46E-09
	Psyr_1960	384	Secondary metabolites biosynthesis, transport and catabolism	non-ribosomal peptide synthase:amino acid adenylation; pyoverdine sidechain peptide synthetase IV, D-Asp-L-Ser component	1.3572	2.90E-07
	Psyr_1961		Transport	TonB-dependent siderophore receptor		
	Psyr_1962		Inorganic ion transport and metabolism	TonB-dependent siderophore receptor	1.2245	1.99E-08
pvdE	*Psyr_1963*	385	Multifunctional	cyclic peptide transporter; pyoverdine ABC transporter, ATP-binding/permease protein	1.7947	3.85E-09
	Psyr_1964	385		hypothetical	1.979	3.08E-21
pvdN	*Psyr_1965*	385	Amino acid transport and metabolism	twin-arginine translocation pathway signal; secretion	1.8543	1.00E-16
	Psyr_1966	385		Peptidase M19, renal dipeptidase		
	Psyr_1967		Secretion	twin-arginine translocation pathway signal	1.5448	3.19E-05

[a] Fold change is reflected as *P.s.s.* B728a in comparison to the *ΔacsS* deletion mutant; therefore, a positive fold change reflects a decreased level of gene expression in *P.s.s.* B728a *ΔacsS*

biosynthesis genes was the most substantial, with the achromobactin transporter YhcA having a 41.06 fold decrease in gene expression in *P.s.s. ΔacsS* as compared to the wild type. The achromobactin biosynthesis genes also showed substantial decreases in gene expression in the *acsS* mutant strain with decreases in fold change ranging from 14.85 fold (*acsA*) to 39.57 fold (*acsD*). The TonB-dependent siderophore receptor encoded on *Psyr_2582*, had an 18.37 fold lower expression in the *acsS* mutant. Transcriptome analysis confirms that the deletion of the *acsS* sigma factor gene disrupts the gene expression of the gene cluster responsible for the biosynthesis and transport of the siderophore achromobactin.

Iron responsive genes are regulated by AcsS. After confirming that AcsS is responsive to low iron conditions and regulates the gene expression of the achromobactin siderophore biosynthesis cluster, I hypothesized that other iron responsive genes may also be regulated by the AcsS sigma factor. Amongst the 287 genes differentially expressed between *P.s.s.* B728a and the *acsS* deletion strain, 31 genes with known associations with iron uptake and metabolism were identified (Table 2 and Table 3).

When combined with the achromobactin biosynthesis and transport genes shown to be regulated by AcsS, a total of 43 of the 287 differentially expressed genes identified in the RNA-seq analysis are known to be associated with iron. This includes an uncharacterized RNA polymerase sigma factor gene, *Psyr_4731,* located in an operon with a gene that encodes an iron sensor molecule. Although the fold change for this operon is approximately two, given the regulatory role of sigma factors this could

have substantial impact on downstream gene targets. Since the sigma factor gene *Psyr_4731* is expressed at a higher level in the wild type *P.s.s.* B728a than in the *acsS* deletion mutant, it is likely that some of the differentially expressed genes identified in this study may also be downstream of the sigma factor *Psyr_4731*. Another regulatory gene, *Psyr_2141,* was also differentially expressed in this study and had a 1.46 fold reduction in the *acsS* deletion mutant as compared to the wild type. *Psyr_2141* encodes a protein with a conserved domain containing sequence homology to proteins in the Fur (ferric uptake regulator) family that is also present in *P.s.t.* DC3000 and *P.s.p* 1448a (27). Thus, AcsS plays a broad spectrum role in the regulation of iron and is not limited to the biosynthesis and secretion of achromobactin.

Differential gene expression of several iron associated receptors and secretion genes provides evidence that in low iron conditions a complex network of highly regulated uptake and secretion systems is necessary to maintain cellular functioning (Table 2). Out of the 19 TonB- dependent receptors located in the *P.s.s.* B728a genome, four had decreased expression in *acsS* deletion mutant, *Psyr_2582*, *Psyr_1962*, *Psyr_3243*, and *Psyr_3345* (Table 1, 2, 3) (20). Amongst these, *Psyr_2582* showed the largest fold change, an 18.37 fold decrease in the *P.s.s.* B728a *ΔacsA* strain, which is not surprising given its genomic location within the achromobactin cluster. However, *Psyr_1962* is encoded within the gene cluster associated with the biosynthesis and secretion of pyoverdine, and has homologous genes within *P.s.t.* DC3000 and *P.s.p.* 1448a (20). This implies that the regulatory networks of iron responsive genes may be highly intertwined. The two remaining TonB receptors are located outside of known

iron associated gene clusters and are also conserved amongst *P.s.s.* B728a, *P.s.t.* DC3000, and *P.s.p.* 1448a (20). Thus, three out of the four TonB-dependent receptors regulated by AcsS are conserved amongst *P.s.s.* B728a, *P.s.t.* DC3000, and *P.s.p.* 1448a, despite the fact that *P.s.t.* DC3000 does not contain a gene homologous to *acsS* (20). Thus it is likely that these strains have divergent regulatory networks, despite the conserved gene homology.

Interestingly, this study also showed that many genes necessary for biosynthesis and secretion of the siderophore pyoverdine were also impacted by the *acsS* deletion (Table 3). Although the fold change is relatively small, with most genes showing a 1.5 to 2 fold change, 17 genes associated with pyoverdine biosynthesis and transport had differential gene expression between the *acsS* mutant and the wild type. Moreover, this includes the sigma factor associated with the regulation of pyoverdine biosynthesis, *pvdS*, which had 1.58-fold lower gene expression in the *P.s.s.* B728a *ΔacsS* strain than in the wild type strain. Therefore, the deletion of the sigma factor AcsS resulted in a decrease in expression of both achromobactin and pyoverdine. This was a surprising result, as it was hypothesized that pyoverdine production would increase in this mutant strain to compensate for the loss of the siderophore achromobactin. Based on this study it appears that the regulation and biosynthesis of pyoverdine and achromobactin are extensively intertwined and that these separate iron acquisition systems work collaboratively in low iron environments, rather than competitively.

AcsS regulates an RND-type efflux system. In addition to supporting the hypothesis that AcsS regulates the biosynthesis and transport of achromobactin and other

iron responsive genes, a benefit of performing an RNA-seq analysis is that it provides a comprehensive analysis of the transcriptome and identified differentially expressed genes that may have never been predicted or anticipated. In order to minimize the possibility of false positives and identify the most likely genes that are directly or indirectly regulated by AcsS, a stringent p-value (0.001) was selected for data analysis in this study. The Resistance-Nodulation-Cell division (RND-type) efflux system encoded in operon 516, *pseABC* (*Psyr_2620-2622*), was identified as having over a 10-fold decrease in gene expression in the *acsS* mutant; therefore, this membrane-spanning transport system may play a role in the secretion of achromobactin and/or other metabolites regulated by the AcsS sigma factor (Fig. 5).

RND-type efflux systems are found in prokaryotes, archaea, and eukaryotes and utilize ion gradients to fuel the transport of antibiotics and other compounds across the inner and outer membranes into the environment (2, 93). These Type I secretion systems utilize an inner membrane proton antiporter, in which the transfer of hydrogen ions drives the export of substrate molecules from the cytosol directly into the extracellular environment (2). Much of our knowledge about RND-type efflux systems is based on extensive research on the AcrAB-TolC efflux system found in *Escherichia coli* K-12 and *Salmonella enterica* serovar Typhimurium SH5014, with the primary focus being the implications of multidrug (antibiotic) resistance (10, 53, 93). However, RND-type efflux systems are not limited to the transport of antibiotics. Recent studies have diversified our understanding of these transporters and emphasized their roles in not only antimicrobial resistance, but also in environmental adaptation and pathogen

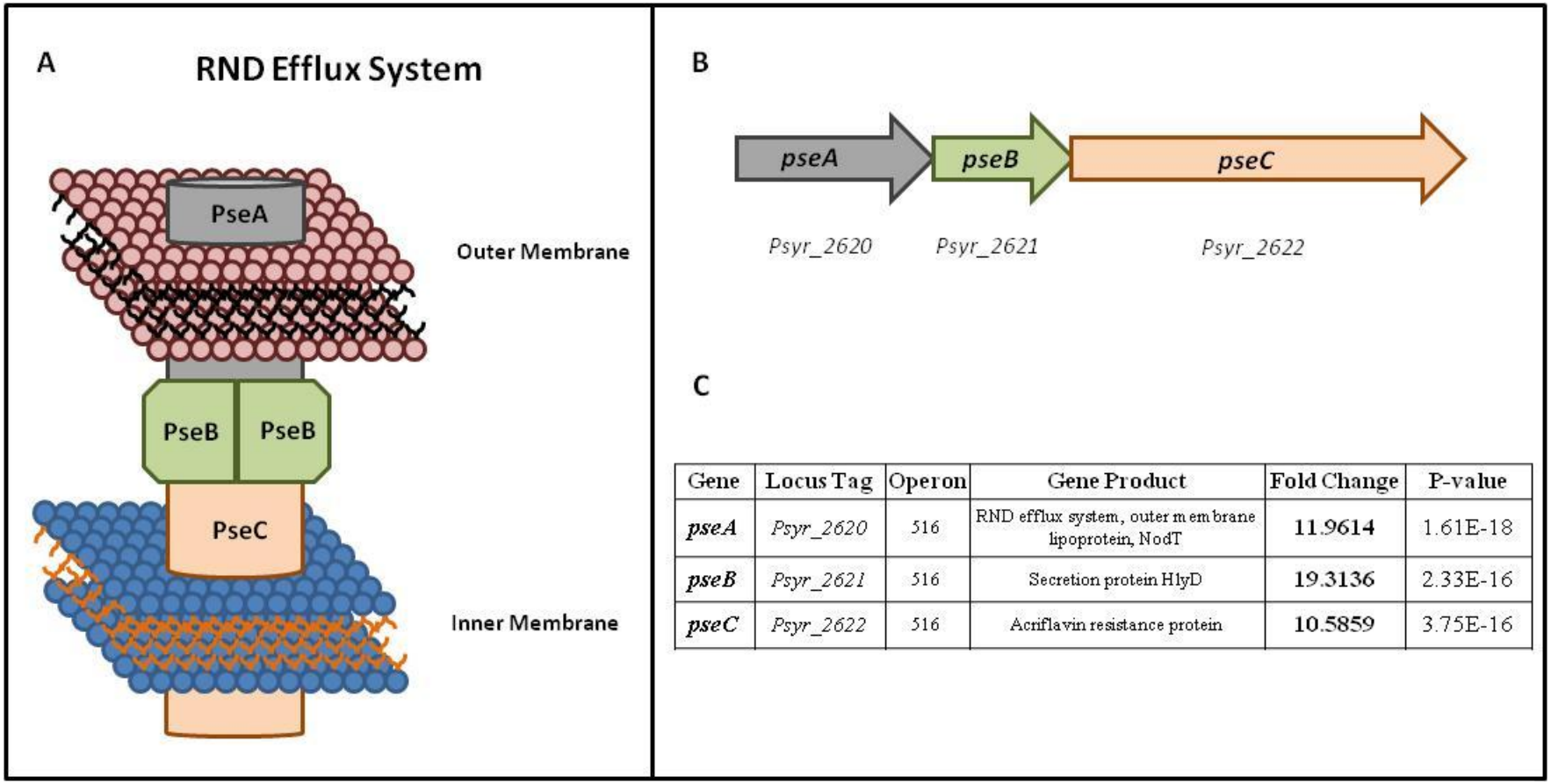

C

Gene	Locus Tag	Operon	Gene Product	Fold Change	P-value
pseA	*Psyr_2620*	516	RND efflux system, outer membrane lipoprotein, NodT	**11.9614**	1.61E-18
pseB	*Psyr_2621*	516	Secretion protein HlyD	**19.3136**	2.33E-16
pseC	*Psyr_2622*	516	Acriflavin resistance protein	**10.5859**	3.75E-16

FIG. 5. The *P.s.s.* B728a RND efflux system PseABC. A. An illustration of the RND efflux system PseABC wherein PseC permeates the bacterial inner membrane, PseA spans the bacterial outer membrane, and the PseB proteins are homologous to membrane fusion proteins. B. The gene order and directionality of *pseABC* on the *P.s.s.* B728a genome are reflected by the colored arrows. The arrow colors coincide to the proteins in illustration A. The locus tag for each gene is listed below each arrow. C. Differential gene expression data for *pseABC* based on the RNA-seq analysis. The fold change is based on a comparison of *P.s.s.* B728a to *P.s.s.* B728a *ΔacsS*; therefore, the fold change values reflect that expression is higher in the wild type than in the *acsS* mutant.

virulence. The rice pathogen, *Xanthamonas oryzae* pv. *oryzae,* requires an RND-efflux system for the transport of the yellow pigment, xanthomonadin, which plays an important role pathogen protection against UV radiation and photo-oxidative stress on the leaf surface (32). Xanthomonadin deficient mutants have a severely decreased ability to survive epiphytically compared to wild type strains; therefore, the ability of this pathogen to transport xanthomonadin to the extracellular environment is an important component of the pathogen's ability to adapt to the leaf surface environment (32). Likewise, *P.s.s.* B301D utilizes an RND-type efflux system, PseABC, and an ATP-binding cassette (ABC) transporter for the secretion of the lipopeptide phytotoxins, syringomycin and syringopeptin, which serve as major virulence factors for this strain (53). In addition to involvement in the transport of pigments and phytotoxins, there is some evidence supporting the involvement of RND-type efflux systems in the transport of the *Escherichia coli* siderophore enterobactin (11). Thus, based on the over 10 fold decrease in gene expression in the *P.s.s.* B728a *ΔacsS* strain, it can be postulated that the *P.s.s.* B728a RND-efflux system, PseABC, is being directly regulated by the AcsS sigma factor and is involved in the transport of achromobactin. However, it also possible that the PseABC RND transporter is involved in the transport of other secondary metabolites regulated by the AcsS sigma factor, such as the antimetabolite toxin, mangotoxin.

AcsS regulates the antimetabolite toxin, mangotoxin. Mangotoxin is a non-host specific antimetabolite toxin that inhibits ornithine acetyl transferase, thereby disrupting the ornithine and arginine biosynthetic pathways (4). This toxin was first identified as a product of *Pseudomonas syringae* pv. *syringae* UMAF0158 (*P.s.s.*

UMAF0158), a pathogen that causes apical necrosis of mango (4). *P.s.s.* B728a, *P.s.t.* DC3000, and *P.s.p.* 1448a contain genes with > 80% sequence similarity to the mangotoxin nonribosomal peptide synthetase gene (*mgoA*), as well as, neighboring genes that are hypothesized to be involved in the biosynthesis of the antimetabolite toxin (4). In *P.s.s.* B728a the gene homologous to *mgoA* (*Psyr_5011*) is encoded within an operon with three hypothetical genes. Interestingly, all four of the genes in this operon were differentially expressed at a statistically relevant level in the RNA-seq analysis; with each having at least 3.9-fold lower expression in the AcsS mutant than in the wild-type strain (Fig. 6).

Gene	Locus Tag	Operon	Gene Product	Fold Change	P-value
	Psyr_5009	983	hypothetical protein, mangotoxin biosynthesis	**4.7447**	4.39E-19
	Psyr_5010	983	hypothetical protein, mangotoxin biosynthesis	**4.0186**	3.36E-10
mgoA	*Psyr_5011*	983	mangotoxin biosyntheis, Amino acid adenylation:Thioester reductase	**5.2527**	2.27E-13
	Psyr_5012	983	hypothetical protein, mangotoxin biosynthesis	**3.9592**	8.07E-07

FIG. 6. The *P.s.s.* B728a gene cluster homologous to the mangotoxin biosynthesis cluster found in *P.s.s.* UMAF0158. RNA-seq analysis of *P.s.s.* B728a versus *P.s.s.* B728a *ΔacsS* established that the operon has lower gene expression in the *P.s.s.* B728a *ΔacsS* than in the wildtype strain.

In the mango pathogen, *P.s.s.* UMAF0158, mangotoxin serves as a virulence factor, wherein mangotoxin deficient strains show a definitive delay in symptom

initiation and progression (3, 4). Mangotoxin deficient strains showed no statistically relevant difference from the wild type strain in their ability to survive epiphytically (3). However, when co-inoculated on the leaf surface, the mangotoxin deficient strain was less efficient at surviving in the epiphytic environment (3). Thus, it is hypothesized that mangotoxin plays a role in epiphytic fitness and competitiveness (3). Mangotoxin biosynthesis by *P.s.s.* B728a has not been investigated; however, based on this study the genes predicted to be involved in this process (*Psyr_5009-Psyr_5012*) are being expressed in limited iron conditions. Gene expression for this cluster was also seen in the microarray study discussed in Chapter III, thereby implying that a mangotoxin-like protein product is being produced by *P.s.s.* B728a. This study supports that the biosynthesis of this mangotoxin-like product is positively regulated by the sigma factor AcsS. Further studies could elucidate if this product contributes to the survival of *P.s.s.* B728a on the leaf surface by providing a competitive advantage, similarly to the mangotoxin produced by *P.s.s.* UMAF0158.

Synthesis of the exopolysaccharide Psl is positively regulated by AcsS.

Although the roles of the *P.s.s.* B728a exopolysaccharides (EPS), alginate and levan, have been extensively studied, recently a putative novel EPS has been identified in this strain, called Psl (99). This EPS was first identified in *P. aeruginosa* PAO1 as a galactose and mannose rich EPS that serves as an essential component of biofilm formation, which is an important component of pathogenicity for this organism (29, 48, 75). It is also known that in *P. aeruginosa* PAO1 environmental iron serves as a signal for biofilm formation and iron uptake is required for such formation to occur (5).

Unfortunately, the role of Psl within the life cycle of *P.s.s.* B728a has not been determined. However, in this study six out of 11 of the genes in the predicted *psl* operons (*Psyr_3301* to *Psyr_3311*) were expressed at approximately 2-fold higher levels in the wild type than in the *acsS* deletion strain (Table 4). Moreover, the Psl biosynthesis clusters are located in three operons and genes from each of these operons are differentially expressed in the RNA-seq analysis. Similarly to what is seen in *P. aeruginosa* PAO1, siderophores and other iron acquisition methods may play an important role in *P.s.s.* B728a's ability to synthesize EPS and biofilms. Therefore, the

TABLE 4. RNA-seq analysis of the Psl exopolysaccharide gene cluster.

Gene	Locus Tag	Op.	Functional Category	Gene Product	Fold Change[a]	P-value
pslA	*Psyr_3301*	639	Cell wall/ Membrane biogenesis	orthologs to Psl polysaccharide genes, Undecaprenyl-phosphate galactosephosphotransferase		
pslB	*Psyr_3302*	639	Cell wall/ Membrane biogenesis	Mannose-1-phosphate guanylyltransferase/mannose-6-phosphate isomerase	2.0125	4.09E-05
pslD	*Psyr_3303*	640	Cell wall/ Membrane biogenesis	Polysaccharide export protein	1.9102	0.0005779
pslE	*Psyr_3304*	640	Cell wall/ membrane biogenesis	Lipopolysaccharide biosynthesis	1.7539	0.0004174
pslF	*Psyr_3305*	640	Cell wall/ Membrane biogenesis	Glycosyl transferase, group 1	2.1287	1.16E-06
pslG	*Psyr_3306*	640	Carbohydrate metabolism	glycoside hydrolase family protein		
pslH-1	*Psyr_3307*	640		Glycosyl transferase, group 1		
pslI	*Psyr_3308*	641	Cell wall/ Membrane biogenesis	Glycosyl transferase, group 1	1.9131	7.44E-05
pslj	*Psyr_3309*	641		hypothetical protein	1.9076	0.0007773
	Psyr_3310	641		hexapaptide repeat-containing transferase		
pslK	*Psyr_3311*	641		Virulence factor MVIN-like		

[a] Fold change is reflected as *P.s.s.* B728a in comparison to the *ΔacsS* deletion mutant; therefore, a positive fold change reflects a decreased level of gene expression in *P.s.s.* B728a *ΔacsS*

biosynthesis of these EPS systems, such as Psl, may be regulated in conjunction with iron acquisition systems. It is not known if Psl is regulated directly by the AcsS sigma factor or if this differential expression is merely a secondary effect of the bacteria's

decreased efficiency in iron acquisition. Biofilm formation is a complicated process and involves numerous cellular functions, with iron sensing and acquisition being only a small piece of this process. However, numerous functions known to be involved in biofilm formation were impacted by the AcsS muatation. Another aspect of biofilm formation identified in this study as being impacted by the deletion of the AcsS sigma factor is cellular motility.

Cell motility genes are regulated by AcsS. *P. aeruginoasa* PAO1 cells that are exposed to extreme iron limitation by the addition of lactoferrin, an iron chelator, are incapable of forming mature biofilms (5). Instead these bacteria convert from a planktonic to a sessile state and display persistent twitching motility; however, complex biofilm structure and EPS production does not occur (5). In *P. aeruginosa* PA14 flagellar-mediated motility, as well as, twitching motility via Type IV pili are both necessary for mature biofilm formation (90). Mutants deficient in Type IV pili were only capable of forming a thin layer of cells on the attachment surface and could not form mature biofilm structures (90). In this study two genes predicted to be associated with Type IV pilus formation were identified that were expressed at higher levels in wild type *P.s.s.* B728a than in the *acsS* mutant, *Psyr_0799* and *Psyr_1661*. Non-motile strains of *P. aeruginosa* PA14 with mutations in the flagellar hook-associated gene, *flgK*, were not capable of making surface attachment and were thus incapable of forming biofilms (90). The RNA-seq analysis in this study revealed 19 flagella genes with lower gene expression in the *acsS* mutant than in the wild type strain (Fig. 7). The proteins encoded by these flagellar genes consist of major conserved structural elements of the

flagella including: the filament (*fliC/Psyr_3466*), the hook-filament junction (*flgK*/*Psyr_3471*, *flgL*/*Psyr_3470*), the hook (*flgE*/ *Psyr*_3478), the rod (*flgC*/*Psyr_3480*, *flgG*/*Psyr_3475*, *flgF*/*Psyr_3476*), the MS ring (*fliF*/*Psyr_3457*), the C ring (*fliG*/ *Psyr_3456*), and the hook-capping protein (*flgD*/*Psyr_3479*) (69). Noticeably the *fleS/fleR* genes encoding a two-component regulatory system involved in flagellar regulation are also differentially expressed with approximately 2-fold lower expression in the *acsS* mutant than in the wild type (Fig. 7) (23). In *P. aeruginosa* PAK and *P. aeruginosa* PAO1 the regulatory hierarchy of flagella genes has been extensively studied and the flagella genes *flgBCDE*, *flgFGHIJKL* and *fliK* are all regulated by the FleS/FleR two-component system (23). Thus, at least 10 of the flagella genes showing differential gene expression in this study are probably being directly regulated by FleR/FleS, which is also being regulated by AcsS. Further studies are necessary to demonstrate the phenotypic effect that a 1.5 to 2 fold decrease in flagella gene expression has on *P.s.s.* B728a. However, this finding emphasizes the advantage of RNA-seq analyses in identifying gene expression changes that although not astronomical in numerical value can substantially contribute to our biological understanding of the organism.

AcsS may contribute to epiphytic survival and competitiveness. This study has shown based on RNA-seq analysis that the sigma factor AcsS is involved in the regulation of the siderophores achromobactin and pyoverdine, several iron transporter systems, TonB-siderophore receptors, an RND-efflux system, mangotoxin-like biosynthesis, Psl biosynthesis, Type IV pili, and cell motility. When considered in totality I hypothesize that AcsS plays an important role in the epiphytic stage of the

A

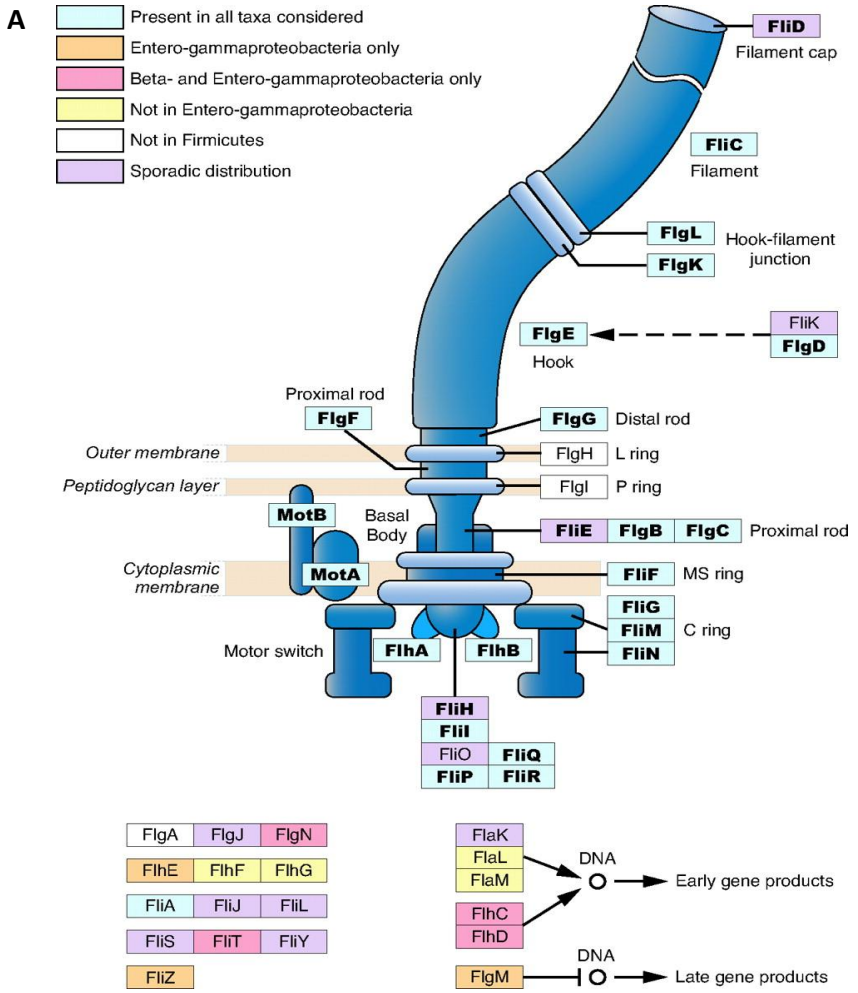

B

Gene	Locus Tag	Operon	Fold Change	P-value
fleN	*Psyr_3438*	661	1.9377	2.95E-06
fliO	*Psyr_3445*	663	1.6107	0.0008848
fliK	*Psyr_3449*		1.5039	6.16E-05
fliG	*Psyr_3456*	664	1.5511	0.0005783
fliF	*Psyr_3457*	664	1.7168	0.0007626
fleR	*Psyr_3459*	665	2.3948	9.08E-05
fleS	*Psyr_3460*	665	2.0208	0.0001672
fliS	*Psyr_3463*	666	1.3776	0.0005087
fliD	*Psyr_3464*	667	1.3248	4.50E-18
fliC	*Psyr_3466*		1.507	1.00E-82
flgL	*Psyr_3470*	668	1.4728	0.0001811
flgK	*Psyr_3471*	668	1.5146	4.12E-05
flgJ	*Psyr_3472*	668	1.6801	4.00E-06
flgH	*Psyr_3474*	668	1.5438	7.86E-05
flgG	*Psyr_3475*	668	1.6098	1.12E-11
flgF	*Psyr_3476*	668	1.4724	4.96E-05
flgE	*Psyr_3478*	669	1.4926	7.76E-10
flgD	*Psyr_3479*	669	1.5067	1.63E-14
flgC	*Psyr_3480*	669	1.4372	3.05E-09

FIG. 7. RNA-seq analysis of flagellar genes. A. Flagellar protein distribution. Reprinted from "Stepwise formation of the bacterial flagellar system" by R. Liu and H. Ochman, 2007. *PNAS.* 104, 7116-7121, with permission from the KEGG pathway database (www.genome.jp/kegg/pathway/eco/eco02040.html).
B. Differential gene expression data based on RNA-seq analysis in this study. The fold change is based on a comparison of *P.s.s.* B728a to *P.s.s.* B728a *ΔacsS*; therefore, the fold change values reflect that expression is higher in the wild type than in the *acsS* mutant.

P.s.s. B728a lifecycle. Interest in this hypothesis is further peaked by the decreased expression of the ice nucleation gene (*Psyr_1608*) in the AcsS mutant strain. Although further studies are certainly required, the completion of a transcriptome analysis of the *P.s.s.* B728a *ΔacsS* strain has provided a vast amount of gene expression data that leads to more detailed and directed future hypotheses and research pursuits.

Purification of achromobactin and mass spectrometry

Although the RNA-seq analysis confirms that AcsS regulates the achromobactin gene cluster, further analysis was necessary to confirm the absence of a molecular product. Therefore, by utilizing the procedure outlined by Berti and Thomas with slight modifications purified achromobactin samples were obtained (8). Purified products were analyzed by Dr. Benjamin Philmus, with the support of Dr. Tadhg Begley at Texas A&M University. Siderophore analysis was accomplished by liquid chromatography-electro spray ionization-time of flight- mass spectrometry (LC-ESI TOF MS). Based upon the ESI-MS study performed by Berti and Thomas, the mass ions of achromobactin are $[M-H]^{-1}$ 590.14, $[M-2H]^{-2}$ 294.57. Initially extraction procedures were performed using media conditions identical to those used for the RNA-seq analysis, HMM with limited iron. In this condition using the pyoverdine deficient mutant *P.s.s.* B728a ADB1005 (PVD^-) I was able to replicate the ESI-MS results seen by Berti and Thomas; however, no product was detected for the *P.s.s.* B728a strain (8). Since the mutant strains were developed in a wild type *P.s.s.* B728a background, in order to compare siderophore products it was necessary to identify culturing conditions in which the wild

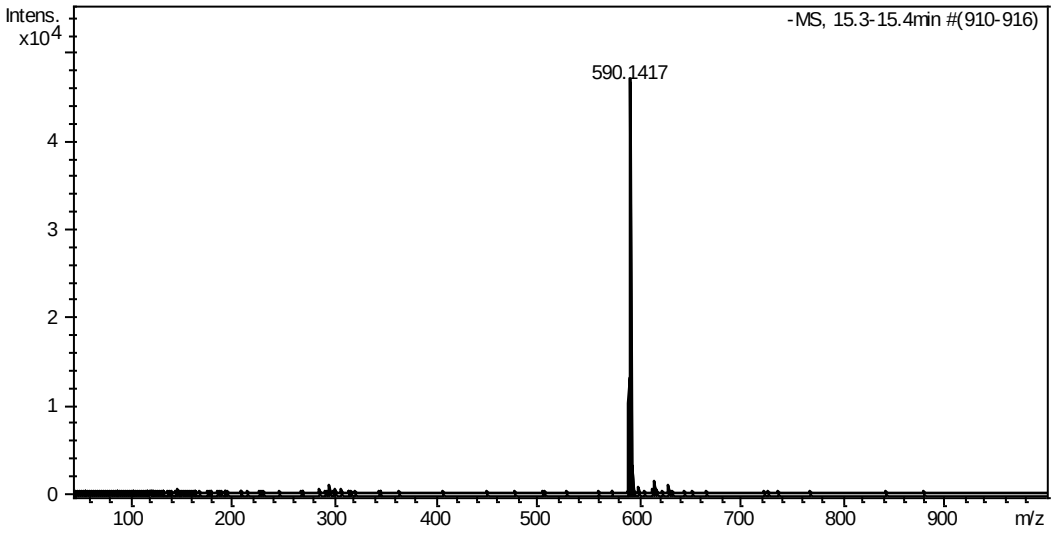

FIG. 8. LC-ESI TOF MS analysis of *P.s.s.*B728a purified from 1L of limited iron HMM + 1.7 mM citrate for four days and purified in a silica resin column. The mass seen here $[M-H]^{-1}$ 590.14, is equivalent to that seen in a study by Berti and Thomas, 2009 (8) with a pyoverdine deficient mutant, *P.s.s.* B728a ADB1005. *P.s.s.* B728a ADB1005 was used as a positive control in this study and displayed an identical mass peak to the P.s.s. B728a strain

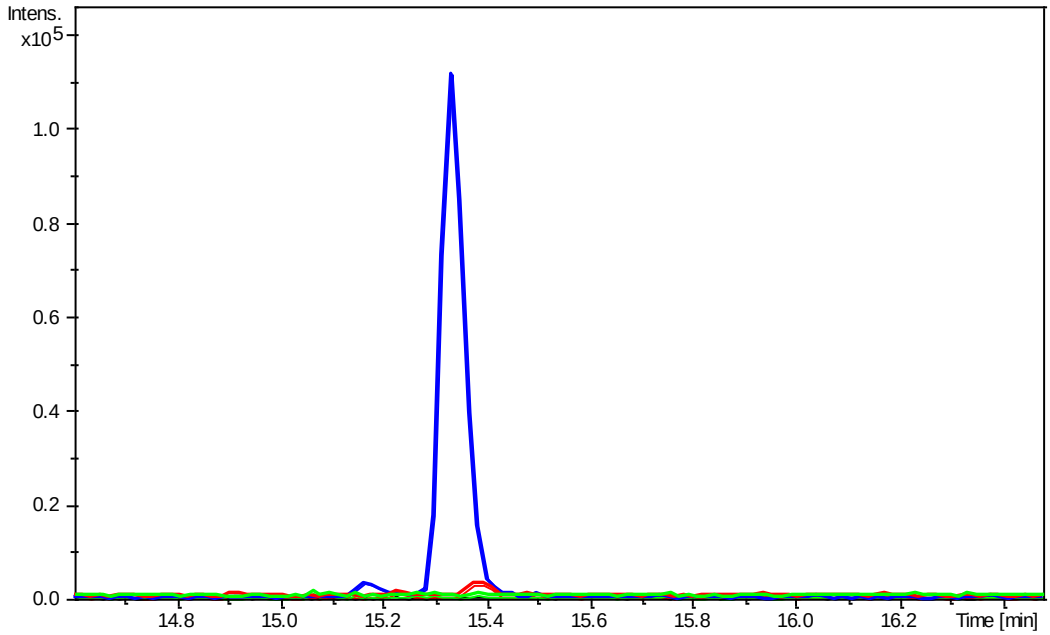

FIG 9. LC-ESI TOF MS analysis of *P.s.s.* B728a from various media conditions. Samples were purified from culture supernatant of the following media conditions: HMM + 1.7 mM sodium citrate (blue line), HMM + 1.7mM sodium citrate + 1 uM iron (red line); HMM + 1.7 mM sodium citrate + 5 uM iron (green line), HMM + 1.7 mM sodium citrate + 10 uM iron (black line).

type *P.s.s.* B728a produced the achromobactin siderophore at a detectable level. Therefore, the limited iron HMM media was modified by adding 1.7 mM sodium citrate, as seen in the media used by Berti and Thomas (8). Several other conditions were also tested including the addition of both citrate and iron; iron levels of 1 μM, 5 μM, and 10 μM were added to the HMM plus 1.7 mM citrate media. This was performed to test whether the low iron conditions were too extreme and was limiting the production of the achromobactin siderophore. The addition of citrate was sufficient for the detection of achromobactin by LC-ESI TOF MS in the wild type *P.s.s.* B728a strain (Fig. 8). The addition of both citrate and iron, even at the lowest level of 1 μM iron, achromobactin production was severely decreased (Fig. 9). Thus, the limited iron HMM media with 1.7 mM sodium citrate media was utilized for the remainder of the purification studies.

The supernatant from one liter cultures of *P.s.s.* B728a, *P.s.s.* B728a *ΔacsS*, *P.s.s.* B728a *ΔacsS* pPROBE-KT':*acsS*, and *P.s.s.* B728a ADB1005 were extracted through silica resin to purify achromobactin. LC-ESI TOF MS analysis revealed that *P.s.s.* B728a *ΔacsS* produces approximately half as much achromobactin as the wild type *P.s.s.* B728a (Fig. 10). Additionally, complementation of the *acsS* deletion mutant was able to restore wild type production levels of achromobactin (Fig. 10). This data confirms that AcsS regulates the biosynthesis and secretion of achromobactin; however, since achromobactin levels were only severely reduced but not eliminated, it implies that there may be other regulators of the citrate siderophore.

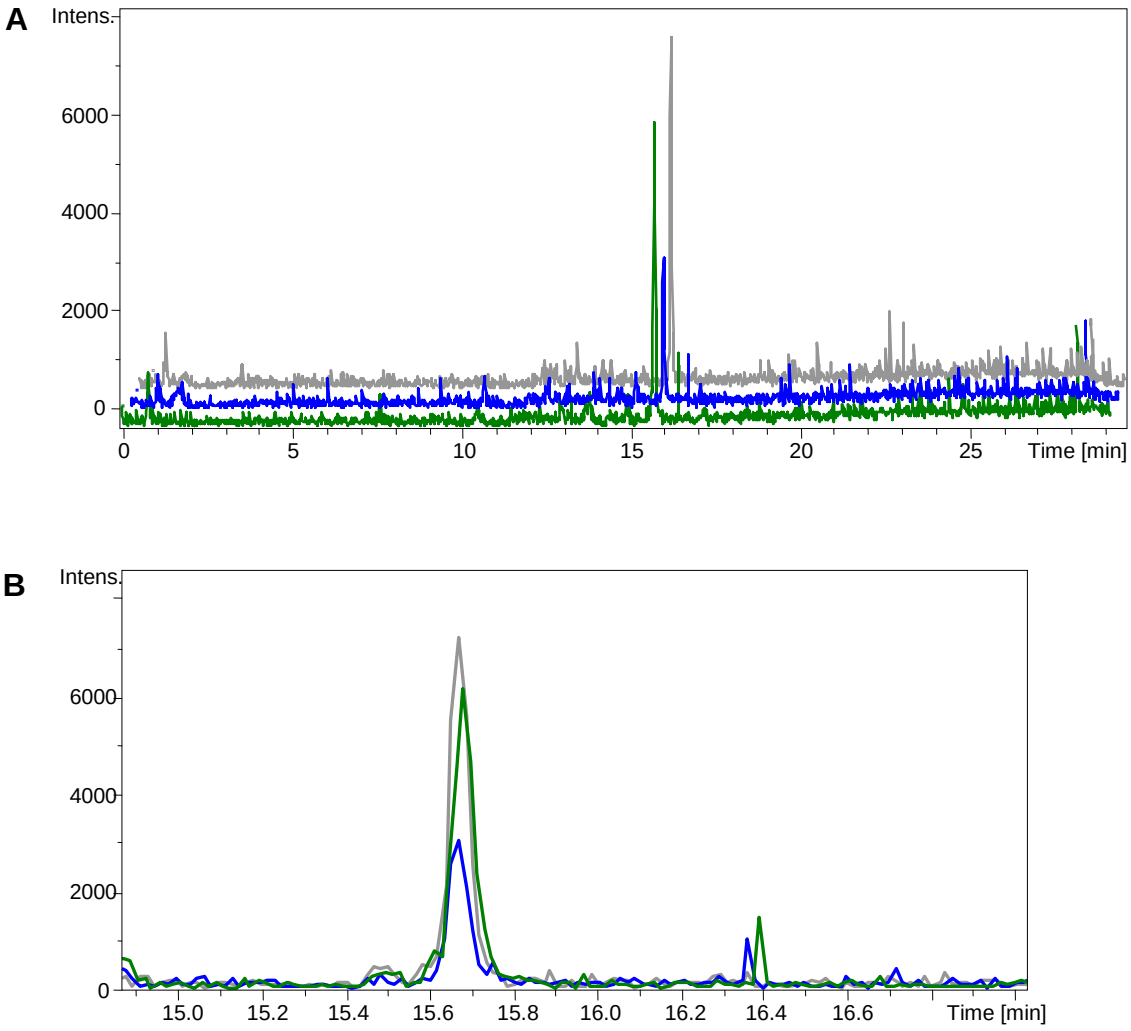

FIG 10. LC-ESI TOF MS analysis of achromobactin from the AcsS mutant. **A.** Samples were purified from culture supernatant of the following strains grown in HMM + 1.7 mM sodium citrate for four days: *P.s.s.* B728a (green line), *P.s.s.* B728a *ΔacsS* (blue line), and *P.s.s.* B728a *ΔacsS* pPROBE-KT':*acsS* (grey line). **B.** A zoomed in view of the LC-ESI TOF MS peaks seen in A.

Conclusions

This study illustrates the power and utility of transcriptome analysis by fulfilling the initial objective of this study and providing valuable data for the pursuit of more in-depth analysis of the overall regulation of iron by *P.s.s.* B728a. Herein it has been established that the regulation of the siderophores achromobactin and pyoverdine are not compensatory, but are intricately intertwined. A transcriptome analysis of a deletion mutant of the pyoverdine sigma factor, PvdS, could further elucidate the interactions between these two regulons. Likewise, this study implies that achromobactin and the AcsS sigma factor are important for pathogen survival and function on the leaf surface. Many of the differentially expressed genes between the AcsS deletion mutant and the wild type strain in this study were involved in functions that are important during the epiphytic stage of *P.s.s.* B728a including genes involved in iron response, secretion, extracellular polysaccharide production, and cell motility. This leads to questions regarding the role of the siderophore pyoverdine in the *P.s.s.* B728a. One is left wondering about the role of pyoverdine in plant disease, and whether these two siderophores are both important for epiphytic survival. Furthermore, one wonders whether either or both of these siderophores play a role in planta during infection. Thus, this study has answered a fundamental question about the regulation of iron acquisition in *P.s.s.* B728a and has provided an abundance of initiation points for new hypotheses and research.

CHAPTER III

TRANSCRIPTOME ANALYSIS OF GLOBAL REGULATORS GacS AND SalA

Overview

A microarray analysis of *Pseudomonas syringae* pv. *syringae* B728a and nine deletion mutant strains grown in seven treatment conditions was performed as part of a collaboration between Dr. Gwyn Beattie (Iowa State University, Dr. Steven Lindow (University of California, Berkley), Dr. Dennis Gross (Texas A&M University), and Dr. Dan Nettleton (Iowa State University). This dissertation addresses the regulatory networks of the sensor kinase, GacS, and the transcription factor, SalA, that were included as deletion mutant strains in this microarray analysis.

Analysis of these microarray anlyses reveals that GacS is a global regulator of *P.s.s.* B728a with 3,314 genes and small RNAs displaying differential gene expression at a q-value of less than 0.05 between the GacS deletion mutant and the wild type *P.s.s.* B728a strain. The SalA regulon is also exceptionally large with over 1,500 genes differentially expressed between the mutant and wild type strains. The regulons of GacS and SalA include major virulence factors, as well as, gene clusters that are important for epiphytic survival and function. In elucidating the regulon of GacS/SalA the potential of a larger multisensory complex emerges that may serve as the *P.s.s.* B728a master switch between epiphytic and pathogenic lifestyles.

Introduction and Literature Review

Signal transduction via two-component systems

In bacterial systems, signal transduction pathways monitor the external cellular environment and appropriately modify cellular functions in response to extracellular changes and conditions (62). One common method of signal transduction utilized by bacteria is the two-component system, in which a transmembrane sensor histidine kinase (HK) in conjunction with a cytoplasmic response regulator (RR) transmits a signal in response to extracellular conditions. The signaling domains of HKs and RRs are highly conserved and are essential to the initiation of cellular adaptation to environmental change. Structurally HKs tend to be homodimers containing an N-terminal sensory domain which is specific to its targeted environmental stimuli and a conserved C-terminal transmitter domain which is located in the cytoplasm and communicates with the RR (62). The RR also consists of multiple domains, including a highly conserved receiver domain and at least one output domain specific for the downstream gene regulatory products. The evolutionarily conserved receiver domain is essential to the appropriate phosphotransfer reaction between conserved histidine residues of the HK transmitter domain and the aspartate residues in RR receiver domain (62). The phosphorylation of the RR receiver domain leads to cellular regulation of downstream gene targets in response to the detected extracellular stimulus. For this reason, it is not surprising that many RR are also transcription factors and use DNA-binding domains to directly regulate gene expression. Two-component systems play a major role in the regulation of bacterial genomes in response to extracellular stimuli and are frequently

associated with both global gene regulation and, in pathogens, more localized regulation of factors associated with virulence and disease (62).

Intense genomic mining of several *Pseudomonas syringae* species using a Hidden Markov Model revealed that the *P.s.s.* B728a genome encodes 68 predicted HK proteins and 93 RRs (62). Amongst these there appears to be a number of two component systems and elements which are highly conserved between *P.s.s.* B728a, *P.s.t.* DC3000, and *P.s.p.* 1448a including: 30 two-component clusters and 44 orphan HKs and RRs, which appear in isolated positions on the genome independent of their reciprocal element, and 16 hybrid HKs, that can transmit a phosphorelay message independently of a RR (62). The high level of conservation of these two-component systems is not surprising given the important role they play in the regulation of cellular activity, both in individual cascades responding to isolated stimuli and the overall global regulatory network (62).

GacS/GacA

The two-component system GacS/GacA is present in a variety of gram-negative bacteria, but has been studied most extensively in enteric bacteria and amongst the fluorescent pseudomonads (41). Although first identified in *P.s.s.* B728a as LemA, due to its involvement in lesion manifestation, the two component system is identified in the literature by the following identifiers: GacS/GacA (*Pseudomonas*, *Erwinia*, *Vibrio fisherii*), VarS/VarA (*Vibrio cholerae*), BarA/UvrY (*Escherichia coli*), BarA/SirA (*Salmonella*), and LetS/LetA (*Legionaella*) (13). Extensive research on this two-

component system continues due to the global effects that these regulators have on their respective organisms. For instance in pseudomonads mutations in the *gacS/gacA* genes result in drastic phenotypic effects including dramatically reduced virulence in pathogenic organisms and decreased biocontrol activity in plant-beneficial pseudomonads (41). In *P.s.s.* B728a strains containing mutation in either *gacS* or *gacA* are unable to cause necrotic lesions on infected plant hosts (58).

Following the discovery of the major virulence effect of the *gacS/gacA* mutation in *P.s.s.* B728a, determining the downstream cellular products and systems impacted by this two-component system became a major research focus. Interestingly, researchers found that regardless of the lifestyle of their organism of interest, whether commensal or pathogenic, the GacS/GacA two-component system is involved in the synthesis of secondary metabolites, polysaccharides, and other extracellular products (41). In *P.s.s.* B728a the GacS/GacA system positively controls the synthesis of the phytotoxins syringomycin and syringopeptin, as well as, the cyclic peptide syringolin and the polysaccharide alginate (41, 125). Similar regulation of secondary metabolites by homologs to the GacA/GacS system is seen in other fluorescent pseudomonad and enteric bacterial species such as: tolaasin, exoprotease (*Pseudomonas tolaassii* PT814); pyocyanin , cyanide, lipase (*Pseudomonas aeruginosa* PAO1); phenazine antibiotics, chitinase, protease (*Pseudomonas chlororaphis* PCL1391); pyrrolnitrin, pyoluteorin, 2,4-diacetylphloroglucinol, cyanide, exoprotease (*Pseudomonas fluorescens* Pf-5; and cholera toxin (*Vibrio cholerae*) (41).

From a pathogenicity perspective, the phenotype associated with the GacA/GacS mutations in *P.s.s.* B728a is intriguing. Although these mutant strains do not cause necrotic lesions on the plant, the bacteria are still capable of growing as epiphytes and colonizing the apoplastic spaces (46). These mutant strains are also capable of causing a hypersensitive response on non-host species, the plant's utilization of programmed cell death as a defense mechanism through rapid cell collapse and tissue death at the site of inoculation (1). The continued capability of causing a hypersensitive response on non-host plants indicates that the bacterial Type III secretion system is operating at a basic level in these mutants and remains capable of synthesizing a Type III pillus and transporting effector molecules into host cells. Therefore, the reduced virulence of GacA/GacS strains with their absence of necrotic lesions can be largely attributed to the loss of potent phytotoxins, syringomycin and syringopeptin. These observations have been confirmed through toxicity assays using bacterial and fungal cultures which are sensitive to these phytoxins (6, 58). The significant role which syringomycin and syringopeptin play in plant disease contributed a desire to further research this branch of the GacA/GacS regulatory pathway and to identify other regulators downstream of the two-component system.

Syringomycin and syringopeptin

The genes necessary for the biosynthesis, transport, and regulation of syringomycin and syringopeptin are encoded on the *P.s.s.* B301D genome within two adjacent gene clusters (*syr/syp*) approximately 55 kb and 80 kb in length, respectively

(105). This *syr/syp* region is also present in *P.s.s.* B728a. These large genomic regions encode the nonribosomal peptide synthetases necessary for the incorporation of the amino acids into a peptide chain. The syringomycin cluster assembles the peptide via a thiotemplate mechanism encoded by the genes, *syrB1, syrB2, syrC* and *syrE* (6, 105). Until recently, the last gene in this cluster, *syrP,* was thought to have a regulatory function. However, recent biochemical analysis of this gene has revealed that *syrP* encodes a non-heme mononuclear iron hydroxylase that lends the l-threo-3-OH-Asp diastereomer structure of mature syringomycin (106). Like syringomycin, syringopeptin's 22 amino acids are also incorporated via a thiotemplate mechanism by the synthetase genes, *sypA*, *sypB*, and *syp C* (104). Once nonribosomally synthesized the extracellular transport of both phytotoxins occurs through the ABC transporter protein encoded by *syrD* (6).

In addition to biosynthesis and transport genes, the *syr/syp* cluster also encodes several regulatory genes including *salA, syrF*, and *syrG,* which have high sequence similarity to the LuxR family of regulatory proteins (73, 104). The regulatory role of *syrG* appears to be complex and may involve virulence mechanisms outside of the *syr* cluster. However, it is known that *syrG* regulates syringomycin biosynthesis but has no role in syringopeptin production (73). The other two regulatory genes in the *syr/syp* cluster, *salA* and *syrF,* are necessary for the biosynthesis of both syringomycin and syringopeptin. This demonstrates that the regulatory networks of these two phytotoxins may overlap, but are not identical. The formation of homodimers of SyrF and SalA allows these proteins to bind to the promoter regions of their regulatory targets (118).

SyrF directly binds to the conserved *syr-syp* boxes of the promoter regions of its gene targets within the *syr/syp* cluster (120). Meanwhile SalA moderates the genes in the *syr/syp* cluster through its regulation of SyrF (120). SalA has a complex regulatory network and has been defined as a key regulatory factor due to its positive regulatory effect on syringomycin and syringopeptin biosynthesis genes, as well as, other virulence-associated genes including the syringolin biosynthesis gene, *sylD* (74).

While searching for downstream regulators of the *syr/syp* cluster, researchers have also expanded our knowledge of the elements upstream of the GacA/GacS system. Through this research scientists have found that the external signals detected by the transmembrane histidine protein kinase, GacS, include plant signal molecules such as arbutin and D-fructose (119). In response to these external signals, GacS phosphorylates its response regulator GacA, thereby activating downstream regulatory elements, including *salA* (119). Although there are several defined regulatory elements of the *syr/syp* cluster, the regulatory pathway is far from complete. It is unclear whether GacS directly senses the plant signal molecules or whether a secondary sensor molecule or two-component system is involved. There may be novel members of the defined *salA/syrF* regulatory pathway or an entirely separate regulation system that has yet to be discovered. Additionally the ECF sigma factor associated with the transcription of genes within and the *syr/syp* cluster has yet to be identified. However, significant advances in our knowledge of the GacA/GacS pathway have resulted from this two-component systems association with biologically important secondary metabolites such as syringomycin and syringopeptin.

Syringolin

P.s.s. B301D and *P.s.s.* B728a produce another cyclic lipopeptide called syringolin that is also regulated by the GacA/GacS two-component system (41, 125). Syringolin is synthesized via a mixed non-ribosomal peptide synthetase/polyketide synthetase encoded on two genes *sylC* and *sylD* (97). Three adjacent genes, *sylA*, *sylB*, and *sylE*, encode a LuxR-like regulatory gene, a desaturase-like protein, and an efflux transport respectively (97). Although several derivatives of this peptide may be synthesized, syringolin A is the most abundantly produced variant (97). When spray inoculated on bean plants mutant strains of *P.s.s.* B728a that were not able to synthesize syringolin had a significant reduction in the number of necrotic lesions that developed (35). Syringolin A is able to uniquely form an irreversible covalent bond with eukaryotic proteasomes; thereby inhibiting all three of the proteasomes catalytic activities (35). Although it is not clear whether this is the mechanism utilized by *P.s.s.* B728a in nature, the inhibition of plant proteosomes by syringolin A causes the opening of stomatal guard cells providing a potential route of entry for the pathogen into the apoplastic spaces (102). The continued expansion of our knowledge of the virulence mechanisms of *P.s.s.* B728a only elevates the importance of GacA/GacS as a global regulatory system.

Exopolysaccharide

In addition to its role in the regulation of secondary metabolites which have a role in virulence, the GacA/GacS two-component system may also be involved in the

ability of *P.s.s.* B728a to thrive as an epiphyte. Although the exopolysaccharide (EPS) alginate is produced by *P.s.s.* B728a during plant disease and is the dominant EPS produced in water-soaked lesions, alginate deficient mutants produced comparable quantities and sized lesions as the wild type strain when vacuum infiltrated into the leaves (125, 128). However, alginate deficient mutants were less effective than wild type strains in colonizing leaf surfaces, and when evaluated for population size and symptom development from a dip inoculation the alginate deficient mutant had smaller in planta populations and less severe disease symptoms (128). Thus increased knowledge regarding the regulation of alginate by the GacA/GacS two-component system could contribute to our understanding of the role of EPS in both epiphytic growth and plant disease.

Quorum sensing

The GacA/GacS two-component system is also directly involved in the cellular regulation of cell signaling via quorum sensing. Quorum sensing is a cellular signaling system utilized by bacteria to monitor and respond to population density (113). Bacteria utilize small molecules, such as acylated homoserine lactone (AHL) molecules in many gram negative bacteria, as a method of detecting the surrounding bacterial population. As the bacterial population increases so does the concentration of signal and, upon reaching and detecting a threshold level of signal (or "quorum"), the expression of quorum sensing gene targets is altered via a signal transduction cascade (124). Quorum sensing is utilized in the regulation of cell density dependent bacterial functions, such as

virulence factor synthesis, formation of biofilms, swarming motility, and bioluminescence (113). By using quorum sensing to mount a concentrated attack, bacterial systems increase their likelihood of successfully overcoming host-defense mechanisms or outcompeting other microorganisms in their ecological niche.

The gram negative AHL based quorum sensing systems have been well studied and rely upon *luxI*/*luxR* gene homologs for transcriptional activation and synthesis of signaling molecules (30). The quorum sensing system in *P.s.s.* B728a utilizes 3-oxo-hexanoyl-homoserine lactone (3-oxo-C6-HSL) as its predominant AHL, which is synthesized by the LuxI homolog, AHL synthase, AhlI (95). The LuxR homolog, AhlR stably binds to 3-oxo-C6-HSL and activates transcription of *ahlI* via a positive feedback mechanism (96). Thus, as the environmental concentrations of 3-oxo-C6-HSL continue to increase, increasing copies of *ahlI* are transcribed to synthesize additional 3-oxo-C6-HSL. GacA is a positive regulator of the AhlI-AhlR quorum sensing system and is required for transcription of *ahlI* (96). Interestingly, another quorum-sensing regulator AefR is also required for appropriate expression of *ahlI*; however, this regulator is not impacted by mutations in the GacA/GacS two-component system. GacA/GacS and AefR are believed to function via independent cellular pathways in their regulation of quorum-sensing (96).

In *P.s.s.* B728a the role of GacA/GacS in quorum sensing may also directly tie to the role of this two-component system in swarming motility, a flagellar driven movement of bacterial cells spreading on a surface as a biofilm. Mutations in either the *gacS* or *gacA* genes of *P.s.s.* B728a result in bacteria that are completely deficient in

their capability of swarming (57). Due to the importance of quorum sensing for swarming in *Serratia liquefaciens*, the AHL synthase, *ahlI,* of P.s.s. B728a was mutated and evaluated for its ability to swarm; however, no swarm phenotype was observed (57). Thus the swarm phenotype associated with mutations in the GacA/GacS two-component system, is not the result of the bacteria's inability to produce AHL via the AHL synthase *ahlI* (57). However, whether quorum sensing plays a role in swarming motility in *P.s.s.* B728a has not been fully elucidated.

As the global regulon of GacA/GacS continues to be researched, the basic inquiry to determine what genes are positively or negatively regulated by this two-component system becomes excessively more complex. The downstream impact of this two-component system is far-reaching, with effects on secondary metabolites, EPS, quorum sensing, and numerous other pathogenicity and fitness gene targets. As the known downstream targets continue to rise, the question is then raised: how do these down-stream gene targets interact with each other? And what role do these complicated regulatory networks play in *P.s.s.* B728a's abilities as both an epiphyte and a plant pathogen?

Experimental design for a transcriptome analysis

To begin investigating and answering these scientific queries, it is necessary first to expand our knowledge of the GacA/GacS downstream gene targets. This is one small part of a larger collaborative effort in which *P.s.s.* B728a gene expression was evaluated across seven experimental conditions using microarray analysis. This project was

funded by USDA-NIFA NRI/AFRI Microbial Biology Program and Microbial Functional Genomics Program and is entitled "Functional genomics of the epiphytic and pathogenic lifestyles of the bacterial plant pathogen *Pseudomonas syringae"* (NIFA Award Number: 2008-35600-18766). The project director is Dr. Gwyn Beattie (Iowa State University). Co- Project Directors are Dr. Steven Lindow (University of California, Berkley), Dr. Dennis Gross (Texas A&M University), and Dr. Dan Nettleton (Iowa State University). Graduate students and postdoctoral researchers who contributed to this project are (listed in alphabetical order): Jessica W. Greenwald (Texas A&M University), Steven P. Lund (Iowa State University), Dr. Angela Records (Texas A&M University); Russell A. Scott (University of California, Berkley), and Xilan Yu (Iowa State University).

For this study Dr. Gwyn Beattie and Dr. Dan Nettleton, in conjunction with Roche Nimblegen, designed a *P.s.s.* B728a specific microarray that encompasses 5,076 predicted open reading frames and 61 putative small RNAs. The commercial services of Roche Nimblegen were utilized to analyze the transcriptome of *P.s.s.* B728a via microarray in order to gain further knowledge of gene networks, especially those involved in growth, survival, and pathogenicity. Transcriptomes were evaluated in seven conditions designed for the expression of the regulons of interest, notably those known to be involved in pathogenicity and epiphytic survival. The base medium is a modified hrp-inducing minimal media (HMM-basal) which was first used for analyses of the Type III secretion system (47). The HMM described by Huynh et al. was modified to: have sufficient iron for phytotoxin production; high water availability; sufficient

nitrogen to support growth of mutant strains; support moderate growth rates; support growth to high cell density; and permit expression of relevant regulons including those involved in phytotoxin biosynthesis, quorum sensing, and Type III secretion. Treatment conditions were modifications of the HMM-basal condition, which serves as the baseline in this study. Treatment conditions included: osmotic stress, oxidative stress, limited iron, and limited nitrogen. Since *P.s.s.* B728a is both an efficient epiphyte and a plant pathogen, transcriptome analyses of bacteria from both epiphytic and apoplastic conditions were also performed.

This study involves the analysis of expression of not only the wild type *P.s.s.* B728a, but also, non-polar deletion strains of *P.s.s.* B728a regulatory genes including: quorum sensing regulators (AhlR and AefR), global regulators (GacS, RetS, and SalA), and sigma facors (RpoE, RpoS, RpoN, and HrpL). Here I will focus on the results obtained from the *P.s.s.* B728a, *P.s.s. ΔgacS*, and *P.s.s.* B728a *ΔsalA* microarray analyses.

Materials and Methods

Bacterial strains, plasmids, and growth conditions

The bacterial strains and plasmids used in this study are listed in Table A-1. For general cloning *Escherichia coli* DH10B was cultured in Luria-Bertani (LB) liquid or agar medium at 37°C (100, 101). For topoisomerase reactions One Shot® TOP10 *Escherichia coli* cells were used in accordance with the manufacturer's protocol (Invitrogen, Carlsbad, CA). *P.s.s.* B728a strains were grown at 26°C with shaking at 200 rotations per minute (rpm). King's B (56) and LB served as media for general growth of *P.s.s.* B728a. Growth medium for treatment conditions was evaluated to determine the conditions most conducive to gene expression of the applicable gene regulons of interest. Conditions were also evaluated to ensure that comparison across conditions mimicking environmental stress stimuli would be appropriate. The basal medium selected is a modified hrp-inducing minimal media (HMM-basal) containing 10% 10×HrpMM Salts [0.2 M KH_2PO_4 (Fisher Scientific, P285-3), 1.2 M K_2HPO_4 (Fisher Scientific, BP363-1), 1.3 M $(NH_4)_2SO_4$ (SigmaUltra, A2939), 5.9 M $MgCl_2$ (Fisher Scientific, M33), 5.8 M NaCl (Fisher Scientific, S271-3) (pH 5.7)], 0.2% fructose (Sigma, F-0127), 0.2% mannitol (Sigma, M-4125), 0.2% sodium succinate (Sigma, S5047), 10 µM N-(B-ketocaproyl)-L-homoserine lactone (AHL)(Sigma, K3007), 10 mM L-glutamine (Sigma, F2877), and 10 µM $FeCl_3$ (Sigma, F2877) (47).

General DNA manipulations

Restriction enzymes, Calf Intestinal Phosphatase (CIP), and T4 DNA ligase were purchased from New England Biolabs (Beverly, Mass.) and used according to the manufacturers' protocols. Thermo Scientific Phusion High-Fidelity DNA polymerase was purchased from Fisher Scientific. Cloning strategies involved the amplification of target genes via PCR and utilization of Gateway technology to insert the PCR product into the pENTR/D-TOPO vector were done in accordance with manufacturers' protocols (Invitrogen) (61). Recombination between pENTR constructs and Gateway destination vectors were performed in accordance with the manufacturers' instructions provided for LR clonase (Invitrogen). Plasmids were incorporated into *E.coli* via chemical transformation or electroporation (101). Tri-parental mating with the helper plasmid pRK2073 was utilized for the incorporation of plasmids in *P.s.s.* B728a for recombination events (63). Primer sequences are listed in Table A-2 and standard PCR cycling conditions were used.

Construction of markerless deletion mutations in* P.s.s. *B728a

Targeted deletion mutants in *P.s.s.* B728a were made utilizing a modified version of the phage lambda Red recombinase system developed by Datsenko and Wanner (24, 99). With this strategy, the gene of interest (GOI) along with 3 to 4 kb of flanking DNA on each side was PCR amplified using Phusion® high fidelity, long-range proofreading polymerase (ThermoScientific F-553S) (flank-GOI-flank). The primers for the PCR reaction creation of a *salA* mutation, PrrsalAF and PrrsalAR, were designed to add a

TOPO cloning tag onto the 5' end of the PCR product (Table A-2). The purified PCR product was then transferred into the Gateway entry vector pENTR/D-TOPO (Invitrogen pENTR/D-TOPO cloning kit catalog #45-0218) and transformed into chemically competent *E. coli* Mach 1 cells (pENTR: flank-GOI-flank). The gene of interest with its flanking regions were recombined into the *Pseudomonas* suicide vector, pLVC-D, using a Gateway reaction (Invitrogen LR Clonase II catalog #11791-020). Site specific recombination proteins from the bacteriophage lambda are utilized to recombine the gene of interest and flanking region from the pENTR vector into the pLVC-D destination vector (pLVC-D: flank-GOI-flank).

The pLVC-D: flank-GOI-flank destination vector was then transformed into the recombineering (recombination-mediated genetic engineering) strain *E. coli* SW105 (http://recombineering.ncifcrf.gov/). The genome of this strain contains a defective lambda prophage containing the Red recombinase genes. These genes are regulated by a temperature sensitive repressor, *cI857*, which is active at 32°C thereby preventing any recombination proteins from being produced. A 15 minute heat-shock at 42°C inactivates the *cI857* repressor and allows transcription of the Red recombinase proteins. The Red recombinase proteins allow the insertion of linear DNA directly into the target DNA molecule, pLVC-D: flank-GOI-flank. The linear DNA is a PCR product containing 36 bp of DNA flanking each side of the gene of interest and a kanamycin (Km) resistance cassette amplified from the vector pKD13 using primers PrrsalAKmF and PrrsalAKmR (Table A-2). The pKD13 vector was used to amplify the FRT (FLP recognition target) sites that can be utilized to remove the Km cassette. The linear DNA

is recombined into the destination plasmid by electroporation of heat-shocked *E.coli* SW105: pLVC-D: flank-GOI-flank with the linear DNA product. The resulting *E.coli* SW105: pLVC-D: flank-Km-flank is utilized for triparental mating to introduce the Km cassette in place of the gene of interest. The Km cassette was later removed using FLP recombinase. Colony PCR and Southern blot analysis were utilized to confirm all double recombination mating events.

Clean deletion mutant strains *P.s.s.* B728a *ΔgacS* and *P.s.s.* B728a *ΔretS* were constructed by Dr. Angela Records and are described in Records and Gross, 2010 (99).

Growth medium treatments

Bacterial strains were taken from glycerol stocks and streaked for isolation on KB plates containing 100 mg/mL rifampicin and incubated at 26°C for 48 hours. Isolated colonies were utilized to inoculate 5 mL cultures of HMM-basal in glass test tubes (17×150mm) and grown overnight at 26°C, shaking at 200 rpm until a dense cell growth is present. 10 µL of these overnight cultures were used to inoculate 5mL cultures of HMM-basal in glass test tubes (17×150mm) and grown overnight at 26°C, shaking at 200 rpm. 125 mL Erlenmeyer flasks containing 30 mL HMM-basal were inoculated with 300 µL of the overnight cultures and grown at 26°C, shaking at 200 rpm until late-logarithmic phase (OD_{600} of 0.6, 5×10^8 CFU/mL). 10 mL of the late-logarithmic phase cultures were transferred to centrifuge tubes and the cells pelleted at 5000×g for 10 min. Cell pellets were washed twice in HMM-basal medium lacking L-glutamine, $(NH_4)SO_4$, $FeCl_3$, and AHL [10% 10×HrpMM Salts lacking nitrogen [0.2 M

KH_2PO_4 (Fisher Scientific, P285-3), 1.2 M K_2HPO_4 (Fisher Scientific, BP363-1), 5.9 M $MgCl_2$ (Fisher Scientific, M33), 5.8 M NaCl (Fisher Scientific, S271-3) (pH 5.7)], 0.2% fructose (Sigma, F-0127), 0.2% mannitol (Sigma, M-4125), 0.2% sodium succinate (Sigma, S5047)](HMM-Fe&N). Washed cells were resuspended in 2 mL of (HMM-Fe&N) medium pre-warmed to 26°C, giving a final concentration of approximately 2.5×10^9 CFU/mL.

Treatment conditions were established as follows in glass test tubes (17×150mm): Treatment A is 1 mL HMM-basal medium; Treatment B is 1 mL HMM-basal medium with 253 mM NaCl; Treatment C is 1 mL HMM-basal medium with 0.55 mM H_2O_2; Treatment D is 1 mL HMM-basal lacking the 10 μM $FeCl_3$ with 110 μM N,N'-Di(2-hyrdroxybenzyl)-ethylenediamine-N,N'-diacetic acid monohydrochloride hydrate (HBED) (Strem Chemicals, 07-0422); Treatment E is 1 mL HMM-Fe&N with 10 μM $FeCl_3$ (Sigma, F2877) added. Each treatment was inoculated with 0.1 mL (approximately 2.5×10^8 CFU/mL) of the overnight cells that were washed and resuspended in HMM-Fe&N. Treatments A, B, and C were incubated at 26°C, shaking at 200 rpm for 15 min. Treatments D and E were incubated at 26°C, shaking at 200 rpm for 2 hours. After incubation the cultures were fixed using RNA protect™ Bacterial Reagent (Qiagen), in a ratio of 2 mL of reagent per 1 mL of bacterial culture. Duplicate treatment tubes were combined and centrifugation was used to pellet the cells (5000×g, 10 min, room temperature), the supernatant was discarded. Pellets were flash frozen in liquid nitrogen and stored for up to 2 weeks at -20°C prior to RNA extraction.

In planta treatments

Inoculum for in planta treatments was grown in 250 mL Erlenmeyer flasks containing 50 mL HMM-basal medium inoculated with 1 mL of an overnight culture grown in HMM-basal. Inoculum was grown at 26°C, shaking at 200 rpm, to an OD_{600} of 0.6 (5×10^8 CFU/mL). Cultures were pelleted at 5000 rpm for 10 min at room temperature. Cell pellets were washed in sterile distilled water. After washing cell pellets were resuspended to an OD_{600} of 0.3, which is equivalent to 5×10^8 colony forming units (CFU) per mL. Bacterial suspensions of 5×10^6 CFU/mL were made in sterile distilled water with 1% Silwet L-77 (Vac-In- Stuff) surfactant (Lehle Seeds, Round Rock, TX). Vacuum infiltration of two week old Blue Lake 274 (Burpee Seeds, Warminster, PA) bean plants (*Phaseolis vulgaris* L.) was performed by suspending the plants in the inoculums and establishing a vacuum. The vacuum was held at 20 in. Hg. for 3 min and slowly released. Plants were rinsed with distilled water and allowed to air dry. The plants were maintained at room temperature on the laboratory bench for 48 hours. After 48 hours the leaves were harvested individually and bacteria were extracted.

Bacterial extraction from in planta treatments

Endophytic bacteria were extracted using an acidic ethanol/phenol solution composed of 9 mL buffer-saturated phenol (pH 6.6), 171 mL absolute ethanol (200 proof), 420 mL sterile distilled water (total 600 mL). Leaves were individually removed from the plants, and hastily cut into thin ribbon-like strips using paper shredding

scissors. The plant tissue strips were immediately submerged in the ethanol/phenol solution. Approximately 100 leaves were shredded into each batch of 600 mL ethanol/phenol. The ethanol/phenol/leaf tissue slurry was sonicated for 10 min then leaf tissue was removed by draining the slurry through sterile cheese cloth. The filtered ethanol/phenol was centrifuged to remove bacterial cells at 5500×g for 10 min. The supernatant was removed and set aside for disposal. The cell and plant debris pellet was resuspended in approximately 5 mL of the supernatant and filtered through a Luer-Lock syringe packed with sterile cheesecloth and fitted with a Millipore Millex 25mm Durapore® PVDF 5 μm filter unit. Cells were pelleted (5000×g, 10 min, room temperature) and the supernatant was discarded. Pellets were flash frozen in liquid nitrogen and stored for up to 2 weeks at -20°C prior to RNA extraction. For these treatments two RNA samples were obtained for each strain per biological replicate, with each RNA sample including samples from 40-80 leaves.

Epiphytic treatments

Epiphytic treatments for this collaboration were performed by Russell A. Scott (University of California, Berkley) in the laboratory of Dr. Steven Lindow (University of California, Berkley). Inoculum for epiphytic treatments was grown in 250 mL Erlenmeyer flasks containing 50 mL HMM-basal medium inoculated with 1 mL of an overnight culture grown in HMM-basal. Inoculum was grown at 26°C, shaking at 200 rpm, to an OD_{600} of 0.6 (5×10^8 CFU/mL). Cultures were pelleted at 5000 rpm for 10 min at room temperature. Cell pellets were washed in sterile distilled water. After washing

cell pellets were resuspended to an OD_{600} of 0.3, which is equivalent to 5×10^8 colony forming units (CFU) per mL. Bacterial suspensions of 5×10^6 CFU/mL were made in sterile distilled water with 1% Silwet L-77 (Vac-In- Stuff) surfactant (Lehle Seeds, Round Rock, TX). Two week old Blue Lake 274 (Burpee Seeds, Warminster, PA) bean plants (*Phaseolis vulgaris* L.) were immersed in the inoculums for 20 seconds and then enclosed in a plastic bag which was misted with sterile distilled water. Bagged plants were placed on the laboratory bench at room temperature for 24 hours. After 24 hours the bags were removed and plants were incubated in Conviron growth chamber with a 16 hour light/ 8 hour dark cycle, 25°C, 98% humidity for 48 hours. After 48 hours the leaves were harvested individually and bacteria were extracted.

Bacterial extraction from epiphytic treatments

Epiphytic bacteria were extracted using an acidic ethanol/phenol solution composed of 9 mL buffer-saturated phenol (pH 6.6), 171 mL absolute ethanol (200 proof), 420 mL sterile distilled water (total 600 mL). Leaves were individually removed from the plants, were immediately submerged in the ethanol/phenol solution. Approximately 100 leaves were submerged into each batch of 600 mL ethanol/phenol. The ethanol/phenol/leaf tissue slurry was sonicated for 10 min then leaf tissue was removed by draining the slurry through sterile cheese cloth. The filtered ethanol/phenol was centrifuged to remove bacterial cells at 5500×g for 10 min. Pellets were flash frozen in liquid nitrogen and stored for up to 2 weeks at -20°C prior to RNA extraction.

For these treatments two RNA samples were obtained for each strain, with each RNA sample including samples from 400-600 leaves.

RNA isolation for microarray analysis

Cell lysis was performed using 7 mg/mL lysozyme (M.P. Biomedicals) in TE buffer (10mM TrisCl, 1 mM EDTA, pH 8.0) with frequent vortexing for 7 min at room temperature. Samples were extracted using the RNeasy® Mini Kit (Qiagen) and eluted in RNase/DNase free water. Those RNA samples gathered from in planta and epiphytic growth were extracted using the RNeasy® Mini Plant Kit (Qiagen). RNA samples were on-column DNase treated during the extraction procedure using Quiagen RNase-free DNase (Qiagen) following the manufacturer's protocol. The RNA was tested for DNA contamination using quantitative Real-Time reverse-transcription PCR (qRT-PCR) in which the RNA is utilized as the template and reverse transcription reaction is not performed. The RNA quality was measured by Regina M. Hokanson at the Texas AgriLife Genomics and Bioinformatics Services using an Agilent 2100 Bioanalyzer (Agilent Technologies, Inc.) and only RNA samples with an RNA Integrity Number (RIN) above 8.0 were selected (49). Total RNA samples were quantified using micro-spectrophotometry (Nano-Drop Technologies, Inc.).

Gene-based microarray analysis

Total RNA samples were sent to Roche Nimblegen for cDNA synthesis, labeling with U-CYA-3 fluorophore, and hybridization to an ORF-based microarray. In

consultation with Roche Nimblegen a custom microarray was designed using bioinformatic analysis of the *P.s.s.* B728a genome, the custom array included 5,071 predicted open reading frames and 75 putative small RNA genes. The latter included 13 sRNAs that were known or similar to known sRNAs, 46 putative sRNAs that were predicted using the Small RNA Identification Protocol using Highthroughput Technologies (SIPHT) (70), and 16 putative sRNAs that were identified in a previous screen for plant-inducible genes (77, 78). Each ORF and sRNA was represented by 14 60-mer nucleotide probes, with a few exceptions, namely 11 ORFs and 4 sRNAs that were represented by fewer probes due to their short size or low complexity. Two ORFs, *Psyr_2216* and *Psyr_3732*, and 13 sRNA genes were omitted from the array due to their extreme shortness or low complexity, while another 16 ORFs and 1 sRNA showed sufficiently high sequence similarity to other probe sets to enable them to be represented by the remaining probes. A total of 5,137 features were represented on the final microarray, including 5,076 ORFs and 61 putative sRNAs. Each slide contained 4 replicate arrays and the treatments were arranged on the slides to maximize the pairing of treatment comparisons of interest.

Microarray data analysis

Operon prediction was performed by Steven Lund and Dr. Daniel S. Nettleton at Iowa State University. Adjacent genes in the *P.s.s.* B728a genome, transcribed in the same direction, were analyzed to determine whether they were in common operons. To classify potential operon pairs in *P.s.s.* B728a the differences between assumed operon

pairs (Ops) and assumed non-operon pairs (NOPs) in the distributions of distance and correlation of expression data was considered to classify a potential operon pair as either an OP or a NOP. The previously annotated genome *Pseudomonas aeruginosa* strain PAO1 was used to provide OP probabilities for assumed OPs and NOPs. Gene pairs with OP probabilities above 0.9 were assumed to be OPs and gene pairs with OP probabilities below 0.1 were assumed to be NOPs.

Microarray expression data was analyzed by Steven Lund and Dr. Daniel S. Nettleton at Iowa State University. The fluorescence intensity level for each probe was measured and the fluorescent intensities subjected to robust multi-array averaging (RMA), which included adjustment for the background intensity, quantile normalization and median polishing. A robust estimated mean value was determined for each feature on the array. For each feature of a given strain that was subjected to a given treatment, the average fluorescence intensity was estimated based on the following model: $Log_2(F_{ijk}) = B_o + B_i rep_k + B_{2i} trt_i + B_{3j} strain_j + B_{4ij}$ trtxstrain$_{ij}$, where $Log_2(F_{ijk})$ is the estimated average fluorescence intensity of given gene of strain *i* that was subjected to treatment *j* in replicate sample *k*,B_o is the average fluorescence intensity for the wild type in the HMM medium treatment in replicate sample 1, and the replicate effect was assumed to be constant. LIMMA analysis was applied to share information across genes when estimating error variances. This was done separately for distinct groups of treatments that had similar absolute median residuals. The resulting variance estimates were used to calculate Welch *t*-statistics, and corresponding p-values, among all pair-wise treatments of interest. For each comparison of interest, q-values were estimated

from the corresponding distribution of p-values according to Nettleton's method (88). Features exhibiting a q-value < 0.05 were identified as differentially expressed.

Purification of achromobactin from P.s.s. *B728a*

Achromobactin was purified from *P.s.s.* B728a, *P.s.s.* B728a ADB1005 (PVD-), and *P.s.s.* B728a Δ*gacS*. The purification procedure is modified from Berti and Thomas (8). Cultures of the *Pseudomonas* strains were grown to late logarithmic phase (OD_{600} of 0.6). One milliliter of the culture was pelleted and washed three times in iron limited HMM media. Cell pellets were re-suspended in one milliliter of iron limited HMM media and used to inoculate 2800 milliliter flasks containing 1 liter of iron limited HMM media with 1.7 mM sodium citrate. These cultures were grown at 26°C, shaking at 250 rotations per minute (rpm) for 4 days. Cells were removed by centrifugation at 5000 rpm for 30 minutes. Rotary evaporation was used to concentrate the supernatant to 10 milliliters. The supernatant was then brought to a 90% methanol concentration and filtered through 125 mm Whatman paper followed by a 0.2 μm diameter pore size filter. The filtered supernatant was diluted 1:1 with ethyl acetate. Column chromatography was performed using a column of silica resin (SiliaFlash F60 40-63 μm, 230-400 mesh, SiliCycle, Quebec City, Canada). The column was washed with two column volumes of 10:9:1 solution ethyl acetate/methanol/water, and eluted in 1 liter of 9:1 methanol/water. The eluted achromobactin was rotary evaporated to a final volume of 3 mL.

Mass spectrometry

Mass spectrometry analysis was performed by Dr. Benjamin Philmus with the support of Dr. Tadhg Begley at Texas A&M University. Siderophore analysis was accomplished by liquid chromatography- electro spray ionization-time of flight- mass spectrometry (LC-ESI TOF MS) analysis using an Agilent 1260 HPLC equipped with a binary pump, thermostated autosampler, heated column compartment and diode array detector in line with a MicroToF-QII MSD (Bruker Daltonics, Billerica, MA) equipped with an ESI source operating in negative ionization mode monitoring from *m/z* 50 – 2500. The crude media preparation from above was separated using a Poroshell 120 EC-C18 HPLC column (3.0 x 100 mm, 2.7 µm, Agilent Technologies, Santa Clara CA) held at 30 ^{o}C with the following program using a flow rate of 0.5 mL/min, where bottle A was 10 mM *N*,*N*-dimethylhexylamine, 10 mM ammonium acetate, pH 7.1 and bottle B was 75% methanol/25% water. The column was pre-equilibrated in 100% A for 2 min prior to injection. The mobile phase was held at 100 % A for 5 minutes and then changed to 100 % B over the following 15 min using a linear gradient, at which time the mobile phase was held at 100 % B for 5 additional minutes followed by recycling the mobile phase to 100% A over 2 min and the column was held at 100% A for 2 min to equilibrate the column prior to the next injection. The MSD had the following settings: Capillary, 3000 V; End plate offset, -500 V; Nebulizer gas, 3.0 bar; Drying gas, 10 L/min; Drying gas temperature, 200^{o}C; Funnel 1 RF, 300 Vpp; Funnel 2 RF, 300 Vpp; ISCID energy, 0.0 eV; Hexapole RF, 300 Vpp; Quadrapole Ion energy, 5 eV; Low mass filter, 300 *m/z*; Collision cell RF, 300 Vpp; Collison energy, 8.0 eV, Transfer time, 100.0

μsec; Prepulse storage, 10.0 μsec. The MSD was calibrated using ESI tune mix-low solution (Agilent Technologies) prior to running a set of samples and each run contained an internal standard derived from an automatic injection of 20 μL sodium acetate (0.4 mg/mL). Data was processed using DataAnalysis 4.0 software (Bruker Daltonics, Billerica, MA).

N,N-dimethylhexylamine, sodium acetate, ammonium acetate were purchased from Sigma-Aldrich and used without purification. All solvents used during LC-MS analysis were of LC-MS grade.

Results and Discussion

Although there have been a significant number of studies on components of the GacS/GacA regulon in *P.s.s.* B728a, the outcome of this collaborative microarray project serves as an example of the scientific power that these types of expression analyses provide. Despite the breadth of our previous knowledge about this specific regulon, this study reveals that the two-component system GacS/GacA is an integral component of the *P.s.s.* B728a regulatory network, with 3,314 genes and small RNAs showing differential expression at a q-value of less than 0.05. For the remainder of this report all references to differential gene expression are based upon this statistical limit of a q-value less than 0.05. The SalA regulon has been less extensively studied than that of GacS/GacA, but is known to be involved in the regulation of some major pathogenicity factors such as the biosynthesis of syringomycin and syringopeptin. However, the extensive number of genes revealed in this study was unexpected, with 1,636 genes and

small RNAs showing differential expression. This study has provided an overwhelming abundance of data, but by utilizing previous studies and compiling predicted regulatory pathways this data will greatly enhance our understanding of the regulation of *P.s.s.* B728a at a global level.

Notably, this data draws attention to the limitations of expression studies performed in isolated experimental conditions and the precautions that should be taken when analyzing data from these studies. In this study a very small number of genes were differentially expressed across all of the treatment conditions tested. Only 11 genes were differentially expressed by the *P.s.s.* B728a *ΔgacS* strain in comparison to the wild type for all seven experimental conditions, while nine genes were differentially expressed by *P.s.s.* B728a *ΔsalA* across all seven experimental conditions (Table 5). Thus, although it is tempting to assume that transcriptome data can be applied to an organism universally, this data is in fact limited to the specific conditions in which the experiments were performed. Thus regulation and gene expression must be approached in a cautious fashion, and diligence is necessary in specifying the experimental conditions when referring to regulatory networks and transcriptome data.

The minimum regulon of GacS/SalA

The minimum regulon of GacS/SalA includes chemotaxis and quorum sensing genes. Likewise, when transcriptomes are analyzed in multiple environmental conditions it is possible to begin compiling what might be referred to as a minimal

TABLE 5. Genes showing differential gene expression in all seven treatment conditions between the GacS and/or SalA deletion mutants and wild type *P.s.s.* B728a.

Gene	Locus Tag	Op.	Function	Basal[a]		NaCl[a]		H_2O_2[a]		Low Fe[a]		Low N[a]		Epiphytic[a]		Apoplastic[a]	
				GacS	SalA	GacS	SalA	GacS	SalA	GacS	SalA	GacS	SalA	GacS	SalA	GacS	SalA
cheR-1	*Psyr_0783*	157	Protein-glutamate O-methyltransferase, chemosensing and chemotaxis	-3.06	-3.52	-5.53	-5.58	-2.87	-3.29	-3.73	-3.41	-6.84	-7.01	-4.34	-4.06	-5.48	1
cheA-1	*Psyr_0786*	157	CheW-like protein:	1	-3.44	-6.33	-5.77	-3.6	-4.48	-5.83	-4.76	-9.66	-7.62	-4.87	-5.60	-7.17	-4.68
cheY-1	*Psyr_0788*	157	Response regulator receiver, chemosensing and chemotaxis	-4.64	-4.73	-12.45	-9.68	-4.16	-11.24	-9.13	-6.54	-16.47	-11.89	-15.41	-15.58	-20.88	-17.36
	Psyr_0871		PAS, cell motility	-4.54	-5.59	-5.36	-5.46	-4.30	-7.88	1	-6.39	-15.80	-20.28	-7.92	-7.08	-9.75	-6.44
	Psyr_0907		hypothetical protein	-10.98	-8.64	-14.25	-10.26	-7.79	-14.10	1	-9.79	-37.74	-29.50	-39.53	-32.05	-46.51	-28.90
ahlI	*Psyr_1621*		Autoinducer synthesis protein, quorum sensing	-6.17	-6.54	-7.33	-10.10	-7.70	-6.00	-9.77	-7.34	-4.98	-6.12	-2.92	-2.45	-5.60	1
aceE	*Psyr_1625*		2-oxoacid dehydrogenase subunit E1	-19.84	-16.64	-18.28	-20.04	-31.65	-15.43	-23.81	-28.57	-6.79	-4.32	-3.45	-3.88	-11.75	-8.03
	Psyr_2279		hypothetical protein	-10.74	-6.21	-7.01	-4.18	-3.74	-9.44	-7.20	1	-4.06	-2.20	-6.20	-4.06	-4.13	1
	Psyr_2624	517	putative lipoprotein	-13.61	-16.58	-11.98	-14.51	-18.90	-11.76	-14.03	-31.25	-5.42	-7.58	-3.91	-4.36	-5.91	1
	Psyr_2860		hypothetical protein	-3.89	-4.40	-12.09	-8.38	-5.84	-5.21	-4.96	1	-12.79	-7.62	-3.08	1	-6.79	-4.46
	Psyr_3163		Serralysin, predicted zinc endopeptidase	-29.50	-22.94	-32.05	-21.93	-17.57	-37.74	-46.51	-27.70	-48.54	-55.25	-28.90	-26.81	-36.10	-41.49
pslD	*Psyr_3303*	640	Polysaccharide export protein, Psl biosynthesis and transport	-2.76	-4.37	-2.93	1	-4.04	-7.40	-5.31	-5.43	-12.38	-11.96	-5.26	-5.17	-5.46	1
psil	*Psyr_3308*	641	Glycosyl transferase, group 1, Psl biosynthesis and transport	-3.84	-5.71	-3.28	-3.86	-9.28	-10.49	-8.06	-6.62	-9.09	-15.50	-3.64	-5.11	-8.33	-4.63
	Psyr_3372	649	hypothetical protein	-9.84	-8.54	-13.77	-10.70	-9.79	-12.33	-4.85	-3.27	-11.03	-13.85	-8.33	-10.88	-12.06	-8.96
	Psyr_3548		glutathione S-transferase	1	-4.54	1	-4.44	1	-4.31	1	-3.59	1	-4.07	1	-2.02	1	-4.56

[a] Values shown are the fold change, with positive numbers reflecting an increase in gene expression in the deletion strain as compared to the wild type, a a negative number reflecting a decrease in gene expression in the deletion strain as compared to the wild type.

regulon, those genes that are constitutively regulated in a specified regulon regardless of the environmental conditions. For GacS/SalA the minimum regulon includes chemotaxis genes (*cheR-1*, *cheA-1*, *cheY-1*) that fall in an eight-gene operon (*Psyr_0781-0788*). Accordingly, based on this study GacS/SalA regulates the chemotaxis operon encoded by *Psyr_0781-0788* regardless of environmental conditions. Similarly this study confirms studies performed by Quinones et al, 2005 (96) in which the quorum sensing gene *ahlI,* which encodes the synthesis of the autoinducer signal AHL, is regulated by GacS/GacA. Additionally, this study confirms that SalA is also a regulator of *ahlI*, downstream of GacS/GacA. Thus the minimum regulon as determined by this study confirms the role of GacS/SalA in both quorum sensing and chemotaxis that have been previously explored experimentally.

This is further supported by looking at the remainder of the genes known to be involved in the quorum sensing and chemotaxis systems that show differential gene expression in this study. As seen in Table 6, the LuxR-like transcriptional regulator of quorum sensing, AhlR, is also differentially expressed in multiple experimental conditions. Likewise, when other known chemotaxis associated genes were analyzed, many displayed differential expression by the GacS and/or SalA mutants as compared to the wild type. Furthermore, several fell in operons in which multiple genes were differentially expressed and in multiple environmental conditions (Table A-4).

A serralysin-like gene is part of the GacS/SalA minimum regulon. One major advantage of transcriptome analysis is the ability to form sound hypothesis based on the novel data regarding previously unstudied genes. For example, the gene

TABLE 6. Quorum sensing genes differentially expressed between deletion mutants of GacS and/or SalA compared to wild type.

Gene	Locus Tag	Op.	Function	Basal[a]		NaCl[a]		H_2O_2[a]		Low Fe[a]		Low N[a]		Epiphytic[a]		Apoplastic[a]	
				GacS	SalA	GacS	SalA	GacS	SalA	GacS	SalA	GacS	SalA	GacS	SalA	GacS	SalA
ahlI	***Psyr_1621***		Autoinducer synthesis protein	-6.17	-6.54	-7.33	-10.10	-7.70	-6.00	-9.77	-7.34	-4.98	-6.12	-2.92	-2.45	-5.76	1
ahlR	***Psyr_1622***		LuxR transcriptional regulator	-4.09	-4.21	-4.22	-5.07	-5.77	-4.00	1	1	-4.18	-3.28	-4.26	-2.70	1	1
hacA	***Psyr_1971***		AHL acylase	1	1	1	1	1	1	-7.46	-21.19	1	1	1	1	1	1

[a] Values shown are the fold change, with positive numbers reflecting an increase in gene expression in the deletion strain as compared to the wild type, a negative number reflecting a decrease in gene expression in the deletion strain as compared to the wild type.

TABLE 7. Type VI secretion associated gene clusters showing differentially expressed between deletion mutants of GacS and/or SalA compared to *P.s.s.* B728a.

Gene	Locus Tag	Op.	Function	Basal[a]		NaCl[a]		H_2O_2[a]		Low Fe[a]		Low N[a]		Epiphytic[a]		Apoplastic[a]	
				GacS	SalA	GacS	SalA	GacS	SalA	GacS	SalA	GacS	SalA	GacS	SalA	GacS	SalA
	Psyr_2624	**517**	putative lipoprotein	-13.61	-16.58	-11.98	-14.51	-18.90	-11.76	-14.03	-31.25	-5.42	-7.58	-3.91	-4.36	-5.91	1
	Psyr_2625	**517**	hyp. protein	-12.33	-13.87	-10.46	-16.08	-18.08	-12.21	-12.59	-21.14	-8.44	-8.70	-4.77	-5.34	1	1
	Psyr_2626	**517**	hyp. protein	-7.34	-8.66	-7.84	-12.84	-14.04	-7.92	-8.42	-10.49	-4.73	-3.47	-2.49	-2.20	1	1
	Psyr_2627	**517**	T6SS island protein	-4.67	-5.20	-5.21	-7.12	-6.99	-4.48	1	1	-2.88	1	1	1	1	1
	Psyr_2628	**517**	ABC transporter	-6.63	-9.07	-6.22	-15.60	-15.34	-6.66	-7.50	-10.42	-6.24	-3.57	-3.08	1	1	1
	Psyr_2629	**517**	von Willebrand factor	-6.30	-8.18	-7.10	-14.33	-17.64	-6.75	-8.67	-13.00	-6.42	-4.29	-5.03	-3.62	1	1
	Psyr_2630	**517**	hyp. protein	-6.21	-8.47	-7.30	-12.97	-17.54	-8.46	-8.40	-12.74	-6.25	-5.62	-4.79	-4.89	1	1
	Psyr_2631	**517**	hyp. protein	-4.40	-6.58	-6.12	-8.35	-10.05	-7.34	-8.61	-7.99	-4.08	-5.46	1	-3.08	1	1
	Psyr_2632	**517**	virulence protein SrfB	-6.84	-7.09	-5.14	-8.49	-10.95	-7.50	-10.14	-10.54	-5.77	-6.01	-3.37	-4.06	1	1
	Psyr_2633	**517**	hyp. protein	-6.63	-6.76	-3.64	-6.92	-10.74	-6.18	-7.12	-7.06	-7.38	-4.72	-4.34	-2.52	1	1

[a] Values shown are the fold change, with positive numbers reflecting an increase in gene expression in the deletion strain as compared to the wild type, a negative number reflecting a decrease in gene expression in the deletion strain as compared to the wild type.

TABLE 7. Continued

Gene	Locus Tag	Op.	Function	Basal[a]		NaCl[a]		H_2O_2[a]		Low Fe[a]		Low N[a]		Epiphytic[a]		Apoplastic[a]	
				GacS	SalA	GacS	SalA	GacS	SalA	GacS	SalA	GacS	SalA	GacS	SalA	GacS	SalA
	Psyr_4952	971	hypothetical protein	1	1	1	1	1	1	1	1	1.63	1	1	1	1	1
tssB	*Psyr_4953*	971	T6SS;	-1.64	1	1	1	-1.40	-1.62	1	1	1	1	1	-1.48	1	1
tssC	*Psyr_4954*	971	T6SS,	-1.93	-1.70	1	1	-1.77	-2.28	1	1	-1.53	1	-1.59	-1.78	1	1
tssE	*Psyr_4955*	971	T6SS,	-2.69	-2.69	1	1	-4.35	-3.23	1	1	-5.14	-3.48	-2.29	-2.07	1	1
tssF	*Psyr_4956*	971	T6SS,	-2.30	-2.34	1	1	-4.69	-2.95	1	1	-2.35	-2.14	1	1	1	1
tssG	*Psyr_4957*	971	T6SS,	-1.94	-1.77	1	-2.17	-2.81	-1.85	1	1	1	1	1	1	1	1
clpV/tssH	*Psyr_4958*	971	T6SS, AAA ATPase, central region:	-2.13	1	1	-2.83	-9.65	-3.57	1	1	-2.22	-2.14	1	1	1	1
tssJ	*Psyr_4959*	971	T6SS	1	1	1	-3.09	-9.98	-2.50	1	1	-2.51	1	1	1	1	1
tssK	*Psyr_4960*	971	T6SS	1	1	1	-3.45	-10.38	-2.69	1	1	-1.90	1	1	1	1	1
tssLa	*Psyr_4961*	971	T6SS protein	1	1	1	-4.80	-13.32	-2.61	1	1	-2.41	1	1	1	1	1
icmF/tssM	*Psyr_4962*	971	T6SS; icmF	-2.41	-2.63	-3.30	-4.54	-8.53	-2.47	1	1	1	1	1	1	1	1
tagF	*Psyr_4963*	971	T6SS protein	1	1	-4.53	-3.25	-5.28	1	1	1	1	1	1	1	1	1
	Psyr_4964	971	OmpA/MotB	1	1	-23.70	1	-4.86	1	1	1	1	1	1	1	1	1
hcp	*Psyr_4965*		hyp. protein	-2.32	-1.89	-3.30	1	-2.78	-2.00	1	1	-3.58	-1.77	-1.93	-2.34	1	1
	Psyr_4966		ImpA, N-terminal	1	1	1	1	-5.31	1	1	1	-2.47	1	1	1	1	1
	Psyr_4967		hyp. protein	-3.64	-4.78	1	-3.33	-9.65	1	1	1	-9.91	1	-3.56	1	1	1
	Psyr_4968	972	hyp. protein	-3.87	-4.23	-2.76	-3.09	-11.36	-2.87	1	1	-9.18	1	-4.04	1	1	1
	Psyr_4969	972	PAAR	-4.57	-5.05	-3.19	-3.77	-13.04	-3.24	1	1	-8.01	-3.06	-4.46	-3.39	1	1
	Psyr_4970	972	Phospholipase D/Transphosphatidylase	-4.42	-5.80	-3.46	-3.62	-5.97	-3.32	1	1	-6.63	-2.96	-4.20	-3.14	1	1
	Psyr_4971		Sel1 repeat-containing protein	-5.78	-7.13	-3.63	-4.66	-9.25	-3.74	1	1	-9.07	-2.50	-3.33	-3.16	1	1
	Psyr_4972		Sel1 repeat-containing protein	-11.24	-9.90	-4.07	-6.51	-11.38	-5.07	1	1	-7.59	-2.75	-4.19	1	1	1
	Psyr_4973	973	hyp. protein	-5.20	-5.79	-2.98	-3.99	-4.42	-3.35	1	1	-2.39	1	1	1	1	1
vgrG	*Psyr_4974*	973	Rhs element Vgr protein	-5.26	-5.18	-3.41	-3.71	-3.37	-2.96	1	1	-3.46	-2.22	-2.12	1	1	1

[a] Values shown are the fold change, with positive numbers reflecting an increase in gene expression in the deletion strain as compared to the wild type, a negative number reflecting a decrease in gene expression in the deletion strain as compared to the wild type.

Psyr_3163 is part of this minimal regulon that we have defined and has large fold changes between the deletion strains and wild type across all experimental conditions tested. These large fold changes imply that this gene has relatively high expression levels in the wild type strain in the conditions tested. *Psyr_3163* is predicted to encode a serralysin-like zinc-dependent metalloprotease that has homologs in the closely related plant pathogens *P.s.t.* DC3000 and *P.s.p.* 1448a. There are also highly similar genes encoded in the genomes of *Pseudomonas entomophila* strain L48, *Pseudomonas fluorescens* strains, and *Pseudomonas aeruginosa* strains. Serralysin is a protease produced by *Serratia marcescens* that is known to induce inflammatory and immune responses in mammalian hosts (55). The enzymatic activity of a similar metalloprotease in *Pseudomonas aeruginosa* has been investigated, but the role of this enzyme on the virulence of this bacterium was not determined (72). However, this predicted enzyme has not been studied in *P.s.s.* B728a or any other plant pathogen. Given the intensity and universality of expression changes we predict that the serralysin-like protease encoded by *Psyr_3163* may play a significant role in the lifecycle of *P.s.s.* B728a.

The Type VI secretion system is part of the GacS/SalA regulon. Another gene that showed differential gene expression across all seven conditions in this study was *Psyr_2624*, which is part of an operon containing 10 genes (Table 7). This operon contains elements of the Type VI secretion system, a system that is not yet completely understood but appears to utilize a self-assembling hexameric ring proteins, Hcp1, to form nanotubules (98, 99). These nanotubes are similar in size and structure to the phage λ tail protein (98). Likewise, another known Type VI protein, VgrG, also has

homology and structural similarity to bacteriophage proteins (98). Regulation of the *P.s.s.* B728a Type VI secretion system was recently found to be reciprocally regulated by the hybrid sensor proteins, LadS and RetS. The role of GacS in Type VI secretion was also analyzed via quantitative Real Time PCR and the Type VI genes *icmF* and *hcp* had decreased expression in the GacS deletion mutant (99). This study provides support for the findings of Records and Gross as many of the Type VI secretion genes are expressed at lower levels in the GacS deletion mutant than in the wild type strain, including *icmF* and *hcp* (Table 7).

Research on the Type VI secretion system is still in its infancy; however, bioinformatic analysis of sequenced genomes has identified the genes necessary for this secretion system in at least one-fourth of gram negative bacteria (98). Interestingly in this study differential gene expression of the Type VI associated gene clusters between the GacS/SalA deletion mutant and the wild type *P.s.s.* B728a was seen predominantly in the epiphytic condition and not in planta (Table 7). In conjunction with observations by Records and Gross that a mutation in the Type VI secretion gene, *clpV*, does not decrease pathogen virulence when vacuum infiltrated, it can be hypothesized that the Type VI secretion system may be functioning primarily in the epiphytical portion of the P.s.s. B728a lifecycle (99).

To further evaluate these findings the expression data in this study was analyzed to determine if GacS/SalA were involved in the regulation of the regulators of the Type VI secretion system identified by Records and Gross, RetS and LadS (99). In this study the sensor kinase LadS, encoded on gene *Psyr_4339,* did not have differential gene

expression for either the GacS or SalA deletion mutant strains as compared to the wild type *P.s.s.* B728a. However, in the oxidative stress and nitrogen stress conditions the GacS deletion mutant showed differential gene expression of the *retS* (*Psyr_4408*) gene at fold change values of -3.57 and -1.91 respectively. This implies that in certain conditions expression of the sensor kinase RetS is directly or indirectly influenced by GacS. This coincides with studies in *Pseudomonas aeruginosa* wherein GacS/GacA is required for RetS function and these two regulators directly interact both in vivo and in vitro (33).

In *Pseudomonas aeruginosa* GacS/GacA, RetS, and LadS form a multisensory signaling network in which all three regulators interact through the response regulator GacA, which modulates expression of two small RNAs, RsmY and RsmZ (13, 33, 99). RsmY and RsmZ serve as the only direct transcriptional targets of GacA in *P. aeruginosa,* while all other genes regulated by the GacS/GacA system are regulated by the activity of RsmY and RsmZ (13). RsmY and RsmZ bind and sequester the carbon storage regulator, RsmA, which prevents RsmA from binding its target mRNA molecules and preventing translation (13, 33, 99). Thus in *P. aeruginosa* the large complex regulons of GacS, LadS, and RetS commence at the level of mRNA stability as the small RNAs RsmY and RsmZ interact with RsmA. The transcriptional control of the genes in these large regulons occurs downstream.

In *P.s.s.* B728a the potential for a parallel GacS/LadS/RetS multisensory signaling network has just begun to be researched. In this study the small RNA RsmY was differentially expressed in both the GacS and SalA deletion mutant strains as

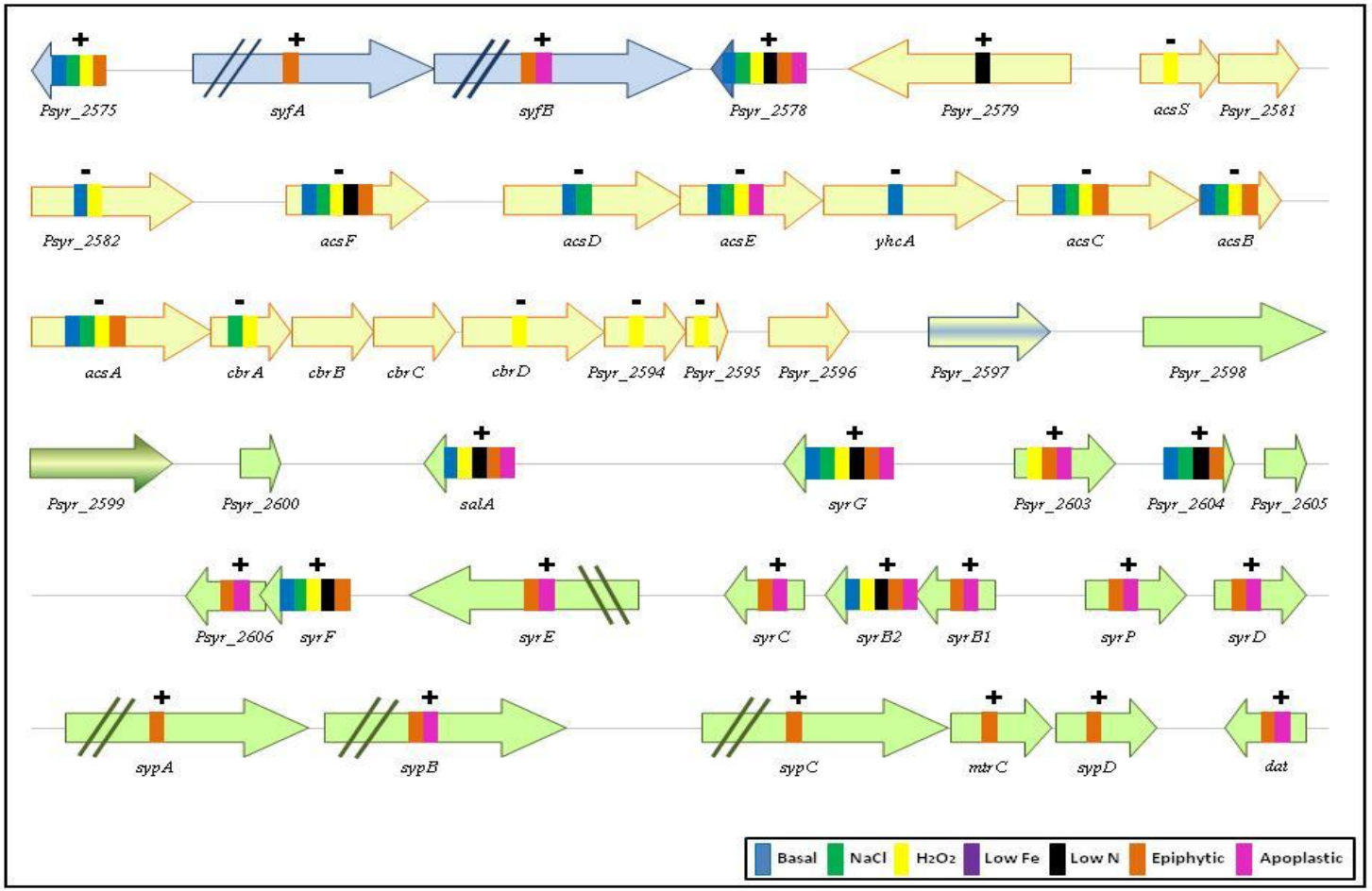

FIG. 11. GacS/SalA regulation of a peptide synthesis rich region of the *P.s.s.* B728a genome. The color coding is based on nucleotide sequence similarity of >80% in the *Pseudomonas* species listed below. *P.s.t.* DC3000 (blue), *P.s.p.* 1448a (yellow), and *P.s.s.* B728a only (green). Those genes with >80% similarity in multiple genomes are striped with the colors of both genomes. Microarray results displaying differential gene expression of *P.s.s.* B728a *ΔgacS* and *P.s.s.* B728a *ΔsalA* compared to wild type *P.s.s.* B728a using a Q-value cut-off of 0.05. The colored bars in each gene represent those microarray conditions in which differential gene expression with a Q-value of less than 0.05 was seen, with colors being defined in the figure legend. Above each depicted gene is a symbol (+/-) representing the regulatory effect of GacS/SalA on the gene expression. The (+) represents a positive regulatory effect by GacS/SalA with the mutant constructs showing decreased relative gene expression compared to wild type. The (–) represents a negative regulatory effect by GacS/SalA with the mutant constructs showing increased relative gene expression compared to wild type.

TABLE 8**.** Small RNAs RsmY and RsmZ that are differentially expressed between deletion mutants of GacS and/or SalA compared to wild type *P.s.s.* B728a.

Seq.	Basal[a]		NaCl[a]		H2O2[a]		Low Fe[a]		Low N[a]		Epiphytic[a]		Apoplastic[a]	
	GacS	SalA	GacS	SalA	GacS	SalA	GacS	SalA	GacS	SalA	GacS	SalA	GacS	SalA
rsmY	-6.27	-4.34	-8.05	-6.39	-5.16	-6.19	1	1	-2.71	1	-6.03	-4.73	1	1
rsmZ	1	1	1	1	1	1	1	1	-2.88	1	1	1	1	1

[a] Values shown are the fold change, with positive numbers reflecting an increase in gene expression in the deletion strain as compared to the wild type, a negative number reflecting a decrease in gene expression in the deletion strain as compared to the wild type.

compared to the wild type in several experimental conditions (Table 8). However, the small RNA RsmZ was differentially expressed only in one condition for the GacS deletion mutant and was not differentially expressed in any conditions by the SalA deletion mutant strain. The data gathered in this study, in conjunction with the work of Records and Gross, emphasizes the importance of continuing research on the regulatory networks of GacS, RetS, and LadS to determine if this system is a comparable system to the complicated feedback mechanism seen in *P. aeruginosa*.

GacS/SalA regulates a biosynthesis rich region of P.s.s. B728a

As mentioned in Chapter II of this dissertation, *P.s.s.* B728a contains a large genomic region with an abundance of peptide synthesis clusters with distinct homology to closely related pseudomonads. By examining this region for regulation by GacS/SalA using the microarray analysis, the entire region appears to be regulated by the GacS/SalA regulon (Fig. 11, Table 9). Examination of this data can provide valuable

TABLE 9. Expression of genes in a peptide synthesis rich region of *P.s.s.* B728a differentially expressed between deletion mutants of GacS and/or SalA compared to wild type *P.s.s.* B728a.

Gene	Locus Tag	Op.	Function	Basal[a]		NaCl[a]		H2O2[a]		Low Fe[a]		Low N[a]		Epiphytic[a]		Apoplastic[a]	
				GacS	SalA	GacS	SalA	GacS	SalA	GacS	SalA	GacS	SalA	GacS	SalA	GacS	SalA
	Psyr_2575		regulatory protein, LuxR	-3.24	-3.27	-2.39	-2.07	-1.84	-3.74	1	1	1	1	-3.04	-3.62	1	1
syfA	*Psyr_2576*	507	Amino acid adenylation	1	1	1	1	1	1	1	1	1	1	-2.03	-2.55	1	1
syfB	*Psyr_2577*	507	Amino acid adenylation	1	1	1	1	1	1	1	1	1	1	-2.47	-2.89	-2.47	1
	Psyr_2578		regulatory protein, LuxR	-3.02	-3.14	-2.53	1	-2.79	-3.54	1	-2.67	-1.99	1	-3.45	-4.42	-4.87	-5.09
	Psyr_2579		Aldehyde dehydrogenase	1	1	1	1	1	1	1	1	1.52	1	1	1	1	1
acsS	*Psyr_2580*	508	Sigma-70 region 2	1	1	1	1	2.83	1	1	1	1	1	1	1	1	1
	Psyr_2581	508	FecR protein	1	1	1	1	1	1	1	1	1	1	1	1	1	1
	Psyr_2582		TonB-dependent siderophore receptor	1	7.09	1	1	1	4.80	1	1	1	1	1	1	1	1
acsF	*Psyr_2583*		Diaminobutyrate-2-oxoglutarate aminotransferase	1	8.5	1	9.04	5.42	3.69	1	1	1	4.44	3.51	1	1	1
acsD	*Psyr_2584*	509	Achromobactin synthesis, IucA/IucC	1	4.46	1	4.38	1	1	1	1	1	1	1	1	1	1
acsE	*Psyr_2585*	509	Achromobactin synthesis, Orn/DAP/Arg decarboxylase	1	4.15	1	3.58	1	3.34	1	1	1	1	1	1	5.24	1
yhcA	*Psyr_2586*	509	Achromobactin synthesis, EmrB/QacA family drug resistance transporter	1	4.46	1	4.38	1	1	1	1	1	1	1	1	1	1
acsC	*Psyr_2587*	510	Achromobactin synthesis, IucA/IucC	1	5.92	1	7.23	1	4.40	1	1	1	1	2.73	1	1	1
acsB	*Psyr_2588*	510	Achromobactin synthesis, HpcH/HpaI aldolase	1	3.89	1	3.92	1	4.56	1	1	1	1	2.36	1	1	1
acsA	*Psyr_2589*	510	Achromobactin synthesis, IucA/IucC	1	7.00	1	8.02	1	6.29	1	1	1	3.68	3.33	1	1	1
cbrA	*Psyr_2590*	510	Periplasmic binding protein	1	1	1	1.76	1	2.01	1	1	1	1	1	1	1	1
cbrB	*Psyr_2591*	510	Transport system permease protein	1	1	1	1	1	1	1	1	1	1	1	1	1	1
cbrC	*Psyr_2592*	510	Transport system permease protein	1	1	1	1	1	1	1	1	1	1	1	1	1	1
cbrD	*Psyr_2593*	511	ABC transporter	1	1	1	1	1	1.92	1	1	1	1	1	1	1	1
	Psyr_2594	511	hypothetical protein	1	1	1	1	1	1.96	1	1	1	1	1	1	1	1

Table 9. Continued

Gene	Locus Tag	Op.	Function	Basal[a]		NaCl[a]		H2O2[a]		Low Fe[a]		Low N[a]		Epiphytic[a]		Apoplastic[a]	
				GacS	SalA	GacS	SalA	GacS	SalA	GacS	SalA	GacS	SalA	GacS	SalA	GacS	SalA
	Psyr_2595	511	Dimethylmenaquinone methyltransferase	1	1	1	1	1	2.38	1	1	1	1	1	1	1	1
	Psyr_2596		PAS	1	1	1	1	1	1	1	1	1	1	1	1	1	1
	Psyr_2597		GGDEF	1	1	1	1	1	1	1	1	1	1	1	1	1	1
	Psyr_2598		putative DNA helicase	1	1	1	1	1	1	1	1	1	1	1	1	1	1
	Psyr_2599		Metallophosphoesterase	1	1	1	1	1	1	1	1	1	1	1	1	1	1
	Psyr_2600		hypothetical protein	1	1	1	1	1	1	1	1	1	1	1	1	1	1
salA	*Psyr_2601*		regulatory protein, LuxR	-2.21	1	1	1	-2.72	1	1	1	-2.25	1	-8.96	1	-7.60	1
syrG	*Psyr_2602*		regulatory protein, LuxR	-3.42	-4.43	-3.55	-3.44	-3.00	-3.78	1	1	-3.73	-2.80	-10.22	-10.15	-14.88	-8.22
	Psyr_2603		Secretion protein HlyD	1	1	1	1	-1.82	1	1	1	-1.72	1	-2.56	-2.37	1	1
	Psyr_2604		hypothetical protein	-2.03	-2.02	-2.85	-2.54	1	1	1	1	-3.62	1	-2.88	1	1	1
	Psyr_2605		transposase, putative	1	1	1	1	1	1	1	1	1	1	1	1	1	1
	Psyr_2606	512	RND efflux system, outer membrane lipoprotein, NodT	1	1	1	1	1	1	1	1	1	1	1	-3.28	-3.99	1
syrF	*Psyr_2607*	512	regulatory protein, LuxR	-2.43	-2.34	-2.77	-2.72	-2.06	-1.90	1	1	-3.04	1	-8.47	-6.70	1	1
syrE	*Psyr_2608*		Syringomycin synthesis, Amino acid adenylation	1	1	1	1	1	1	1	1	1	1	-3.94	-4.44	-9.75	-7.36
syrC	*Psyr_2609*		Syringomycin synthesis, Alpha/beta hydrolase fold	1	1	1	1	1	1	1	1	1	1	-2.95	-2.84	-7.02	-5.05
syrB2	*Psyr_2610*	513	Syringomycin synthesis, chlorinating enzyme	-2.00	-2.03	1	1	-1.98	1	1	1	-1.63	1	-13.46	-9.78	-34.72	-21.60
syrB1	*Psyr_2611*	513	Syringomycin synthesis, Amino acid adenylation	1	1	1	1	1	1	1	1	1	1	-12.48	-10.53	-34.48	-21.65
syrP	*Psyr_2612*	514	Syringomycin regulation, syrP protein, putative	1	1	1	1	1	1	1	1	1	1	-7.90	-9.18	-47.17	-26.32
syrD	*Psyr_2613*	514	Syringomycin synthesis, Cyclic peptide transporter	1	1	1	1	1	1	1	1	1	1	-7.58	-7.65	-27.93	-8.70
sypA	*Psyr_2614*	514	Syringopeptin synthesis, Amino acid adenylation	1	1	1	1	1	1	1	1	1	1	1	-2.56	1	1
sypB	*Psyr_2615*	514	Syringopeptin synthesis, Amino acid adenylation	1	1	1	1	1	1	1	1	1	1	-1.92	-2.72	-6.83	-3.53
sypC	*Psyr_2616*	515	Syringopeptin synthesis, Amino acid adenylation	1	1	1	1	1	1	1	1	1	1	1	-2.06	1	1

Table 9. Continued

Gene	Locus Tag	Op.	Function	Basal[a]		NaCl[a]		H2O2[a]		Low Fe[a]		Low N[a]		Epiphytic[a]		Apoplastic[a]	
				GacS	SalA	GacS	SalA	GacS	SalA	GacS	SalA	GacS	SalA	GacS	SalA	GacS	SalA
mtrC	*Psyr_2617*	515	Secretion protein HlyD	1	1	1	1	1	1	1	1	1	1	-2.41	-3.19	1	1
sypD	*Psyr_2618*	515	ABC transporter	1	1	1	1	1	1	1	1	1	1	-2.42	-2.35	1	1
dat	*Psyr_2619*		Diaminobutyrate-2-oxoglutarate transaminase	1	1	1	1	1	1	1	1	1	1	-3.23	-3.05	-9.17	-5.27

[a] Values shown are the fold change, with positive numbers reflecting an increase in gene expression in the deletion strain as compared to the wild type, a negative number reflecting a decrease in gene expression in the deletion strain as compared to the wild type.

clues about the regulation of these peptide products and the role of these peptides in the *P.s.s.* B728a lifecycle.

GacS/SalA regulates syringafactin biosynthesis. Within this peptide synthesis rich region of the *P.s.s.* B728a genome a novel NRPS synthesized lipopeptide named syringafactin is encoded by genes *Psyr_2576* and *Psyr_2577*. The syringafactin gene cluster contains eight NRPS modules that produce six highly related linear lipooctapeptides (9). *P.s.s.* B728a mutant constructs that are incapable of producing syringafactin were unable to swarm, thereby suggesting that syringafactin functions as a biosurfactant (9). This biosurfactant quality was confirmed in subsequent analyses (14). Syringafactin is encoded on two NRPS genes (*syfA/syfB*) that are adjacent to two Lux-R like homologs (*Psyr_2575* and *Psyr_2578*), this cluster of genes is homologous to genes found in *P.s.t.* DC3000. The apparent inheritance of this region as a gene cluster leads to the hypothesis that one or both of these Lux-R homologs may be involved in the regulation of syringafactin biosynthesis. Based on the microarray analysis, syringafactin is regulated by GacS/SalA in the plant conditions, with both NRPS genes displaying differential expression in the epiphytic condition. Likewise, both of the adjacent Lux-R homologs (*Psyr_2575* and *Psyr_2578*) are also regulated by GacS/SalA in the epiphytic condition. The biosurfactant qualities of syringafactin combined with these observations suggests that syringafactin may play a role in *P.s.s.* B728a's ability to swarm on the leaf surface. Therefore, further studies should be performed to determine if *Psyr_2575* and/or *Psyr_2578* are involved in the regulation of syringafactin biosynthesis

downstream of GacS/SalA and if syringafactin provides an epiphytic advantage to *P.s.s.* B728a.

GacS/SalA negatively regulates achromobactin biosynthesis. The second biosynthesis cluster in this peptide biosynthesis rich region encodes the citrate siderophore achromobactin. This study found that 13 of the genes in the achromobactin biosynthesis and secretion cluster were differentially expressed between the GacS/SalA deletion mutants and the wild type strain. Differential expression of this cluster was most common in the basal medium condition, and surprisingly differential expression the achromobactin genes were not seen in the iron stress treatment. It is possible that the iron stress condition was too extreme to induce expression of achromobactin, since this siderophore has a lower binding efficiency for iron than pyoverdine. The regulation of iron associated genes, including achromobactin and pyoverdine biosynthesis genes, by GacS/SalA will be discussed in a later portion of this chapter. It is also interesting to note that differential gene expression was seen in media treatment conditions that contain 10 μM iron, relatively high iron content for significant siderophore expression. I anticipate that larger fold changes would have occurred if slightly lower iron conditions were utilized for the media conditions, or if a less extreme iron stress condition were selected. Unlike syringafactin, GacS/SalA had a negative regulatory effect on the achromobactin biosynthesis and secretion cluster in this study, wherein we see higher expression of the achromobactin gene cluster in the GacS/SalA deletion strains.

Syringomycin and syringopeptin are positively regulated by GacS/SalA. The final component of the peptide synthesis rich region encodes biosynthesis, secretion, and

regulatory elements associated with the potent phytotoxins syringomycin and syringopeptin. This study has confirmed the regulatory role of GacS/SalA in the synthesis and secretion of syringomycin and syringopeptin, and has provided additional data regarding the environmental conditions in which these phytotoxin genes are most highly expressed. Not surprisingly, the largest fold changes associated with the regulation of syringomycin and syringopeptin by GacS/SalA were found in the apoplastic treatment condition (Table 9). However, there was a reasonably sized fold change associated with these gene clusters in the epiphytic treatment condition, implying that there may be lower level expression of at least some *syr/syp* genes on the leaf surface.

Analysis of this peptide synthesis rich region reveals that although GacS/SalA regulates all three peptide products in this region, they are not regulated identically. I hypothesize that syringafactin is primarily involved in the epiphytic stage of the *P.s.s.* B728a lifecycle. Meanwhile, syringomycin and syringopeptin may have a previously uncharacterized role on the leaf surface, prior to their role in plant disease. It is unclear in what plant environments achromobactin is most prevalent; however, in stark contrast to the positive regulation of syringafactin, syringomycin, and syringopeptin, this citrate siderophore is negatively regulated by GacS/SalA and has increased expression levels in the deletion mutants.

Additionally, this study provides valuable clues for regulators within the peptide cluster that may work downstream of GacS/SalA in regulating the synthesis and secretion of syringafactin, syringomycin, syringopeptin, and achromobactin. The data

from this study can be used to make educated hypotheses and further define the complex regulatory networks of *P.s.s.* B728a. One logical approach to analyzing this microarray was by beginning with previously identified gene clusters with known regulation by GacS/SalA, such as the NRPS synthesized molecules, syringolin, syringomycin, and syringopeptin. After confirming the known regulatory networks, similarly synthesized molecules were investigated.

GacS/SalA regulate NRPS synthesized toxins

Prior to this study it was known that GacS/SalA was involved in the regulation of several secondary metabolites of *P.s.s.* B728a produced by NRPS enzyme clusters including syringomycin, syringopeptin, and syringolin. This study has confirmed the regulation of the *syr/syp* gene cluster and syringolin by GacS/GacA (Table 10). Likewise, as reported earlier the NRPS synthesized syringafactin is also regulated by GacS/SalA. Despite previous knowledge of GacS/SalA regulation, this study has provided new insights into the regulation of these secondary metabolites. Earlier new hypotheses regarding the *syr/syp* biosynthesis clusters were discussed; however, similar new hypothesis can be proposed concerning the biosynthesis of the peptide syringolin.

GacS/SalA positively regulates syringolin. Similarly to the *syr/syp* gene clusters, the NRPS/polyketide synthetase biosynthesis cluster that encodes syringolin had the largest differential gene expression between the GacS/SalA deletion mutants and the wildtype in the apoplastic condition (Table 10). This is an interesting observation given that syringolin functions as an irreversible eukaryotic proteasome inhibitor (97).

TABLE 10. Syringolin genes of *P.s.s.* B728a differentially expressed between deletion mutants of GacS and/or SalA compared to wild type.

Gene	Locus Tag	Op.	Function	Basal[a]		NaCl[a]		H2O2[a]		Low Fe[a]		Low N[a]		Epiphytic[a]		Apoplastic[a]	
				GacS	SalA	GacS	SalA	GacS	SalA	GacS	SalA	GacS	SalA	GacS	SalA	GacS	SalA
sylA	*Psyr_1702*		Syringolin D regulator, LuxR	-2.19	1	-2.04	1	1	1	1	1	-3.66	1	-2.54	-1.94	1	1
sylB	*Psyr_1703*		Fatty acid desaturase	1	1	1	1	1	1	1	1	-3.87	1	1	1	1	1
sylC	*Psyr_1704*		Amino acid adenylation	1	1	1	1	1	1	1	1	-2.00	1	-2.12	1	-9.84	-6.73
sylD	*Psyr_1705*		Syringolin D synthesis, Amino acid adenylation	1	1	1	1	1	1	1	1	-1.65	1	1	1	1	1
sylE	*Psyr_1706*		Syringolin D exporter, major facilitator transporter	1	1	1	1	1	1	1	1	1	1	1	1	1	1

[a] Values shown are the fold change, with positive numbers reflecting an increase in gene expression in the deletion strain as compared to the wild type, a negative number reflecting a decrease in gene expression in the deletion strain as compared to the wild type.

TABLE 11. Mangotoxin genes of *P.s.s.* B728a differentially expressed between deletion mutants of GacS and/or SalA compared to wild type.

Gene	Locus Tag	Op.	Function	Basal[a]		NaCl[a]		H2O2[a]		Low Fe[a]		Low N[a]		Epiphytic[a]		Apoplastic[a]	
				GacS	SalA	GacS	SalA	GacS	SalA	GacS	SalA	GacS	SalA	GacS	SalA	GacS	SalA
	Psyr_5009	983	hypothetical protein	-5.27	-4.17	-5.84	-4.22	-5.25	-4.46	**1**	-5.24	-8.45	-5.71	-3.86	-3.40	1	1
	Psyr_5010	983	hypothetical protein	-3.19	-3.20	-3.49	-3.04	-3.86	-3.25	1	1	-3.99	-3.48	1	-2.34	1	1
mgoA	***Psyr_5011***	983	Amino acid adenylation:Thioester reductase	-2.84	-3.35	-3.81	-3.51	-5.01	-3.78	1	-4.57	-4.53	-3.01	1	-2.27	1	1
	Psyr_5012	983	hypothetical protein	1	1	1	1	-2.50	1	1	1	-3.72	-2.27	1	1	1	1

[a] Values shown are the fold change, with positive numbers reflecting an increase in gene expression in the deletion strain as compared to the wild type, a negative number reflecting a decrease in gene expression in the deletion strain as compared to the wild type.

Although it has been reported that the proteasome inhibiton property of syringolin A assists *P.s.s.* B728a in invading the plant host via the stomates, this study suggests that syringolin may also play an important role in planta (102).

Mangotoxin-like toxin is regulated by GacS/SalA. As discussed in Chapter II, the *P.s.s.* B728a genome encodes a predicted NRPS synthesized, non-host specific, antimetabolite toxin, mangotoxin. In this study the predicted mangotoxin gene cluster had the largest fold change between the GacS/SalA deletion mutant strains and the wild type in the nitrogen stress treatment. However, differential gene expression for the predicted mangotoxin cluster was seen in all of the experimental conditions except the apoplast (Table 11). This supports the hypothesis made in Chapter II, that mangotoxin contributes to the survival of *P.s.s.* B728a on the leaf surface as seen in *P.s.s.* UMAF0158 (3).

In addition to the NRPS synthesized toxin regions, this study also analyzed the NRPS synthesized siderophore, pyoverdine, and the NIS synthesized citrate siderophore, achromobactin. The analysis of these regions involved not only the siderophore biosynthesis clusters, but also known and predicted iron responsive genes within the *P.s.s.* B728a genome.

Iron responsive genes are regulated by GacS/SalA

Prior to this study the role of GacS/SalA in the regulation of iron responsive genes had not been extensively researched. Earlier in this study it was reported that GacS/SalA serve as negative regulators of the achromobactin gene cluster (Table 9, Fig.

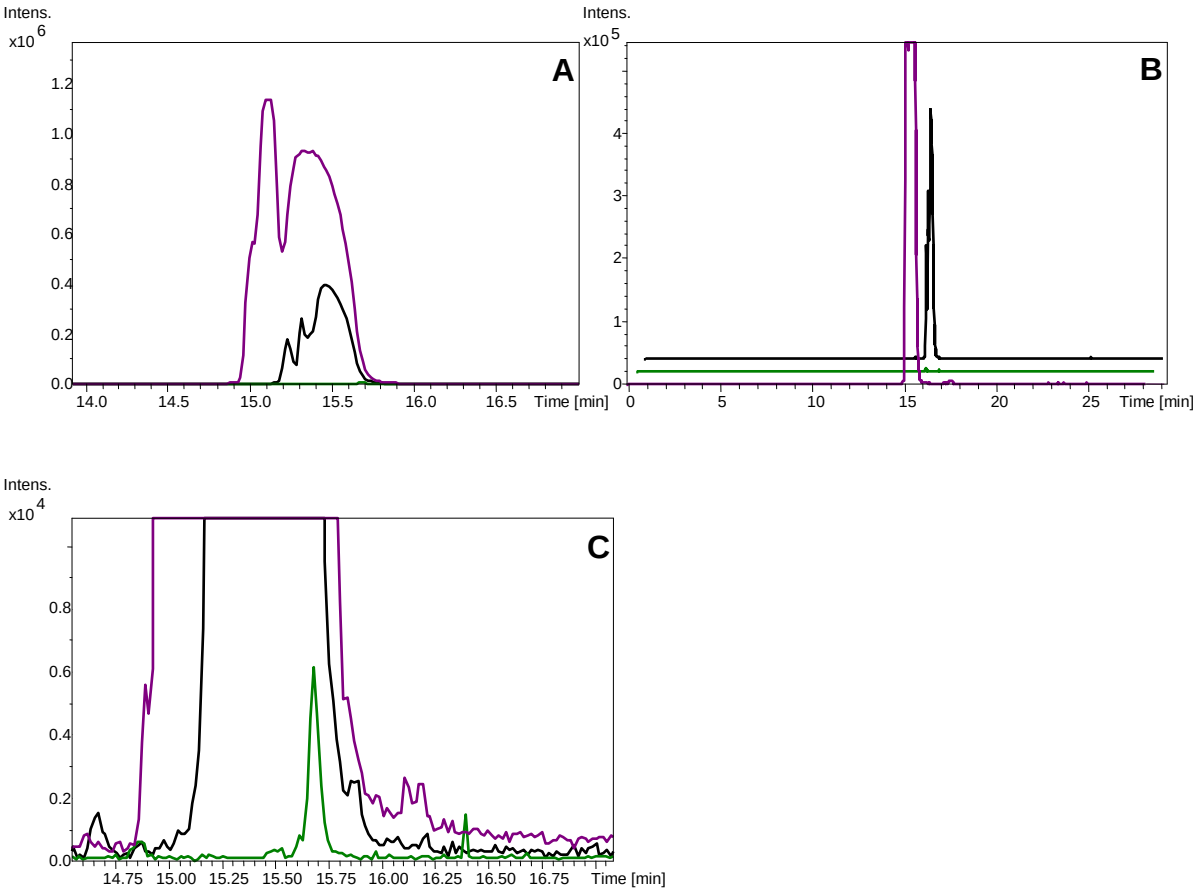

FIG. 12. LC-ESI TOF MS analysis of achromobactin from the *gacS* deletion mutant. **A.** Samples were purified from culture supernatant of the following strains grown in HMM + 1.7 mM sodium citrate for four days: *P.s.s.* B728a (green line), *P.s.s.* B728a ADB1005 (PVD)(black line), and *P.s.s.* B728a *ΔgacS* (purple line). **B.** A zoomed in view of the LC-ESI TOF MS peaks seen in A. **C.** Increased zoom to allow the visualization of the *P.s.s.* B728a achromobactin peak (green line).

11). To biologically confirm these results achromobactin was purified from the culture supernatant of *P.s.s.* B728a and *P.s.s.* B728a *ΔgacS* via a silica resin column and analyzed by liquid chromatography- electro spray ionization-time of flight- mass spectrometry (LC-ESI TOF MS). For this analysis the strain *P.s.s.* B728a ADB1005 (PVD^-) was utilized as a positive control (8). This strain has an insertion in the pyoverdine biosynthesis cluster and therefore only produces the siderophore achromobactin. Interestingly, the *P.s.s.* B728a *ΔgacS* strain with a LC-ESI TOF MS produces the largest quantity of achromobactin with an intensity of 1.15×10^6 (Fig. 12). This is over three times the intensity of the achromobactin purified from the positive control strain *P.s.s.* B728a ADB1005 (PVD^-). The achromobactin peak from wild type *P.s.s.* B728a yielded an intensity of only 0.6×10^4, 191.7 times less than the *P.s.s.* B728a *ΔgacS* strain. This data confirms the expression data from the microarray analysis, wherein expression of the achromobactin biosynthesis genes was increased in the *gacS* deletion mutant in comparison to the wild type *P.s.s.* B728a (Table 9).

The negative regulation of the siderophore achromobactin is exceptionally interesting when evaluated in context with the regulation of *P.s.s.* B728a's second siderophores, pyoverdine. As seen in Table 12, 18 pyoverdine biosynthesis and secretion genes were differentially expressed in the iron stress treatment condition showing decreased gene expression for the *gacS/salA* deletion mutant in comparison to the wild type. It is fascinating that in this study GacS/SalA appears to regulate achromobactin and pyoverdine in contrasting expression patterns. However, since this pattern is not seen in identical experimental conditions further analysis is necessary. In

the low iron treatment conditions large fold changes are seen for the pyoverdine genes; however, the achromobactin gene cluster is not differentially expressed in this condition. Furthermore, differential expression of the pyoverdine genes is not seen in the basal conditions wherein achromobactin differential expression occurs. As mentioned earlier, it is possible that the extreme iron stress of this treatment condition was not conducive for achromobactin biosynthesis. Likewise, it is likely that the basal based treatment conditions (Treatments A, B, C, and E) contained an iron concentration that was too high for pyoverdine biosynthesis.

In order to further study the dual regulation of achromobactin and pyoverdine by GacS/SalA, the deletion mutants could be grown in a more moderate low iron condition, such as the limited iron HMM media used for the achromobactin LC-ESI TOF MS analyses. The gene expression levels could then be evaluated in identical media conditions. Additionally, the production of pyoverdine could be evaluated by measuring fluorescence. Gaining further knowledge about the regulation of achromobactin and pyoverdine could greatly increase understanding of the role these siderophores play in the *P.s.s.* B728a lifecycle and whether these siderophores work in tandem with each other.

TABLE 12. Pyoverdine associated gene clusters of *P.s.s.* B728a differentially expressed between deletion mutants of GacS and/or SalA compared to wild type *P.s.s.* B728a.

Gene	Locus Tag	Op.	Function	Basal[a]		NaCl[a]		H2O2[a]		Low Fe[a]		Low N[a]		Epiphytic[a]		Apoplastic[a]	
				GacS	SalA	GacS	SalA	GacS	SalA	GacS	SalA	GacS	SalA	GacS	SalA	GacS	SalA
pvdS	*Psyr_1943*		sigma-70 factor	1	1	1	1	4.78	-2.73	1	1	1	1	1	1	1	1
	Psyr_1944		Thioesterase	1	1	1	1	4.05	1	-7.39	-27.25	1	1	1	1	1	1
	Psyr_1945		peptide synthase	1	1	1	1	1	1	-8.78	-16.69	1	1	1	1	1	1
dat	*Psyr_1946*		Diaminobutyrate-2-oxoglutarate aminotransferase	1	1	1	1	1	1	1	-28.99	1	1	1	1	1	1
	Psyr_1947		MbtH-like protein	1	1	1	1	1	1	1	-7.56	1	1	1	1	1	1
	Psyr_1948	383	ABC transporter,	1	1	1	1	1	1	1	1	1	1	1	1	1	1
	Psyr_1949	383	hypothetical protein	1	1	1	1	1	1	1	1	1	1	1	1	1	1
	Psyr_1950	383	ABC transporter	1	1	1	1	1	1	1	1	1	1	1	1	1	1
	Psyr_1951	383	Periplasmic solute binding protein	1	1	1	1	1	1	1	1	1	1	1	1	1	1
	Psyr_1952	383	hypothetical protein	1	1	1	1	1	1	1	1	1	1	1	1	1	1
	Psyr_1953	383	hypothetical protein	1	1	1	1	1	1	1	1	1	1	1	1	1	1
	Psyr_1954	383	hypothetical protein	1	1	1	1	1	1	1	-3.00	1	1	1	1	1	1
	Psyr_1955	383	peptidase	1	1	1	1	1	1	1	1	1	1	1	1	1	1
	Psyr_1956		pyoverdine biosynthesis	1	1	1	1	5.11	1	-5.97	-33.11	1	1	1	1	1	1
	Psyr_1957	384	Amino acid adenylation	1	1	1	1	1	1	1	-12.05	1	1	1	1	1	1
	Psyr_1958	384	NRPS:Amino acid adenylation	1	1	1	1	1	1	1	-11.66	1	1	1	1	1	1
	Psyr_1959	384	Amino acid adenylation	1	1	1	1	1	1	1	-18.59	1	1	1	1	1	1
	Psyr_1960	384	NRPS:Amino acid adenylation	1	1	1	1	1	1	-6.36	-11.34	1	1	1	1	1	1
	Psyr_1961		TonB-dependent siderophore receptor	1	1	1	1	1	1	1	1	1	1	1	1	1	1
	Psyr_1962		TonB-dependent siderophore receptor	1	1	1	1	9.11	1	1	-19.53	1	1	1	1	1	1
	Psyr_1963	385	Cyclic peptide transporter	1	1	1	1	1	1	1	-7.21	1	1	1	1	1	1
	Psyr_1964	385	hypothetical protein	1	1	1	1	1	1	1	-18.76	1	1	1	1	1	1
	Psyr_1965	385	Aminotransferase	1	1	1	1	1	1	1	-14.25	1	1	1	1	1	1
	Psyr_1966	385	Peptidase M19, renal dipeptidase	1	1	1	1	1	1	-5.17	-19.38	1	1	1	1	1	1
	Psyr_1967		TAT path. signal	1	1	1	1	1	1	1	-11.51	1	1	1	1	1	1
	Psyr_1968	386	RND efflux system, NodT	1	1	1	1	1	1	1	1	1	1	1	1	1	1
	Psyr_1969	386	ABC transporter	1	1	1	1	1	1	1	-7.71	1	1	1	1	1	1
	Psyr_1970	386	Secretion protein HlyD	1	1	1	1	1	1	1	-6.01	1	1	1	1	1	1

[a]Values shown are the fold change, with positive numbers reflecting an increase in gene expression in the deletion strain as compared to the wild type, a negative number reflecting a decrease in gene expression in the deletion strain as compared to the wild type.

TABLE 13. EPS gene clusters of *P.s.s.* B728a differentially expressed between deletion mutants of GacS and/or SalA compared to wild type *P.s.s.* B728a.

Gene	Locus Tag	Op.	Function	Basal[a]		NaCl[a]		H2O2[a]		Low Fe[a]		Low N[a]		Epiphytic[a]		Apoplastic[a]	
				GacS	SalA	GacS	SalA	GacS	SalA	GacS	SalA	GacS	SalA	GacS	SalA	GacS	SalA
	Psyr_3301	639	galactose phosphotransferase	1	-2.32	-2.79	-2.66	-3.45	-4.50	1	1	-6.12	-7.84	-3.29	-3.06	1	1
	Psyr_3302	639	phosphate guanyltransferase/isomerase	1	-2.57	-2.75	-2.43	-2.44	-5.15	1	-3.15	-8.16	-11.12	-4.18	-4.28	-6.16	1
	Psyr_3303	640	polysaccharide export protein	-2.76	-4.37	-2.93	1	-4.04	-7.40	-5.31	-5.43	-12.38	-11.96	-5.26	-5.17	-5.46	1
	Psyr_3304	640	lipopolysaccharide biosynthesis	-3.79	-5.89	-3.90	-3.06	-6.93	-10.35	1	-6.73	-14.73	-13.35	-6.60	-8.06	1	1
	Psyr_3305	640	glycosyl transferase	1	-3.28	1	1	-3.69	-4.31	1	1	-5.45	-6.44	1	-3.11	1	1
	Psyr_3306	640	glycoside hydrolase	1	-3.39	1	1	-4.86	-6.09	1	1	-7.94	-7.48	-4.77	-4.58	1	1
	Psyr_3307	640	glycosyl transferase	1	-3.23	1	1	-6.23	-6.24	1	-3.86	-7.62	-9.18	-3.46	-4.03	-5.04	1
	Psyr_3308	641	glycosyl transferase	-3.84	-5.71	-3.28	-3.86	-9.28	-10.49	-8.06	-6.62	-9.09	-15.50	-3.64	-5.11	-8.33	-4.63
	Psyr_3309	641	hypothetical	-4.04	-5.21	-4.05	-5.55	-12.71	-11.40	1	-4.74	-6.66	-5.16	-3.87	-4.41	1	1
	Psyr_3310	641	transferase	-2.64	-3.38	-2.88	-3.34	-5.91	-6.42	1	-3.62	-6.54	-6.31	-4.36	-3.37	1	1
	Psyr_3311	641	virulence factor MVIN-like	1	1	1	1	-2.57	-3.03	1	1	1	1	1	1	1	1
algA	*Psyr_1052*		phosphate guanyltransferase/isomerase	-4.85	1	-5.07	1	-9.14	-2.46	1	1	-8.55	-3.56	1	1	1	1
algF	*Psyr_1053*	215	alginate biosynthesis protein	-4.19	1	-3.77	1	-10.40	1	1	1	-2.31	1	1	1	1	1
algJ	*Psyr_1054*	215	alginate biosynthesis protein	-3.48	1	-3.89	1	-10.68	1	1	1	1	1	1	1	1	1
algI	*Psyr_1055*	215	membrane bound O-acyl transferase	-3.91	1	-3.88	1	-12.06	1	1	1	1	1	1	1	1	1
algL	*Psyr_1056*	216	poly(beta-D-mannuronate) lyase	-3.12	1	-2.51	1	-6.59	-2.74	1	1	1	1	1	1	1	1
algX	*Psyr_1057*	216	alginate biosynthesis protein	-3.12	1	-4.14	-4.55	-13.44	-4.12	1	1	-2.26	1	1	1	1	1
algG	*Psyr_1058*	216	parallel beta-helix repeat containing protein	-3.06	1	-4.42	-5.25	-20.88	-5.97	1	1	1	1	1	1	1	1
algE	*Psyr_1059*	216	alginate biosynthesis protein	-3.68	1	-3.86	-4.02	-22.88	-7.36	1	1	1	1	1	1	1	1
algK	*Psyr_1060*	216	Sel1 repeat containing protein	-2.94	1	-3.45	-3.38	-15.92	-6.79	1	1	1	1	1	1	1	1
alg44	*Psyr_1061*	216	alginate biosynthesis protein	-4.10	1	NA	1	-16.75	-7.71	1	1	-2.74	1	1	1	1	1
alg8	*Psyr_1062*	216	alginate biosynthesis protein	-4.20	1	-3.57	1	-18.25	-5.83	1	1	-3.23	1	1	1	1	1
algD	*Psyr_1063*		GDP mannose-6-dehydrogenase	-3.60	1	-3.58	1	-14.84	-3.54	1	1	-10.44	1	1	1	1	1
lsc-1	*Psyr_0754*		levansucrase	-2.72	-3.44	1	-3.27	1	1	1	-10.09	1.00	-3.62	1	1	1	1
lsc-2	*Psyr_2103*		levansucrase	1	1	1	1	1	1	1	1	1	1	1	1	1	1

[a]Values shown are the fold change, with positive numbers reflecting an increase in gene expression in the deletion strain as compared to the wild type, a negative number reflecting a decrease in gene expression in the deletion strain as compared to the wild type.

GacS/SalA regulates extracellular polysaccharides

The *P.s.s.* B728a genome encodes three extracellular polysaccharides, alginate, levansucrase, and Psl (99). Interestingly in the HMM basal medium the genes encoding all three of these EPS clusters showed differential gene expression in the GacS and/or SalA deletion mutants compared to the wild type (Table 13, Fig. 13). Regardless of the EPS cluster or the condition, GacS and SalA were consistently positive regulators of the EPS genes, with the deletion strains having lower gene expression than the wild type strain. The Psl gene cluster (*Psyr_3301-Psyr_3311*) showed differential gene expression in all 7 experimental conditions with the largest fold changes being seen in the nitrogen stress and oxidative stress conditions. Additionally the Psl genes were the only EPS genes to have significant differential gene expression in the plant conditions, both the GacS and SalA deletion mutants expressed the Psl genes at a lower level both in planta and epiphytically. The role of Psl in *P.s.s.* B728a survival and pathogenicity is not known; however, this study shows that Psl is being expressed both in planta and epiphytically and is regulated by GacS/SalA which makes it an interesting topic for further research.

Although this study did not show differential gene expression between the GacS/SalA deletion mutants and the wild type for the alginate and levansucrase genes in the plant conditions, these genes were differentially expressed in multiple experimental conditions. Similarly to the Psl gene cluster, the largest fold changes between the GacS/SalA deletion mutants and *P.s.s.* B728a for the alginate gene cluster were seen in the nitrogen stress and oxidative stress conditions. Further research is necessary to

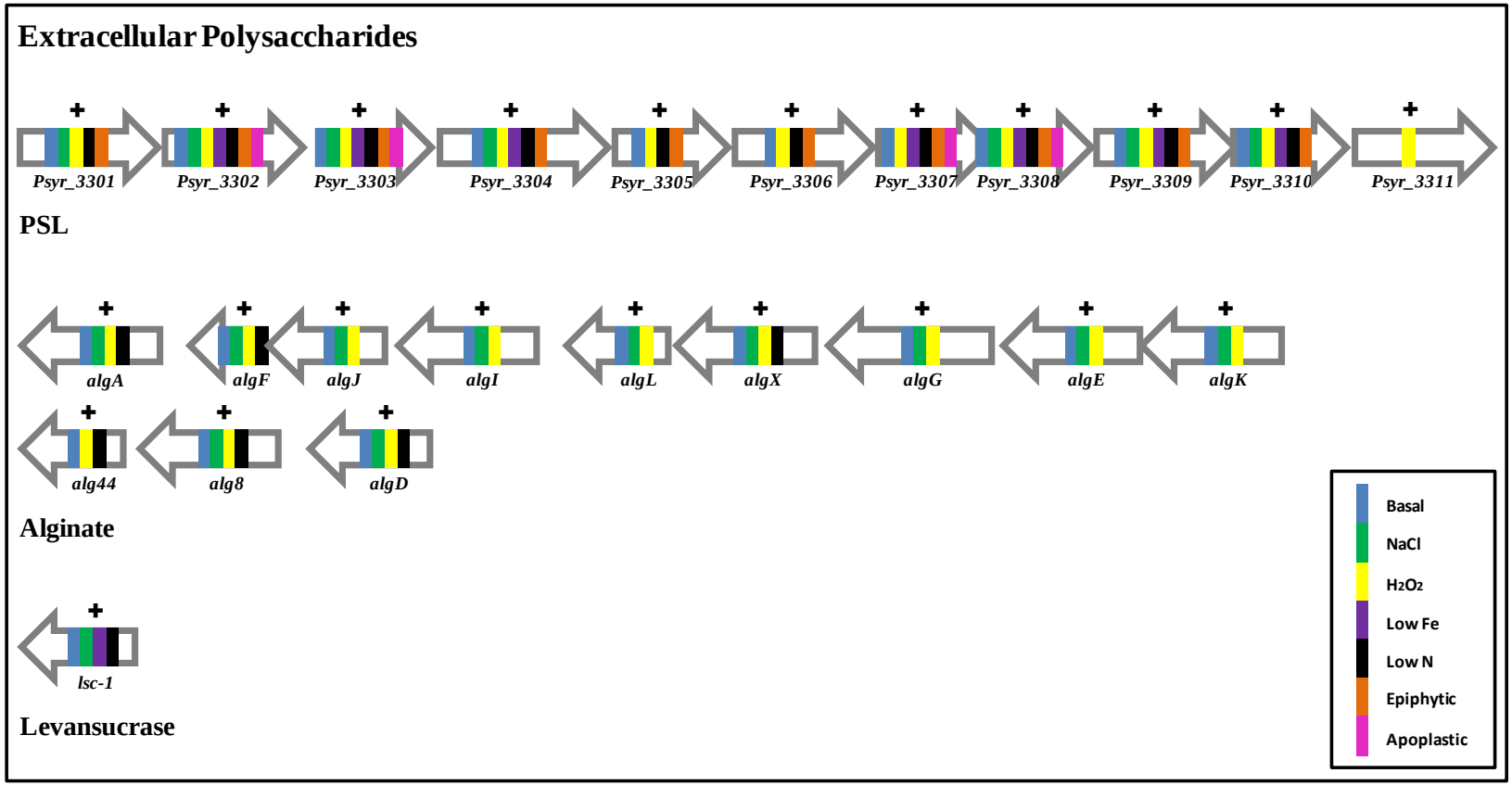

FIG 13. GacS/SalA regulation of EPS gene clusters of the *P.s.s.* B728a genome. Microarray results displaying differential gene expression of *P.s.s.* B728a *ΔgacS* and *P.s.s.* B728a *ΔsalA* compared to wild type *P.s.s.* B728a using a Q-value cut-off of 0.05. The colored bars in each gene represent those microarray conditions in which differential gene expression with a Q-value of less than 0.05 was seen, with colors being defined in the figure legend. Above each depicted gene is a symbol (+/-) representing the regulatory effect of GacS/SalA on the gene expression. The (+) represents a positive regulatory effect by GacS/SalA with the mutant constructs showing decreased relative gene expression compared to wild type. The (–) represents a negative regulatory effect by GacS/SalA with the mutant constructs showing increased relative gene expression compared to wild type.

TABLE 14. Type III secretion and effector gene clusters of *P.s.s.* B728a differentially expressed between deletion mutants of GacS and/or SalA compared to wild type *P.s.s.* B728a.

Gene	Locus Tag	Op.	Function	Basal[a]		NaCl[a]		H2O2[a]		Low Fe[a]		Low N[a]		Epiphytic[a]		Apoplastic[a]	
				GacS	SalA	GacS	SalA	GacS	SalA	GacS	SalA	GacS	SalA	GacS	SalA	GacS	SalA
avrRpm1	*Psyr_0738*		type III effector protein AvrRpm1	1	1	1	1	1	1	1	1	-2.07	1	1	1	1	1
hopAG1	*Psyr_0778*			1	1	1	1	1	1	1	1	-2.94	1	1	1	1	1
hopAH1	*Psyr_0779*			1	1	1	1	1.77	1	1	1	1	1	1	1	1	1
hopJ1	*Psyr_1017*	209	type III effector HopJ1	1	1	1	1.72	1	1	1	1	2.65	1	1	1	1	1
	Psyr_1018	209	hypothetical protein	1.47	1	1	1.85	1	1	1	1	3.40	1.88	1	1	1	1
folX	*Psyr_1019*	209	D-erythro-7,8-dihydroneopterin triphosphate 2'-epimerase	1.73	1	1	1.86	1.90	1.56	1	1	3.67	2.08	1.70	1.76	1	1
folE	*Psyr_1020*	209	GTP cyclohydrolase I	1.89	1.73	1	1.93	2.28	1.61	1	1	4.58	2.89	1.74	1	1	1
	Psyr_1021	209	short chain dehydrogenase	1.55	1	1	1.89	2.22	1	1	1	2.34	1.91	1	1	1	1
hopAA1	*Psyr_1183*		type III effector HopAA1	1	1	1	1	1	1	1	1	1	1	2.22	1	1	1
hrpW1	*Psyr_1184*		type III helper protein HrpW1	1	1	1	1	1	1	1	1	1	1	4.24	1	11.03	1
	Psyr_1185	240	effector locus protein	1	1	1	1	1	1	1	1	-1.78	1	1	1	1	1
hopM1	*Psyr_1186*	240	type III effector HopM1	1	1	1	1	1	1	1	1	1	1	1.72	1	1	1
	Psyr_1187		DspFAvrF	1	1	1	1	1	1	1	1	1	1	1	1	1	1
avrE1	*Psyr_1188*		type III effector protein AvrE1	-1.75	-1.67	1	1	1	1	1	1	-3.85	-2.44	1	1	1	1
hrpR	*Psyr_1190*	241	type III transcriptional regulator HrpR	1	1	1	1	-2.87	1	1	1	1	1	1	1	1	1
hrpS	*Psyr_1191*	241	type III transcriptional regulator HrpS	1	1	1	1	-2.09	1	1	1	1	1	1	1	1	1
hrpA2	*Psyr_1192*	242	type III helper protein HrpA2	1	1	1	1	1	1	1	1	1	2.2	4.15	2.93	1	1
hrpZ1	*Psyr_1193*	242	type III helper protein HrpZ1	-2.27	-2.80	1	1	1	1	1	1	1	1	4.16	3.18	1	1
hrpB	*Psyr_1194*	242	type III secretion protein HrpB	1	-2.44	1	1	1	1	1	1	1	1	4.34	3.10	1	1
hrcJ	*Psyr_1195*	242	type III secretion protein HrcJ	1	1	1	1	1	1	1	1	1	1	3.34	2.57	1	1
hrpD	*Psyr_1196*	242	type III secretion protein HrpD	1	1	1	1	1	1	1	1	1	1	1.90	1	1	1
hrpE	*Psyr_1197*	242	type III secretion protein HrpE	1	1	1	1	1	1	1	1	1	1	1	1	1	1
hrpF	*Psyr_1198*	242	type III secretion protein HrpF	1	1	1	1	1	1	1	1	1.46	1.64	1.97	1	1	1
hrpG	*Psyr_1199*	242	type III secretion protein HrpG	1	1	1	1	1	1	1	1	1	1	2.61	1	1	1
hrcC	*Psyr_1200*	242	outer-membrane type III secretion protein HrcC	1	1	1	1	1	1	1	1	1	1	2.39	1	1	1
hrpT	*Psyr_1201*	242	type III secretion protein HrpT	1	1	1	1	1	1	1	1	1	1	3.38	1	1	1
hrpV	*Psyr_1202*	242	negative regulator of hrp expression HrpV	1	1	1	1	1	1	1	1	1	1	1.95	1	1	1
hrcU	*Psyr_1205*	244	type III secretion protein HrcU	1	1	1	1	1	1	1	1	-1.50	1	1	1	1	1
hrcT	*Psyr_1206*	244	type III secretion protein HrcT	1	1	1	1	1	1	1	1	1	1	1	1	1	1
hrcS	*Psyr_1207*	244	type III secretion protein HrcS	1	1	1	1	1	1	1	1	-1.71	1	1	1	1	1

Table 14. Continued

Gene	Locus Tag	Op.	Function	Basal[a]		NaCl[a]		H2O2[a]		Low Fe[a]		Low N[a]		Epiphytic[a]		Apoplastic[a]	
				GacS	SalA	GacS	SalA	GacS	SalA	GacS	SalA	GacS	SalA	GacS	SalA	GacS	SalA
hrcR	*Psyr_1208*	244	type III secretion system protein	1	1	1	1	1	1	1	1	1	1	1	1	1	1
hrcQb	*Psyr_1209*	244	type III secretion protein HrcQb	1	1	1	1	1	1	1	1	1	1	1.71	1	1	1
hrcQa	*Psyr_1210*	245	type III secretion protein HrcQa	1	1	1	1	1	1	1	1	1.44	1	1	1	1	1
hrpP	*Psyr_1211*	245	type III secretion protein HrpP	1	1	1	1	1	1	1	1	1.57	1	1.66	1	1	1
hrpO	*Psyr_1212*	245	type III secretion protein HrpO	1	1	1	1	1	1	1	1	1	1	1	1	1	1
hrcN	*Psyr_1213*	245	type III secretion cytoplasmic ATPase HrcN	1	1	1	1	1	1	1	1	1.41	1	1	1	1	1
hrpQ	*Psyr_1214*	245	type III secretion protein HrpQ	1	1	1	1	1	1	1	1	1	1	1	1	1	1
hrcV	*Psyr_1215*	245	Type III secretion protein HrcV	1	1	1	1	1	1	1	1	1	1	1	1	1	1
hrpJ	*Psyr_1216*	245	type III secretion protein HrpJ	1	1	1	1	1	1	1	1	1	1	1.58	1	1	1
hrpL	*Psyr_1217*	246	Sigma-70 region 2:Sigma-70 region 4	1	1	1	1	-1.96	1	1	1	1	1	2.42	1	1	1
hrpK1	*Psyr_1218*	246	type III helper protein HrpK1	1	1	1	1	1	1	1	1	1	1	3.83	2.47	1	1
avrB3	*Psyr_1219*		type III effector protein AvrB3	1	1	1	1	1	1	1	1	2.19	2.67	6.23	4.22	1	1
hopX1	*Psyr_1220*		type III effector HopX1	1	1	1	1	1	1	1	1	1	1	2.58	1	1	1
hopZ3	*Psyr_1224*	247	type III effector HopZ3	1	1	1	1	1	1	1	1	-3.66	1	1	1	1	1
	Psyr_1225	247	hypothetical protein	1	1	1	1	1	1	1	1	-4.91	1	1	1	1	1
hopAF1	*Psyr_1889*		type III effector HopH1	-2.38	-3.26	1	1	-1.93	1	1	1	-2.42	1	2.63	1	1	1
	Psyr_1890		type III effector HopAP1	1	1	1	1	1	1	1	1	-2.37	1	1	1	1	1
	Psyr_3123		type III effector HopAH2	1.63	1.89	1	1	1	1.83	1	1	1	1.65	1	1.57	1	1
hopl1	*Psyr_4326*		type III effector HopI1	1	1	1	1	1	1	1	1	1	1	1.70	1.70	1	1
hopAB1	*Psyr_4659*		type III effector HopAB1	1	1	1	1	1	1	1	1	1	1	1.72	1.60	1	1
avrPto1	*Psyr_4919*		type III effector protein AvrPto1	1	1	1	1	2.65	1	1	1	1	1	10.36	5.19	1	1

[a]Values shown are the fold change, with positive numbers reflecting an increase in gene expression in the deletion strain as compared to the wild type, a negative number reflecting a decrease in gene expression in the deletion strain as compared to the wild type.

elucidate the roles that the three EPS systems of *P.s.s.* B728a play in both survival and pathogenicity. Furthermore, additional studies involving regulators of the EPS gene clusters that occur downstream of GacS/SalA may contribute to our understanding of these clusters and the specific role that each plays in the *P.s.s.* B728a lifecycle.

The role of GacS/SalA in the Type III secretion system

Early studies of GacS insertional mutants in *P.s.s.* B728a revealed that these strains maintain the ability to cause a hypersensitive response on non-host species thereby leading to the conclusion that GacS does not regulate the Type III secretion system in this strain. However, this study reveals that in the epiphytic condition GacS/SalA is negatively regulating many components of the Type III secretion system including both the secretion apparatus and effector proteins (Table 14). In *P. syringae* strains the genes encoding the Type III secretion apparatus are found in a conserved pathogenicity island called the hrp cluster (hypersensitive response and pathogenesis) (39). Amongst this cluster is the HrpZ operon (*Psyr_1192-Psyr_1202*) which encodes one of the most abundantly secreted proteins, the harpin HrpZ (40). With both membrane binding and pore-forming functions, this protein is predicted to form the pores in host cell membranes that permits the Type III pillus structure to permeate the host (39, 40). The Type III pilus structure is composed of self-assembling HrpA proteins, which are also encoded in the HrpZ operon (39). Another Type III apparatus associated protein encoded in this operon is HrcJ, which is believed to be embedded in the bacterial cell membranes and associated with the foundation of the Type III pilus

(39). As seen in Table 14, in the epiphytic condition of the microarray analysis the Type III pilus associated genes HrpZ, HrpA, and HrcJ showed differential gene expression between the wild type *P.s.s.* B728a and the GacS and SalA deletion mutants. For each of these mutants the expression of these genes was over 2.5 fold higher in the GacS/SalA mutants than in the wild type.

In addition to the Type III secretion apparatus, *P.s.s.* B728a encodes 23 genes that have been identified as Type III effectors (66). Most effector molecules are transported through the Type III pilus and translocated directly into the plant cell; although a few Hrp outer protein (Hop) effectors are function as helper proteins at the surface between the plant and the bacterium (66). Characterization of individual effectors has proven difficult, as most mutations do not result in detectable phenotypes. Additionally, several effectors are encoded in operons which have yet to be fully defined. In this study numerous effector genes displayed differential gene expression between the GacS and/or SalA deletion mutants and the wild type *P.s.s.* B728a, especially in the epiphytic condition (Table 14). The largest fold change between wild type and mutant was seen in the epiphytic condition for the effector gene, *avrPto1,* with over 10 fold higher expression of the *avrPto1* gene in the GacS mutant compared to the wild type. In *P.s.t.* DC3000 the AvrPto1 effector interferes with host map kinase

pathways to suppress host plant resistance responses (64). It is likely that this effector plays a similar role in *P.s.s.* B728a.

It is also noteworthy, that in the epiphytic treatment condition the *hrpL* sigma factor gene has over 2 fold higher expression in the GacS deletion mutant than in the wild type strain (Table 14). Previously it has been postulated that *hrpL* is induced by the interaction of the RpoN-RNA polymerase with the heterodimer protein of the regulators, HrpR and HrpS (110). It is possible that GacS is involved in the regulation of one or more of these *hrpL* inducing factors. It is also possible that GacS regulates alternative transcriptional factors that are involved in the activation of *hrpL* expression.

This study reveals that GacS/SalA are involved in the negative regulation of the Type III secretion apparatus and effectors, as well as, the *hrpL* sigma factor. Previous studies have shown that the sensor kinase proteins RetS and LadS regulate the expression of *hrpL* and *hrpR* in a reciprocal fashion (99). In conjunction with the findings of this microarray, I propose that the *P.s.s. B728a* Type III secretion system is being regulated by a multisensory signaling network composed of GacS, RetS, and LadS, as seen in *P. aeruginosa* (13, 33, 99).

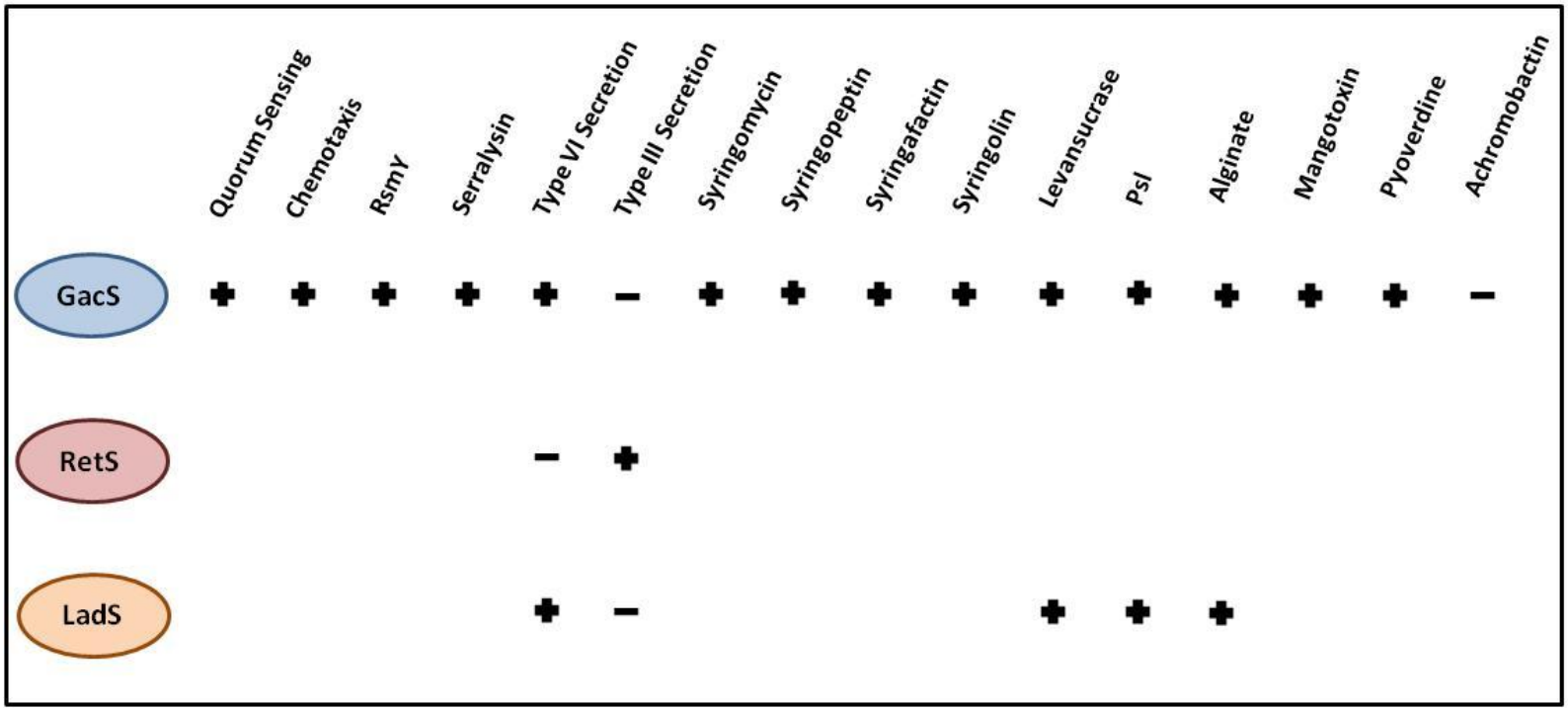

FIG. 14. The regulatory effects of GacS, RetS, and LadS on various virulence and epiphyticly associated systems in *P.s.s.* B728a. A plus sign (+) represents a positive regulatory effect of the sensor kinase on the gene target. A negative (-) sign indicates a negative regulatory effect of the sensor kinase on the gene target. Those spaces left blank denote that the regulatory effect is currently unknown.

Conclusions

With thousands of genes showing differential gene expression between the GacS and SalA deletion mutants and the wild type strain, the process of analyzing this data is both daunting and exhilarating. The strength of the study is reaffirmed by the regulatory patterns of gene clusters that were previously known, such as the positive regulation of syringomycin and syringopeptin by GacS and SalA. Furthermore, new insights arise with findings such as the negative regulation of the Type III secretion system. One consisitent pattern that emerges from this study is the overlapping regulons of the sensor kinases GacS, RetS, and LadS (Figure 14). As the data from this collaborative study continues to be analyzed, especially the expression data from the *retS* deletion mutant strain, the extent of these overlapping regulons should be further elucidated. This study confirms the role of GacS in the regulation of major virulence components of *P.s.s.* B728a such as phytotoxin production and Type III secretion. However, this study has also established the sensor's role in the regulation of factors important for epiphytic survival and function, such as the Type VI secretion system, iron acquisition, and EPS production. Since the GacS/RetS/LadS multisensory regulon of *P. aeruginosa* is essential to the transition from acute to chronic infection of human lungs, I hypothesize that GacS, RetS, and LadS function as a multisensory system that serves as the master switch between the epiphytic and pathogenic lifestyle of *P.s.s.* B728a (99). Thus, this study has provided the foundation and preliminary hypotheses for an abundance of future studies regarding the complex regulation of the *P.s.s.* B728a lifecycle.

CHAPTER IV

CONCLUSIONS

P.s.s. B728a is an exceptionally interesting plant pathogen due to its adeptness at surving as an epiphyte in the phyllosphere. Although the genome of *P.s.s.* B728a is available and many of the key virulence and pathogenicity factors have been identified and studied, key questions remain concerning the lifestyle of this organism. This dissertation reports on the analysis of several gene regulatory networks of *P.s.s.* B728a that have provided valuable insight into the bacterium's ability to acquire iron and a potential mechanism for the transistion between epiphytic and pathogenic lifestyles.

An RNA-seq analysis reveals that the sigma factor AcsS is a positive regulator of the citrate siderophore achromobactin. Other iron associated genes, including the siderophores pyoverdine, are also positively regulated by AcsS. Given these findings I hypothesize that achromobactin and pyoverdine have a collaborative role in the acquirement of iron. In addition to iron associated genes, an RND-efflux system, mangotoxin-like biosynthesis, Psl biosynthesis, Type IV pili, and cell motility genes were also differentially expressed in this study. Independently, these gene clusters are all known or hypothesized to play a role in the epiphytic survival and function of *P.s.s.* B728a. Additionally, the deletion of *acsS* did not have an apparent effect on the amount or severity of disease in vacuum infiltrated plants hosts. Therefore, it is likely that AcsS and the achromobactin siderophores cluster function primarily on the leaf surface.

Future studies should include analysis of the *P.s.s.* B728a *ΔacsS* and its ability to survive and function as an epiphyte. This could include the utilization of *gfp* reporter so that the formation of bacterial colonies could be microscopically evaluated. These studies should evaluate the ability of *P.s.s.* B728a *ΔacsS* to establish bacterial populations' of equivalent size to the wild type strain. Additionally, the *P.s.s.* B728a *ΔacsS* strain should be evaluated for its ability to form biofilms. The regulon of the AcsS sigma factor can be further elucidated by investigating those regulatory factors identified in the RNA-Seq analysis, such as the sigma factor *Psyr_4731*. This study has provided support for numerous novel hypotheses regarding the role of siderophores in the *P.s.s.* B728a lifecycle.

The remainder of this disseratation addresses the regulation of *P.s.s.* B728a at a global level and the nature of the transition between epiphyte and pathogen. Microarray analysis of the GacS and SalA deletion mutants across seven experimental conditions reveals the repeated overlap of the regulons of sensor kinases GacS, RetS, and Lads. Given these consistent overlaps, I propose that GacS, RetS, and LadS function as a multisensory system that serves as the master switch between the epiphytic and pathogenic lifestyle of *P.s.s.* B728a. Further analysis of the microarray study, including the regulon of the *P.s.s.* B728a *ΔretS* strain should be performed. Additionally, the small RNAs RsmY and RsmZ should be analyzed in *P.s.s.* B728a to determine if they are the sole transcriptional targets of the histidine kinase, GacA, as is the case in *P. aeruginosa*.

Further persuit of the role of GacS in the Type III secretion system should also be persued. Since the GacS deletion strain overexpressed the Type III secretion pilus and effector genes, as well as, *hrpL*, I hypothesize that an overexpressor strain of GacS would have a decrease in Type III expression and function.

As high throughput sequencing and expression analysis becomes more inexpensive, the ability of the scientific community to sequence genomes and perform transcriptome analyses can expand. With these studies science can begin to comprehend the regulation of gene networks at a global level. These discoveries should prove invaluable to our understanding of pathogenicity and allow for major breakthroughs in applied protection against plant pathogens. For instance, the long-term outcomes of this study may include the limitation of iron acquisition on the leaf surface to prevent *P.s.s.* B728a from reaching the threshold population for host infection and disease. Alternatively, the microarray aspect of this study could lead to the identification of the signaling molecules directly detected by GacS, RetS, and LadS. If these signals were known, it may be possible to provide constitutive signal to the appropriate regulator that would prevent *P.s.s.* B728a from expressing pathogenicity genes.

REFERENCES

1. **Alfano, J.R. and A. Collmer.** 1997. The type III (Hrp) secretion pathway of plant pathogenic bacteria: trafficking harpins, Avr proteins, and death. J. Bacteriol. **179:**5655-5662.

2. **Anderson, C.** 2003. Channel-tunnels: outer membrane components of type I secretion systems and multidrug efflux pumps of gram-negative bacteria. Rev. Physiol. Biochem. Pharmacol. **147:**122-165.

3. **Arrebola, E., F.M. Cazorla, J.C. Codina, J.A. Gutiérrez-Barranquero, A. Pérez-García, and A. de Vicente.** 2009. Contribution of mangotoxin to the virulence and epiphytic fitness of *Pseudomonas syringae* pv. *syringae*. Int. Microbiol. **12:**87-95.

4. **Arrebola, E., F.M. Cazorla, D. Romero, A. Peréz-Garcia, and A. deVicente.** 2007. A nonribosomal peptide synthetase gene (*mgoA*) of *Pseudomonas syringae* pv. *syringae* is involved in mangotoxin biosynthesis and is required for full virulence. Mol. Plant-Microbe Interact. **20:**500-509.

5. **Banin, E., M.L. Vasil, and E.P. Greenberg.** 2005. Iron and *Pseudomonas aeruginosa* biofilm formation. Proc. Natl. Acad. Sci. U.S.A. **102:**11076-11081.

6. **Bender, C. L., F. Alarcon-Chaidez, and D. C. Gross.** 1999. *Pseudomonas syringae* phytotoxins: mode of action, regulation, and biosynthesis by peptide and polyketide synthetases. Microbiol. Mol. Biol. Rev. **63:**266-292.

7. **Bernard, P. and M. Couturier.** 1992. Cell killing by the F plasmid CcdB protein involves poisoning of DNA-topoisomerase II complexes. J. Mol. Biol. **226:**735-745.

8. **Berti, A.D. and M.G. Thomas.** 2009. Analysis of achromobactin biosynthesis by *Pseudomonas syringae* pv. *syringae* B728a. J. Bacteriol. **191:**4594-4604.

9. **Berti, A.D., N. J. Greve, Q. H. Christensen, and M. G. Thomas.** 2007. Identification of a biosynthetic gene cluster and the six associated lipopeptides involved in swarming motility of *Pseudomonas syringae* pv. *tomato* DC3000. J. Bacteriol. **189:**6312-6323.

10. **Blair, J.M.A. and L.J.V. Piddock.** 2009. Structure, function and inhibition of RND efflux pumps in gram-negative bacteria: an update. Curr. Opin. Microbiol. **12:**512-519.

11. **Bleuel, C., C. Grobe, N. Taudte, J. Scherer, D. Wesenberg, G.J. Kraub, D.H. Nies, and G. Grass.** 2005. TolC is involved in enterobactin efflux across the outer membrane of *Escherichia coli*. J. Bacteriol. **187:**6701-6707.

12. **Briat, J.** 2006. Cellular and whole organism aspects of iron transport and storage in plants. Topics in Current Genetics. **14:**193-213.

13. **Brencic, A., K.A. McFarland, H.R. McManus, S. Castang, I. Mogno, S.L. Dove, and S. Lory.** 2009. The GacS/GacA signal transduction system of *Pseudomonas aeruginosa* acts exclusively through its control over the transcription of the RsmY and RsmZ regulatory small RNAs. Mol. Microbiol. **73:**434-445.

14. **Burch, A.Y., B.K. Shimada, P.J. Browne, and S.E. Lindow.** 2010. Novel high-throughput detection method to assess bacterial surfactant production. Appl. Environ. Microbiol. **76:**5363-5372.

15. **Bustin, S.A., V. Benes, J.A. Garson, J. Hellemans, J. Huggett, M. Kubista, R. Mueller, T. Nolan, M.W. Pfaffl, G.L. Shipley, J. Vandesompele, and C.T. Wittwer.** 2009. The MIQE guidelines: minimum information for publication of quantitative real-time PCR experiments. Clin. Chem. **55:**611-622.

16. **Challis, G.L.** 2005. A widely distributed bacterial pathway for siderophore biosynthesis independent of nonribosomal peptide synthetases. ChemBioChem. **6:**601-611.

17. **Cody, Y. S., and D. C. Gross.** 1987. Characterization of pyoverdin$_{pss}$, the fluorescent siderophore produced by *Pseudomonas syringae* pv. *syringae*. Appl. Environ. Microbiol. **53:**928-934.

18. **Cody, Y. S., and D. C. Gross.** 1987. Outer membrane protein mediating iron uptake via pyoverdine$_{pss}$, the fluorecent siderophore produced by *Pseudomonas syringae* pv. *syringae*. J. Bacteriol. **169:**2207-2214.

19. **Cornelis, P.** 2010. Iron uptake and metabolism in pseudomonads. Appl. Microbiol. Biotechnol. **86:**1637-1645.

20. **Cornelis, P. and J. Bodelis.** 2009. A survey of TonB-dependent receptors in fluorescent pseudomonads. Environ. Microbiol. Reports. **1:**256-262.

21. **Croucher, N.J., M.C. Fookes, T.T. Perkins, D.J. Turner, S.B. Marguerat, T. Keane, M.A. Quail, M. He, S. Assefa, J. Bähler, R.A. Kingsley, J. Parkhill, S.D. Bentley, G. Dougan, and N.R. Thomson.** 2009. A simple method for directional transcriptome sequencing using Illumina technology. Nucleic Acids Res. **22:**e148-e157.

22. **Curie, C. and J. Briat.** 2003. Iron transport and signaling in plants. Annu. Rev. Plant Biol. **54:**183-206.

23. **Dasgupta, N., M.C. Wolfgang, A.L. Goodman, S.K. Arora, J. Jyot, S. Lory, and R. Ramphal.** 2003. A four-tiered transcriptional regulatory circuit controls flagellar biogenesis in *Pseudomonas aeruginosa*. Mol. Microbiol. **50:**809-824.

24. **Datsenko, K. A., and B. L. Wanner.** 2000. One-step inactivation of chromosomal genes in *Escherichia coli* K-12 using PCR products. Proc. Natl. Acad. Sci. U. S. A. **97:**6640-6645.

25. **Expert, D.** 1999. Withholding and exchanging iron: interactions between *Erwinia* spp. and their plant hosts. Annu. Rev. Phytopathol. **37:**307-334.

26. **Feil, H., W. S. Feil, P. Chain, F. Larimer, G. DiBartolo, A. Copeland, A. Lykidis, S. Trong, M. Nolan, E. Goltsman, J. Thiel, S. Malfatti, J. E. Loper, A. Lapidus, J. C. Detter, M. Land, P. M. Richardson, N. C. Kyrpides, N. Ivanova, and S. E. Lindow.** 2005. Comparison of the complete genome sequences of *Pseudomonas syringae* pv. *syringae* B728a and pv. *tomato* DC3000. Proc. Natl. Acad. Sci. U. S. A. **102:**11064-11069.

27. **Filiatrault, M.J., P.V. Stodghill, P.A. Bronstein, S. Moll, M. Lindeberg, G. Grills, P. Schweitzer, W. Wang, G.P. Schroth, S. Luo, I. Khrebtukova, Y. Yang, T. Thannhauser, B.G. Butcher, S. Cartinhour, and D.J. Schneider.** 2010. Transcriptome analysis of *Pseudomonas syringae* identifies new genes, noncoding RNAs, and antisense activity. J. Bacteriol. **192:**2359-2372.

28. **Franza, T., B. Mahe, and D. Expert.** 2005. *Erwinia chrysanthemi* requires a second iron transport route dependent of the siderophore achromobactin for extracellular growth and plant infection. Mol. Microbiol. **55:**261-275.

29. **Friedman, L. and R. Kolter.** 2004. Two genetic loci produce distinct carbohydrate-rich structural components of the *Pseudomonas aeruginosa* biofilm matrix. J. Bacteriol. **186:**4457-4465.

30. **Fuqua, W.C., S.C. Winans, and E.P. Greenberg.** 1994. Quorum sensing in bacteria: the LuxR-LuxI family of cell density-responsive transcriptional regulators. J. Bacteriol. **176:** 269-275.

31. **Glasner, J.D., C. Yang, S. Reverchon, N. Hugouvieux-Cotte-Pattat, G. Condemine, J. Bohin, F. Van Gijsegem, S. Yang, T. Franza, D. Expert, G. Plunkett III, M.J. San Francisco, A.O. Charkowski, B. Py, K. Bell, L. Rauscher, P. Rodriguez-Palenzuela, A. Toussaint, M.C. Holeva, S.Y. He, V. Douet, M. Boccara, C. Blanco, I. Toth, B.D. Anderson, B.S. Biehl, B. Mau, S.M. Flynn, F. Barras, M. Lindeberg, P. Birch, S. Tsuyumu, X. Shi, M. Hibbing, M. Yap, M. Carpentier, E. Dassa, M. Unehara, J.F. Kim, M. Rusch, P. Soni, G.F. Mayhew, D.E. Fouts, S.R. Gill, F.R. Blattner, N.T. Keen, and N.T. Perna.** 2011. Genome sequence of the plant pathogenic bacterium *Dickeya dadantii* 3937. J. Bacteriol. **193:**2076-2077.

32. **Goel, A.K., L. Rajagopal, N. Nagesh, and R.V. Sonti.** 2002. Genetic locus encoding functions involved in biosynthesis and outer membrane localization of xanthomonadin in *Xanthomonas oryzae* pv. *oryzae*. J. Bacteriol. **184:**3539-3548.

33. **Goodman, A.L., M. Merighi, M. Hyodo, I. Ventre, A. Filloux, and S. Lory.** 2009. Direct interaction between sensor kinase proteins mediates acute and chronic disease phenotypes in a bacterial pathogen. Genes Dev. **23:**249-259.

34. **Grant, S.G.N., J. Jessee, F.R.. Bloom, and D. Hanahan.** 1990. Differential plasmid rescue from transgenic mouse DNAs into *Escherichia coli* methylation restriction mutants. Proc. Natl. Acad. Sci. U.S.A. **87:**4645-4649.

35. **Groll, M., B. Schellenberg, A.S. Bachmann, C.R. Archer, R. Huber, T.K. Powell, S. Lindow, M. Kaiser, and R. Dudler.** 2008. A plant pathogen virulence factor inhibits the eukaryotic proteasome by a novel mechanism. Nature. **452:**755-759.

36. **Gross, D. C.** 1985. Regulation of syringomycin synthesis in *Pseudomonas syringae* pv *syringae* and defined conditions for its production. J. Appl. Bacteriol. **58:**167-174.

37. **Guerinot, M. L.** 1994. Microbial iron transport. Annu. Rev. Microbiol. **48:**743-772.

38. **Guerinot, M.L. and Y. Yi.** 1994. Iron: nutritious, noxious, and not readily available. Plant Physiol. **104:** 815-820.

39. **Guttman, D.S., S.J. Gropp, R.L. Morgan, and P.W. Wang.** 2006. Diversifying selection drives the evolution of the type III secretion system pilus of *Pseudomonas syringae.* Mol. Biol. Evol. **23:**2342-2354.

40. **Haapalainen, M., S. Engelhardt, I. Küfner, C. Li, T. Nürnberger, J. Lee, M. Romantschuk, and S. Taira.** 2011. Functional mapping of harpin HrpZ of *Pseudomonas syringae* reveals the sites responsible for protein oligomerization, lipid interactions and plant defence induction. Mol. Plant Pathol. **12:**151-166.

41. **Heeb, S. and D. Haas.** 2001. Regulatory roles of the GacS/GacA two-component system in plant-associated and other gram-negative bacteria. Mol. Plant-Microbe Interact. **14:**1351-1363.

42. **Hirano, S. S., and C. D. Upper.** 1990. Population biology and epidemiology of *Pseudomonas syringae*. Annu. Rev. Phytopathol. **28:**155-177.

43. **Hirano, S.S. and C.D. Upper.** 2000. Bacteria in the leaf ecosystem with emphasis on *Pseudomonas syringae*- a pathogen, ice nucleus, and epiphyte. Microbiol. Mol. Biol. Rev. **64:**624-653.

44. **House, B.L., M.W. Mortimer, and M.L. Kahn.** 2004. New recombination methods for *Sinorhizobium meliloti* genetics. Appl. Environ. Microbiol. **70:**2806-2815.

45. **Howden, A.J.M., A. Rico, T. Mentlak, L. Miguet, and G.M. Preston.** 2009. *Pseudomonas syringae* pv. *syringae* B728a hydrolyses indole-3-acetonitrile to the plant hormone indole-3-acetic acid. Mol. Plant Pathol. **10:**857-865.

46. **Hrabak, E.M. and D.K. Willis.** 1992. The lemA gene required for pathogenicity of *Pseudomonas syringae* pv. *syringae* on bean is a member of a family of two-component regulators. J. Bacteriol. **174:**3011-3020.

47. **Huynh, T. V., D. Dahlbeck, and B. J. Staskawicz.** 1989. Bacterial blight of soybean: regulation of a pathogen gene determining host cultivar specificity. Science. **245:**1374-1377.

48. **Jackson, K.D., M. Starkey, S. Kremer, M.R. Parsek, and D.J. Wozniak.** 2004. Identification of *psl*,a locus encoding a potential exopolysaccharide that is essential for *Pseudomonas aeruginosa* PAO1 biofilm formation. J. Bacteriol. **186:**4466-4475.

49. **Jahn, C.E., A.O. Charkowski, and D.K. Willis.** 2008. Evaluation of isolation methods and RNA integrity for bacterial RNA quantitation. J. Microbiol. Methods. **75:**318-324.

50. **Jones, A. M., S. E. Lindow, and M. C. Wildermuth.** 2007. Salicylic acid, yersiniabactin, and pyoverdin production by the model phytopathogen *Pseudomonas syringae* pv. *tomato* DC3000: Synthesis, regulation, and impact on tomato and *Arabidopsis* host plants. J. Bacteriol. **189:**6773-6786.

51. **Joyner, D. C., and S. E. Lindow.** 2000. Heterogeneity of iron bioavailability on plants assessed with a whole-cell GFP-based bacterial biosensor. Microbiology. **146:**2435-2445.

52. **Kadurugamuwa, J.L., H. Anwar, M.R. Brown, G.H. Shand, and K.H. Ward.** 1987. Media for study of growth kinetics and envelope properties of iron-deprived bacteria. J. Clin. Microbiol. **25:**849-855.

53. **Kang, H. and D. C. Gross.** 2005. Characterization of a resistance-nodulation-cell division transporter system associated with the *syr/syp* genomic island of *Pseudomonas syringae* pv. *syringae*. Appl. Environ. Microbiol. **71:**5056-5065.

54. **Kendziorski, C., R.A. Irizarry, K.S. Chen, J.D. Haag, and M.N. Gould.** 2005. On the utility of pooling biological samples in microarray experiments. Proc. Natl. Acad. Aci. U.S.A. **102:**4252-4257.

55. **Kida, Y., H. Inoue, T. Shimizu, and K. Kuwano.** 2007. *Serratia marcescens* serralysin induces inflammatory responses through protease-activated receptor 2. Infect. Immun. **75:**164-174.

56. **King, E. O., M. K. Ward, and D. E. Raney.** 1954. Two simple media for the demonstration of pyocyanin and fluorescin. J. Lab. Clin. Med. **44:**301-307.

57. **Kinscherf, T. G. and D. K. Willis.** 1999. Swarming by Pseudomonas syringae B728a requires gacS (lemA) and gacA but not the acyl-homoserine lactone biosynthetic gene ahlI. J. Bacteriol. **181:**4133-4136.

58. **Kitten, T., T. G. Kinscherf, J. L. McEvoy, and D. K. Willis.** 1998. A newly identified regulator is required for virulence and toxin production in *Pseudomonas syringae*. Mol. Microbiol. **28:**917-929.

59. **Koorts, A.M. and M. Viljoen.** 2007. Ferritin and ferritin isoforms I: structure-function relationships, synthesis, degradation and secretion. Arch. Physiol. Biochem. **113:**30-54.

60. **Lamont, I. L., L. W. Martin, T. Sims, A. Scott, and M. Wallace.** 2006. Characterization of a gene encoding an acetylase required for pyoverdine synthesis in *Pseudomonas aeruginosa*. J. Bacteriol. **188:**3149-3152.

61. **Landy, A.** 1989. Dynamic, structural, and regulatory aspects of λ site-specific recombination. Annu. Rev. Biochem. **58:**913-949.

62. **Lavin, J.L., K. Kiil, O. Resano, D.W. Ussery, and J.A. Oguiza.** 2007. Comparative genomic analysis of two-component regulatory proteins in *Pseudomonas syringae*. BMC Genomics. **8:**397-408.

63. **Leong, S.A., G.S. Ditta, and D.R. Helinski.** 1982. Heme biosynthesis in *Rhizobium*: identification of a cloned gene coding for δ-aminolevulinic acid synthetase from *Rhizobium meliloti*. J. Biol. Chem. **257:**8724-8730.

64. **Lewis, J.D., D.S. Guttman, and D. Desveaux.** 2009. The targeting of plant cellular systems by injected type III effector proteins. Seminars in Cell & Developmental Biology. **20:**1055-1063.

65. **Lim, S. P., N. Roongsawang, K. Washio, and M. Morikawa.** 2007. Functional analysis of a pyoverdine synthetase from *Pseudomonas* sp MIS38. Biosci. Biotechnol. Biochem. **71:**2002-2009.

66. **Lindeberg, M., S. Cartinhour, C.R. Myers, L.M. Schechter, D.J. Schneider, and A. Collmer.** 2006. Closing the circle on the discovery of genes encoding Hrp regulon members and type III secretion system effectors in the genomes of three model Pseudomonas syringae strains. Mol. Plant-Microbe Interact. **19:**1151-1158.

67. **Lindow, S. E. and M. T. Brandl.** 2003. Microbiology of the phyllosphere. Appl. Environ. Microbiol. **69:**1875-1883.

68. **Liu, F., T. Jenssen, J. Trimarchi, C. Punzo, C.L. Cepko, L. Ohno-Machado, E. Hovig, and W.P. Kuo.** 2007. Comparison of hybridization-based and sequencing-based gene expression technologies on biological replicates. BMC Genomics. **8:**153-166.

69. **Liu, R. and H. Ochman.** 2007. Stepwise formation of the bacterial flagellar system. Proc. Natl. Acad. Sci. U.S.A. **104:**7116-7121.

70. **Livny, J., H. Teonadi, M. Livny, and M.K. Waldor.** 2008. High-throughput, kingdom-wide prediction and annotation of bacterial non-coding RNAs. PLoS ONE. **3:**e3197.

71. **Loper, J.E., and S.E. Lindow.** 1987. Lack of evidence for in situ fluorescent pigment production by *Pseudomonas syringae* pv. *syringae* on bean leaf surfaces. Phytopathology. **77:**1449-1454.

72. **Louis, D., J. Bernillon, and J.M. Wallach.** 1998. Specificity of *Pseudomonas aeruginosa* serralysin revisited, using biologically active peptides as substrates. Biochimica et Biophysica Acta. **1387:**378-386.

73. **Lu, S. E., B. K. Scholz-Schroeder, and D. C. Gross.** 2002. Characterization of the *salA*, *syrF*, and *syrG* regulatory genes located at the right border of the syringomycin gene cluster of *Pseudomonas syringae* pv. *syringae*. Mol. Plant-Microbe Interact. **15:**43-53.

74. **Lu, S. E., N. Wang, J. L. Wang, Z. J. Chen, and D. C. Gross.** 2005. Oligonucleotide microarray analysis of the *salA* regulon controlling phytotoxin production by *Pseudomonas syringae* pv. *syringae*. Mol. Plant-Microbe Interact. **18:**324-333.

75. **Ma, L., H. Lu, A. Sprinkle, M.R. Parsek, and D.J. Wozniak.** 2007. *Pseudomonas aeruginosa* Psl is a galactose- and mannose-rich exopolysaccharide. J. Bacteriol. **189:**8353-8356.

76. **Marahiel, M. A., T. Stachelhaus, and H. D. Mootz.** 1997. Modular peptide synthetases involved in nonribosomal peptide synthesis. Chem. Rev. **97:**2651-2673.

77. **Marco, M.L., J. Legac, and S.E. Lindow.** 2003. Conditional survival as a selection strategy to identify plant-inducible genes of *Pseudomonas syringae*. Appl. Environ. Microbiol. **69:**5793-5801.

78. **Marco, M.L., J. Legac, and S.E. Lindow.** 2005. *Pseudomonas syringae* genes induced during colonization of leaf surfaces. Environ. Microbiol. **7:**1379-1391.

79. **Marioni, J.C., C.E. Mason, S.M. Mane, M. Stephens, and Y. Gilad.** 2008. RNA-seq: An assessment of technical reproducibility and comparison with gene expression arrays. Genome Res. **18:**1509-1517.

80. **Masse, E., H. Salvail, G. Desnoyers, and M. Arguin.** 2007. Small RNAs controlling iron metabolism. Curr. Opin. Microbiol. **10:**140-145.

81. **McMahon, S.A., M. Oke, H. Liu, K.A. Johnson, L. Carter, N. Kadia, M.F. White, G.L. Challis, and J.H. Naismith.** 2008. Purification, crystallization and data collection of *Pectobacterium chrysanthemi* AcsD, a type A siderophore synthetase. Acta Cryst. **F64:**1052-1055.

82. **Miethke, M., and M. A. Marahiel.** 2007. Siderophore-based iron acquisition and pathogen control. Microbiol. Mol. Biol. Rev. **71:**413-451.

83. **Mila, I., A. Scalbert, and D. Expert.** 1996. Iron withholding by plant polyphenols and resistance to pathogens and rots. Phytochemistry. **42:**1551-1555.

84. **Miller, W.G., J.H.J. Leveau, and S.E. Lindow.** 2000. Improved *gfp* and *inaZ* broad-host-range promoter-probe vectors. Mol. Plant-Microbe Interact. **13:**1243-1250.

85. **Mortazavi, A., B.A. Williams, K. McCue, L. Schaeffer, and B. Wold.** 2008. Mapping and quantifying mammalian transcriptomes by RNA-seq. Nat. Methods. **5:**621-628.

86. **Mossialos, D., and G. D. Amoutzias.** 2007. Siderophores in fluorescent pseudomonads: new tricks from an old dog. Future Microbiol. **2:**387-395.

87. **Munzinger, M., H. Budzikiewicz, D. Expert, C. Enard, and J. Meyer.** 2000. Achromobactin, a new citrate siderophore of *Erwinia chrysanthemi*. Z. Naturforsch. **55:**328-332.

88. **Nettleton, D., J.T.G. Hwang, R.A. Caldo, and R.P. Wise.** 2006. Estimating the number of true null hypotheses from a histogram of p-values. Journal of Agricultural, Biological, and Environmental Statistics. **11:**337-356.

89. **Oguiza, J. A., K. Kiil, and D. W. Ussery.** 2005. Extracytoplasmic function sigma factors in *Pseudomonas syringae*. Trends Microbiol. **13:**565-568.

90. **O'Toole, G.A. and R. Kolter.** 1998. Flagellar and twitching motility are necessary for *Pseudomonas aeruginosa* biofilm development. Molecular Microbio. **30:**295-304.

91. **Peng, X., C.L. Wood, E.M. Blalock, K.C. Chen, P.W. Landfield, and A.J. Stromberg.** 2003. Statistical implications of pooling RNA samples for microarray experiments. BMC Bioinformatics. **4:**26-34.

92. **Perkins, T.T., R.A. Kingsley, M.C. Fookes, P.P. Gardner, K.D. James, L. Yu, S.A. Assefa, M. He, N.J. Croucher, D.J. Pickard, D.J. Maskell, J. Parkhill, J. Choudhary, N.R. Thomson, and G. Dougan.** 2009. A strand-specific RNA-seq analysis of the transcriptome of the typhoid bacillus *Salmonella typhi.* PLoS Genetics. **5:**e1000569-e1000581.

93. **Piddock, L.J.V.** 2006. Multidrug-resistance efflux pumps- not just for resistance. Nature Rev. **4:**629-636.

94. **Quigley, N. B., and D. C. Gross.** 1994. Syringomycin production among strains of *Pseudomonas syringae* pv *syringae* : conservation of the *syrB* and *syrD* genes and activation of phytotoxin production by plant signal molecules. Mol. Plant-Microbe Interact. **7:**78-90.

95. **Quinones, B., C.J. Pujol, and S.E. Lindow.** 2004. Regulation of AHL production and its contribution to epiphytic fitness in *Pseudomonas syringae*. Mol. Plant-Microbe Interact. **17:**521-531.

96. **Quinones, B., G. Dulla, and S.E. Lindow.** 2005. Quorum sensing regulates exopolysaccharide production, motility, and virulence in *Pseudomonas syringae*. Mol. Plant-Microbe Interact. **18:**682-693.

97. **Ramel, C., M. Tobler, M. Meyer, L. Bigler, M. Ebert, B. Schellenberg, and R. Dudler.** 2009. Biosynthesis of the proteasome inhibitor syringolin A: the ureido group joining two amino acids originates from bicarbonate. BMC Biochem. **10:**26-35.

98. **Records, A.R. 2011.** The type VI secretion system: a multi-purpose delivery system with a phage-like machinery. Mol. Plant-Microbe Interact. **24:**751-757.

99. **Records, A.R. and D.C. Gross.** 2010. Sensor kinases RetS and LadS regulate *Pseudomonas syringae* Type VI secretion and virulence factors. J. Bacteriol. **192:**3584-3596.

100. **Sambrook, J., E. F. Fritsch, and T. Maniatis.** 1989. Molecular Cloning: A Laboratory Manual. Cold Spring Harbor Lab. Press, Plainview, NY, 2nd Ed.

101. **Sawahel, W., G. Sastry, C. Knight, and D. Cove.** 1993. Development of an electrotransformation system for *Escherichia coli* DH10B. Biotechnol. Tech. **7:**261-266.

102. **Schellenberg, B., C. Ramel, and R. Dudler.** 2010. *Pseudomonas syringae* virulence factor syringolin A counteracts stomatal immunity by proteasome inhibition. Mol. Plant-Microbe Interact. **23:**1287-1293.

103. **Scholz-Schroeder, B. K., M. L. Hutchison, I. Grgurina, and D. C. Gross.** 2001. The contribution of syringopeptin and syringomycin to virulence of *Pseudomonas syringae* pv. *syringae* strain B301D on the basis of *sypA* and *syrB1* biosynthesis mutant analysis. Mol. Plant-Microbe Interact. **14:**336-348.

104. **Scholz-Schroeder, B. K., J. D. Soule, and D. C. Gross.** 2003. The *sypA*, *sypB* and *sypC* synthetase genes encode twenty-two modules involved in the

nonribosomal peptide synthesis of syringopeptin by *Pseudomonas syringae* pv. *syringae* B301D. Mol. Plant-Microbe Interact. **16:**271-280.

105. **Scholz-Schroeder, B. K., J. D. Soule, S. E. Lu, I. Grgurina, and D. C. Gross.** 2001. A physical map of the syringomycin and syringopeptin gene clusters localized to an approximately 145-kb DNA region of *Pseudomonas syringae* pv. *syringae* strain B301D. Mol. Plant-Microbe Interact. **14:**1426-1435.

106. **Singh, G. M., P. D. Fortin, A. Koglin, and C. T. Walsh.** 2008. beta-Hydroxylation of the aspartyl residue in the phytotoxin syringomycin E: characterization of two candidate hydroxylases AspH and SyrP in *Pseudomonas syringae*. Biochemistry **47:**11310-11320.

107. **Sorek, R. and P. Cossart.** 2010. Prokaryotic transcriptomics: a new view on regulation, physiology, and pathogenicity. Nat. Rev. Genet. **11:**9-16.

108. **Stephan, U. W. and G. Scholz.** 1993. Nicotianamine: mediator of transport of iron and heavy metals in the phloem? Physiol. Plant. **88:**522-529.

109. **Swingle, B., D. Thete, M. Moll, C. R. Myers, D. J. Schneider, and S. Cartinhour.** 2008. Characterization of the PvdS-regulated promoter motif in *Pseudomonas syringae* pv. *tomato* DC3000 reveals regulon members and insights regarding PvdS function in other pseudomonads. Mol. Microbiol. **68:**871-889.

110. **Tang, X., Y. Xiao, and J. Zhou.** 2006. Regulation of the type III secretion system in phytopathogenic bacteria. Mol. Plant-Microbe Interact. **19:**1159-1166.

111. **Theil, E. C.** 1987. Ferritin: structure, gene regulation, and cellular function in animals, plants, and microorganisms. Ann. Rev. Biochem. **56:**289-315.

112. **Vansuyt, G., A. Robin, J. F. Briat, C. Curie, and P. Lemanceau.** 2007. Iron acquisition from Fe-pyoverdine by *Arabidopsis thaliana*. Mol. Plant-Microbe Interact. **20:**441-447.

113. **Venturi, V.** 2006. Regulation of quorum sensing in *Pseudomonas*. FEMS Microbiol. Rev. **30:**274-291.

114. **Visca, P., F. Imperi, and I. L. Lamont.** 2007. Pyoverdine siderophores: from biogenesis to biosignificance. Trends Microbiol. **15:**22-30.

115. **Visca, P., L. Leoni, M. J. Wilson, and I. L. Lamont.** 2002. Iron transport and regulation, cell signalling and genomics: lessons from *Escherichia coli* and *Pseudomonas*. Mol. Microbiol. **45:**1177-1190.

116. **Voulhoux, R., A. Filloux, and I. J. Schalk.** 2006. Pyoverdine-mediated iron uptake in *Pseudomonas aeruginosa*: the tat system is required for PvdN but not for FpvA transport. J. Bacteriol. **188:**3317-3323.

117. **Wang, L., Z. Feng, X. Wang, X. Wang, and X. Zhang.** 2009. DEGseq: an R package for identifying differentially expressed genes from RNA-seq data. Bioinformatics. **26:**136-138.

118. **Wang, N., S. E. Lu, A. R. Records, and D. C. Gross.** 2006. Characterization of the transcriptional activators SalA and SyrF, which are required for syringomycin and syringopeptin production by *Pseudomonas syringae* pv. *syringae*. J. Bacteriol. **188:**3290-3298.

119. **Wang, N., S. E. Lu, J. L. Wang, Z. J. Chen, and D. C. Gross.** 2006. The expression of genes encoding lipodepsipeptide phytotoxins by *Pseudomonas syringae* pv. *syringae* is coordinated in response to plant signal molecules. Mol. Plant-Microbe Interact. **19:**257-269.

120. **Wang, N., S. E. Lu, Q. W. Yang, S. H. Sze, and D. C. Gross.** 2006. Identification of the *syr-syp* box in the promoter regions of genes dedicated to syringomycin and syringopeptin production by *Pseudomonas syringae* pv. *syringae* B301D. J. Bacteriol. **188:**160-168.

121. **Wang, Z., M. Gerstein, and M. Snyder.** 2009. RNA-Seq: a revolutionary tool for transcriptomics. Nat. Rev. Genet. **10:**57-63.

122. **Weber, K.A., L.A. Achenbach, and J.D. Coates.** 2006. Microorganisms pumping iron: anaerobic microbial iron oxidation and reduction. Nat. Rev. Microbiol. **4:**752-764.

123. **Wensing, A., S.D. Braun, P. Buttner, D. Expert, B. Volksch, M.S. Ullrich, and H. Weingart.** 2010. Impact of siderophore production by *Pseudomonas syringae* pv. *syringae* 22d/93 on epiphytic fitness and biocontrol activity against *Pseudomonas syringae* pv. *glycinea* 1a/96. Appl. Environ. Microbiol. **76:**2704-2711.

124. **Williams, P.** 2007. Quorum-sensing, communication and cross-kingdom signaling in the bacterial world. Microbiology. **153:**3923-3938.

125. **Willis, D.K., J.J. Holmstadt, and T.G. Kinscherf.** 2001. Genetic evidence that loss of virulence associated with *gacS* or *gacA* mutations in *Pseudomonas syringae* B728a does not result from effects on alginate production. Appl. Environ. Microbiol. **67:**1400-1403.

126. **Yang, C. and D.E. Crowley.** 2000. Rhizosphere microbial community structure in relation to root location and plant iron nutritional status. Appl. Environ. Microbiol. **66:**345-351.

127. **Yang, C., M. Gavilanes-Ruiz, Y. Okinaka, R. Vedel, I. Berthuy, M. Boccara, J. Wei-Ta Chen, N. T. Perna, and N. T. Keen.** 2002. *hrp* genes of *Erwinia chrysanthemi* 3937 are important virulence factors. Mol. Plant-Microbe Interact. **15:**472-480.

128. **Yu, J., A. Penaloza-Vazquez, A.M. Chakrabarty, and C.L. Bender.** 1999. Involvement of the exopolysaccharide alginate in the virulence and epiphytic fitness of *Pseudomonas syringae* pv. *syringae*. Mol. Microbiol. **33:**712-720.

APPENDIX A

TABLE A-1. Strains and plasmids used in this study.

Designation	Relevant Characteristics	Source
Bacterial Strains		
E. coli		
DB3.1	F$^-$ *gyrA462 endA1 glnV44* Δ(*sr1-recA*) *mcrB mrr hsdS20*(rB$^-$ mB$^-$) *ara14 galK2 lacY1 proA rpsL20*(Sm^r) *xyl5* Δ*leu mtl1*	(7)
DH10B	F$^-$ *mcrA* Δ*lacX74* (Φ80d*lacZΔM15*) Δ(mrr-*hsdRMS-mcrB*) *deoR recA1 endA1 araD139* Δ(*ara, leu*)7697 *galU galK λ*$^-$ *rpsL nupG*	(34)
One Shot®TOP10	F$^-$ *mcrA* Δ(mrr-hsdRMS-mcrB) Φ80*lacZΔM15* Δ*lacX74 recA1 araD139* Δ*(ara-leu)7697 galU galK rpsL (Str^R) endA1 nupG*	Invitrogen
Mach1 T1™	F$^-$ Δ*recA1398 endA1 tonA* φ80(*lacZ*)ΔM15 Δ*lacX74 hsdR*(rK$^-$ mK$^+$)	Invitrogen
SW105	DY380 (*cro-bioA*) <>*araC*-P$_{BAD}$*Cre* Δ*galK*	National Cancer Institute
P. syringae* pv. *syringae		
B728a	Wild-type, bean pathogen; Rif^r	(71)
B728aΔ*acsS*	*acsS* mutant derivative of B728a, Rif^r	This study
B728a ADB1005 (PVD$^-$)	*pvdL::nptII* (Kan^r)	(8)
B728aΔ*gacS*	*gacS* mutant derivative of B728a, Rif^r	(99)
B728aΔ*salA*	*salA* mutant derivative of B728a, Rif^r	This study
B728aΔ*retS*	*retS* mutant derivative of B728a, Rif^r	(99)
B728a Δ*acsS* pPROBE-KT': *acsS*	Complemented strain of the *acsS* mutant derivative of B728a, Rif^r Km^r	This study
Plasmids		
pBH474	*flp* constitutively expressed; Gm^r Suc^s	(42)
pENTR/D-TOPO	Gateway entry vector; Km^r	Invitrogen
pE*acsS*	pENTR/D-TOPO carrying *acsS*, Km^r	This study
pE*salA*	pENTR/D-TOPO carrying *salA*, Km^r	This study
pKD13	Template plasmid containing FRT-flanked *nptII*	(23)
pLVCD	Gateway destination vector for mating with *P. syringae*; pBR322 derivative with *mob* genes from RSF1010; Tc^r Ap^r Cm^r	(75)
pLV*acsS*	pLVCD carrying *acsS*; Tc^r Ap^r	This study
pLV*salA*	pLVCD carrying *salA*; Tc^r Ap^r	This study
pLV*acsS*-FP	pLVCD carrying upstream and downstream regions of *acsS* fused to *nptII*; Tc^r Ap^r Km^r	This study
pLV*salA*-FP	pLVCD carrying upstream and downstream regions of *salA* fused to *nptII*; Tc^r Ap^r Km^r	This study
pRK2073	Helper plasmid; Sp^r Trm^r	(61)
pPROBE-KT'	Complementation vector	(81)

TABLE A-2. Primers used for PCR and qRT-PCR amplification.

Name	Sequence	Source
Prr2580F	CACCAAAAACGCCCGCTGATGAG	This study
Prr2580R	GCGCCGGCCGAACTCCA	This study
Prr2580KmF	CTCATTTGGCGCATCCCATCGCTCAAGGCTTTTGACGTGTAGGCTGGAGCTGCTTCG	This study
Prr2580KmR	CTACCTCGCGTTCTTCGTTCGAAGGTGCCGGGCGAAATTCCGGGGATCCGTCGACC	This study
P-*acs*ScompF	ATATCGGAATTCTGGACTCGGGATATAACACTAA	This study
P-*acs*ScompR	ATATATGAATTCTGCCGGGCGAATCACCAGT	This study
PrrsalAF	CACCCACCGAAGCCGAAGCCATTGTCA	This study
PrrsalAR	TTGCCAATACATCCTCGTCCTACC	This study
PrrsalAKmF	AAAATCCCCGAACGTGGGACAGCAATTGGACGCCTTGTGTAGGCTGGAGCTGCTTCG	This study
PrrsalAKmR	GGCGTGTCTCTTTATAAACGGAAAAAGGAACCCCGAATTCCGGGGATCCGTCGACC	This study
qRTrecAF	CTTCGGTACGCCTGGACA	(74)
qRTrecAR	AACTCGGCCTGACGGAAC	(74)
qRT16SF	ACACCGCCCGTCACACCA	(74)
qRT16SR	GTTCCCCTACGGCTACCTT	(74)
qRT2580F	ATCATCATGGCTGGCTGGAAAGC	This study
qRT2580R	TCAAGGCTGCGACGAGTGTAGAAA	This study

TABLE A-3. RNA-Seq analysis of *P.s.s.* B728a and *P.s.s.* B728a *ΔacsS*.

Gene	Locus Tag	Op.	Function	RPKM *P.s.s.* B728a	RPKM *P.s.s.* B728a *ΔacsS*	log2 (Fold_change) normalized	Fold Change	z-score	p-value	q-value[1]	q-value[2]
acsS	*Psyr_2580*	508	Sigma 70 RNA polymerase	136.893	0.000	9.850	**923.156**	10.248	**1.20E-24**	1.60E-22	1.46E-22
yhcA	*Psyr_2586*	509	EmrB/QacA family drug resistance transporter; Acr	249.999	6.075	5.363	**41.160**	16.410	**1.62E-60**	5.99E-58	5.46E-58
acsD	*Psyr_2584*	509	IucA/IucC; Acr biosynthesis	797.588	19.916	5.324	**40.054**	29.297	**1.12E-188**	1.93E-185	1.76E-185
acsB	*Psyr_2588*	509	HpcH/HpaI aldolase; Acr	266.547	6.717	5.311	**39.689**	16.932	**2.61E-64**	1.04E-61	9.48E-62
acsE	*Psyr_2585*	509	Orn/DAP/Arg decarboxylase 2:Orn/DAP/Arg decarboxylase 2; Acr biosynthesis	653.997	20.271	5.012	**32.269**	26.362	**3.74E-153**	3.23E-150	2.94E-150
acsC	*Psyr_2587*	510	IucA/IucC; Acr biosynthesis	370.861	12.322	4.912	**30.103**	19.795	**3.31E-87**	2.14E-84	1.95E-84
acsF	*Psyr_2583*		diaminobutyrate--2-oxoglutarate aminotransferase; Acr	1236.351	48.339	4.677	**25.581**	35.849	**1.92E-281**	9.96E-278	9.07E-278
pseB	*Psyr_2621*	516	secretion protein HlyD	67.474	3.494	4.272	**19.314**	8.204	**2.33E-16**	1.77E-14	1.62E-14
	Psyr_2582		Ton-B dependent siderophore receptor; predicted Acr secretion	340.215	18.525	4.199	**18.368**	18.339	**4.04E-75**	1.90E-72	1.74E-72
acsA	*Psyr_2589*	510	IucA/IucC; Acr biosynthesis	379.257	25.374	3.902	**14.949**	18.944	**4.98E-80**	2.58E-77	2.36E-77
pseA	*Psyr_2620*	516	RND efflux system, outer membrane lipoprotein, NodT	86.604	7.242	3.580	**11.961**	8.782	**1.61E-18**	1.41E-16	1.29E-16
pseC	*Psyr_2622*	516	Acriflavin resistance protein	77.560	7.328	3.404	**10.586**	8.147	**3.75E-16**	2.78E-14	2.53E-14
mgoA	*Psyr_5011*	983	amino acid adenylation:thioester reductase; predicted mangotoxin	89.544	17.050	2.393	**5.253**	7.332	**2.27E-13**	1.29E-11	1.18E-11
	Psyr_5009	983	hypothetical; predicted mangotoxin	143.162	30.178	2.246	**4.745**	8.927	**4.39E-19**	4.14E-17	3.78E-17
cbrA	*Psyr_2590*	510	periplasmic binding protein	126.280	27.467	2.201	**4.598**	8.280	**1.24E-16**	9.57E-15	8.72E-15
	Psyr_5010	983	hypothetical; predicted mangotoxin	81.749	20.346	2.007	**4.019**	6.281	**3.36E-10**	1.57E-08	1.43E-08
	Psyr_5012	983	hypothetical; predicted mangotoxin	51.150	12.922	1.985	**3.959**	4.934	**8.07E-07**	2.30E-05	2.10E-05
	Psyr_0288		carbonate dehydratase	48.010	13.168	1.867	**3.647**	4.587	**4.49E-06**	0.0001152	0.000105

Table A-3. Continued.

Gene	Locus Tag	Op.	Function	RPKM *P.s.s.* B728a	RPKM *P.s.s.* B728a *ΔacsS*	log2 (Fold_change) normalized	Fold Change	z-score	p-value	q-value[1]	q-value[2]
cbrB	*Psyr_2591*	510	transport system permease protein	44.708	13.753	1.701	**3.251**	4.152	**3.30E-05**	0.0007102	0.000647
	Psyr_2595	511	dimethylmenaquinone methyltransferase	62.925	23.454	1.424	**2.683**	4.326	**1.52E-05**	0.0003594	0.000328
	Psyr_1136		hypothetical	61.613	23.196	1.410	**2.657**	4.248	**2.16E-05**	0.0004823	0.000439
	Psyr_3369	648	twin-arginine translocation pathway signal:Tat-translocated enzyme:Dyp-type peroxidase; TAT secretion	411.180	164.543	1.322	**2.499**	10.449	**1.48E-25**	2.08E-23	1.90E-23
	Psyr_3368	648	hypothetical	181.767	72.831	1.320	**2.496**	6.939	**3.95E-12**	2.05E-10	1.87E-10
	Psyr_1950	383	ABC transporter	64.844	26.004	1.318	**2.494**	4.141	**3.46E-05**	0.0007407	0.000675
	Psyr_3632		hypothetical	58.901	24.482	1.267	**2.406**	3.826	**0.000130**	0.0023847	0.002173
fleR	*Psyr_3459*	665	helix-turn-helix, Fis-type; regulation of flagella	62.161	25.961	1.260	**2.395**	3.914	**9.08E-05**	0.0016876	0.001538
	Psyr_4015		hypothetical	99.538	43.932	1.180	**2.266**	4.704	**2.55E-06**	6.85E-05	6.24E-05
	Psyr_3370	648	hypothetical	677.237	302.118	1.165	**2.242**	12.146	**5.99E-34**	1.15E-31	1.05E-31
	Psyr_2594	511	hypothetical	59.100	26.377	1.164	**2.241**	3.585	**0.000336**	0.0056705	0.005167
	Psyr_3023		hypothetical	862.947	396.286	1.123	**2.178**	13.316	**1.86E-40**	4.59E-38	4.18E-38
	Psyr_3305	640	glycocyl transferase, group 1; predicted EPS Psl	120.839	56.778	1.090	**2.129**	4.862	**1.16E-06**	3.25E-05	2.97E-05
fdhD_narQ	*Psyr_4945*	969	formate dehyrogenase, subunit FdhD	75.230	35.606	1.079	**2.113**	3.806	**0.000141**	0.0025676	0.00234
	Psyr_3243		Ton-B dependent siderophore receptor	78.585	37.457	1.069	**2.098**	3.860	**0.000113**	0.0020821	0.001897
	Psyr_3130	607	Secretion protein HlyD; multidrug efflux	63.125	30.179	1.065	**2.092**	3.448	**0.000564**	0.0088666	0.008057
	Psyr_1387		ferredoxin--NADP(+) reductase	89.935	43.250	1.056	**2.080**	4.089	**4.33E-05**	0.0008908	0.000812
	Psyr_3061	593	putative glutathione S-transferase	65.211	31.633	1.044	**2.062**	3.448	**0.000564**	0.0088413	0.008057
	Psyr_1952	383	hypothetical	140.216	68.836	1.027	**2.037**	4.988	**6.10E-07**	1.78E-05	1.62E-05
	Psyr_1938	382	response regulator receiver	71.478	35.136	1.025	**2.035**	3.556	**0.000376**	0.0062432	0.005689

Table A-3. Continued.

Gene	Locus Tag	Op.	Function	RPKM *P.s.s.* B728a	RPKM *P.s.s.* B728a *ΔacsS*	log2 (Fold_change) normalized	Fold Change	z-score	p-value	q-value[1]	q-value[2]
	Psyr_4731	927	RNA polymerase sigma factor	160.586	79.283	1.019	**2.026**	5.303	**1.14E-07**	3.62E-06	3.30E-06
fleS	*Psyr_3460*	665	flagellar sensor histidine kinase FleS	81.380	40.279	1.015	**2.021**	3.764	**0.000167**	0.0030222	0.002754
gidA	*Psyr_5132*	1007	tRNA uridine 5-carboxymethylaminomethyl modification enzyme GidA	107.554	53.303	1.013	**2.018**	4.321	**1.56E-05**	0.0003669	0.000334
pslB	*Psyr_3302*	639	mannose-1-phosphate guanylyltransferase/mannose-6-phosphate isomerase; predicted EPS Psl	97.601	48.507	1.009	**2.012**	4.102	**4.09E-05**	0.0008594	0.000783
	Psyr_0784	157	CheW-like protein	146.608	73.539	0.996	**1.994**	4.973	**6.59E-07**	1.90E-05	1.73E-05
	Psyr_4730	927	FecR protein, Fe dicitrate sensor, membrane component	154.461	77.561	0.994	**1.992**	5.098	**3.44E-07**	1.04E-05	9.44E-06
	Psyr_1964	385	hypothetical	539.980	272.896	0.985	**1.979**	9.460	**3.08E-21**	3.40E-19	3.10E-19
	Psyr_2053	405	moxR protein, putative	74.778	38.232	0.968	**1.956**	3.470	**0.000521**	0.0083173	0.007579
	Psyr_1953	383	hypothetical	137.429	70.415	0.965	**1.952**	4.691	**2.71E-06**	7.26E-05	6.61E-05
	Psyr_4393	853	secretion	68.563	35.323	0.957	**1.941**	3.291	**0.000998**	0.0147201	0.013384
	Psyr_4255		FKBP-type peptidyl-prolyl isomerase, N-terminal:peptidylprolyl isomerase, FKBP-type	536.200	276.244	0.957	**1.941**	9.206	**3.40E-20**	3.39E-18	3.09E-18
	Psyr_2434		carbohydrate kinase, PfkB, fructokinase	106.368	54.857	0.956	**1.939**	4.094	**4.25E-05**	0.0008778	0.0008
	Psyr_4260	829	hypothetical	1027.066	529.941	0.955	**1.938**	12.720	**4.60E-37**	1.04E-34	9.46E-35
fleN	*Psyr_3438*	661	flagellar synthesis regulator, cobyrinic acid a,c-diamide synthase	138.985	71.740	0.954	**1.938**	4.674	**2.95E-06**	7.80E-05	7.11E-05
	Psyr_3308	641	glycosyl transferase, group 1; predicted EPS Psl	103.156	53.930	0.936	**1.913**	3.962	**7.44E-05**	0.001434	0.001307
	Psyr_3303	640	polysaccharide export protein; predicted EPS Psl	78.158	40.923	0.934	**1.910**	3.442	**0.000577**	0.0090031	0.008186
	Psyr_0374		phosphorylase	247.501	129.677	0.933	**1.909**	6.120	**9.36E-10**	4.08E-08	3.72E-08
	Psyr_3309	641	hypothetical; predicted EPS Psl	74.782	39.209	0.932	**1.908**	3.361	**0.000777**	0.0117231	0.010683

Table A-3. Continued.

Gene	Locus Tag	Op.	Function	RPKM *P.s.s.* B728a	RPKM *P.s.s.* B728a *ΔacsS*	log2 (Fold_change) normalized	Fold Change	z-score	p-value	q-value[1]	q-value[2]
	Psyr_4376		LuxR response regulator receiver	201.766	106.256	0.925	**1.899**	5.489	**4.04E-08**	1.40E-06	1.27E-06
	Psyr_4373	851	PAS	108.344	57.257	0.920	**1.893**	4.004	**6.24E-05**	0.0012311	0.001122
	Psyr_2739		ThiJ/PfpI family protein	105.284	55.669	0.920	**1.892**	3.944	**8.02E-05**	0.0015176	0.001383
leuC	*Psyr_1983*	390	isopropylmalate isomerase large subunit	187.768	99.526	0.916	**1.887**	5.250	**1.52E-07**	4.67E-06	4.25E-06
	Psyr_0458		helicase, C-terminal:Type III restriction enzyme, res subunit:DEAD/DEAH box helicase, N-terminal	81.832	43.423	0.914	**1.885**	3.461	**0.000538**	0.0085497	0.007791
	Psyr_3345		TonB-dependent siderophore receptor	211.262	112.174	0.914	**1.884**	5.556	**2.76E-08**	9.80E-07	8.93E-07
	Psyr_1072		extracellular solute-binding protein	264.573	140.547	0.913	**1.883**	6.214	**5.16E-10**	2.37E-08	2.16E-08
	Psyr_1966	385	peptidase M19, renal dipeptidase	534.590	284.774	0.909	**1.878**	8.802	**1.34E-18**	1.20E-16	1.10E-16
gabT	*Psyr_0090*		4-aminobutyrate aminotransferase	124.126	66.546	0.900	**1.866**	4.204	**2.62E-05**	0.0005818	0.00053
	Psyr_0392		hypothetical	130.452	70.201	0.894	**1.859**	4.288	**1.81E-05**	0.0004163	0.000379
	Psyr_4946	969	oxidoreductase alpha (molybdopterin) subunit; TCA cycle	197.110	106.193	0.893	**1.856**	5.263	**1.42E-07**	4.44E-06	4.05E-06
	Psyr_1965	385	twin-arginine translocation pathway signal; secretion	492.200	265.477	0.891	**1.854**	8.304	**1.00E-16**	7.88E-15	7.18E-15
	Psyr_2462	484	nitrite/sulfite reductase, hemoprotein beta-component, ferrodoxin-like:nitrite and sulphite reductase 4Fe-4S region; sulfur metabolism	119.100	64.378	0.888	**1.850**	4.072	**4.66E-05**	0.0009482	0.000864
3xrn	*Psyr_0579*	112	3'-5' exoribonuclease, VacB and RNase II	120.796	65.790	0.877	**1.836**	4.058	**4.94E-05**	0.0009943	0.000905
glgA	*Psyr_2992*	580	trehalose synthesis, glycogen synthase; osmoadaptation	122.629	66.983	0.873	**1.831**	4.072	**4.66E-05**	0.0009509	0.000864
	Psyr_2799		hypothetical	420.648	231.121	0.864	**1.820**	7.481	**7.36E-14**	4.34E-12	3.95E-12
	Psyr_1903	377	hypothetical	82.091	45.152	0.863	**1.818**	3.299	**0.000969**	0.014327	0.013055
	Psyr_0629		aldehyde dehydrogenase	265.302	146.505	0.857	**1.811**	5.898	**3.67E-09**	1.48E-07	1.35E-07
	Psyr_0785	157	histidine kinase, HAMP region: chemotaxis sensory transducer	192.842	106.699	0.854	**1.808**	5.014	**5.32E-07**	1.58E-05	1.44E-05
	Psyr_1770	360	enoyl-CoA hydratase/isomerase	299.818	166.641	0.848	**1.799**	6.212	**5.23E-10**	2.38E-08	2.17E-08

Table A-3. Continued.

Gene	Locus Tag	Op.	Function	RPKM *P.s.s.* B728a	RPKM *P.s.s.* B728a *ΔacsS*	log2 (Fold_change) normalized	Fold Change	z-score	p-value	q-value[1]	q-value[2]
	Psyr_4596	897	hypothetical	266.882	148.478	0.846	**1.798**	5.853	**4.84E-09**	1.92E-07	1.74E-07
	Psyr_1963	385	cyclic peptide transporter; pyoverdine ABC transporter, ATP-binding/permease protein	271.697	151.415	0.844	**1.795**	5.891	**3.85E-09**	1.54E-07	1.40E-07
	Psyr_1477	300	hypothetical	597.108	334.703	0.835	**1.784**	8.660	**4.72E-18**	3.95E-16	3.60E-16
	Psyr_2634		histidine kinase, HAMP region: chemotaxis sensory transducer	183.324	102.849	0.834	**1.783**	4.791	**1.66E-06**	4.50E-05	4.10E-05
	Psyr_3372	649	hypothetical	227.268	127.649	0.832	**1.781**	5.326	**1.01E-07**	3.28E-06	2.99E-06
	Psyr_3060		GAF:ATP-binding region, ATPase-like:histidine kinase A, N-terminal	132.336	74.331	0.832	**1.781**	4.064	**4.83E-05**	0.0009797	0.000893
	Psyr_0200		hypothetical; predicted signal transduction mechanism	112.423	63.249	0.830	**1.778**	3.736	**0.000186**	0.0033193	0.003025
pepA	*Psyr_1091*		leucyl aminopeptidase	424.332	238.739	0.830	**1.778**	7.260	**3.88E-13**	2.19E-11	2.00E-11
	Psyr_1769	360	Acyl-CoA dehydrogenase, C-terminal:Acyl-CoA dehydrogenase, central region:Acyl-CoA dehydrogenase, N-terminal	268.511	152.724	0.814	**1.758**	5.680	**1.34E-08**	4.91E-07	4.47E-07
	Psyr_3304	640	lipopolysaccharide biosynthesis; predicted EPS Psl	104.473	59.578	0.811	**1.754**	3.529	**0.0004174**	0.0068101	0.006206
	Psyr_3024		peptidase M14, carboxypeptidase A	151.451	86.749	0.804	**1.746**	4.220	**2.44E-05**	0.0005434	0.000495
tssA	*Psyr_4966*		ImpA, N-terminal; type VI secretion-associated protein	159.548	91.735	0.799	**1.740**	4.306	**1.66E-05**	0.0003899	0.000355
	Psyr_0391		Poly granule associated	260.053	149.533	0.799	**1.739**	5.497	**3.86E-08**	1.34E-06	1.22E-06
	Psyr_4150	809	hypothetical	294.527	169.704	0.796	**1.736**	5.832	**5.48E-09**	2.11E-07	1.92E-07
	Psyr_4676		hypothetical	165.991	95.717	0.795	**1.734**	4.372	**1.23E-05**	0.0002993	0.000273
	Psyr_4125		hypothetical	193.730	112.437	0.785	**1.723**	4.676	**2.93E-06**	7.79E-05	7.10E-05
fliF	*Psyr_3457*	664	flagellar MS-ring protein	101.617	59.198	0.780	**1.717**	3.366	**0.000762**	0.011534	0.01051
	Psyr_3367	648	Iron permease FTR1	268.993	157.030	0.777	**1.713**	5.459	**4.79E-08**	1.62E-06	1.48E-06
	Psyr_1090	221	DNA polymerase III subunit chi	298.615	174.729	0.773	**1.709**	5.730	**1.00E-08**	3.72E-07	3.39E-07
	Psyr_3373		hypothetical	1243.845	728.437	0.772	**1.708**	11.686	**1.51E-31**	2.70E-29	2.46E-29
	Psyr_0360		Serine O-acetyltransferase	229.524	134.550	0.771	**1.706**	5.009	**5.48E-07**	1.61E-05	1.46E-05
	Psyr_4595	897	Bacteriophage Mu tail sheath	347.656	206.809	0.750	**1.681**	6.018	**1.77E-09**	7.53E-08	6.86E-08

Table A-3. Continued.

Gene	Locus Tag	Op.	Function	RPKM *P.s.s.* B728a	RPKM *P.s.s.* B728a *ΔacsS*	log2 (Fold_change) normalized	Fold Change	z-score	p-value	q-value[1]	q-value[2]
flgJ	*Psyr_3472*	668	flagellar rod assembly protein/muramidase FlgJ	204.719	121.874	0.749	**1.680**	4.611	**4.00E-06**	0.0001033	9.41E-05
	Psyr_4221		EAL:GAF	226.359	134.940	0.747	**1.678**	4.838	**1.31E-06**	3.64E-05	3.32E-05
	Psyr_3592		nitroreductase	148.563	88.583	0.746	**1.677**	3.918	**8.94E-05**	0.0016743	0.001526
algA	*Psyr_1052*		mannose-1-phosphate guanylyltransferase/mannose-6-phosphate isomerase; Alginate synthesis	183.931	110.021	0.742	**1.672**	4.336	**1.45E-05**	0.0003486	0.000318
pyrD2	*Psyr_2106*		dihydroorotate dehydrogenase 2; pyrimidine biosynthesis	121.544	72.928	0.737	**1.667**	3.506	**0.000454**	0.0073712	0.006717
	Psyr_2431		zinc-containing alcohol dehydrogenase superfamily protein	138.220	82.968	0.737	**1.666**	3.736	**0.000186**	0.0033295	0.003025
	Psyr_4254		hypothetical	379.408	227.853	0.736	**1.665**	6.186	**6.16E-10**	2.78E-08	2.53E-08
	Psyr_3401	654	GCN5-related N-acetyltransferase	131.593	79.166	0.733	**1.663**	3.632	**0.000281**	0.0048038	0.004377
	Psyr_3129		3-hydroxyacyl-CoA-acyl carrier protein transferase	468.396	282.511	0.730	**1.658**	6.823	**8.91E-12**	4.58E-10	4.17E-10
	Psyr_4718		zinc-containing alcohol dehydrogenase superfamily protein; methane metabolism	278.509	168.109	0.729	**1.657**	5.254	**1.49E-07**	4.60E-06	4.19E-06
	Psyr_3016	584	cobalamin synthesis protein/P47K:cobalamin synthesis protein/P47K	119.503	72.159	0.728	**1.656**	3.439	**0.000584**	0.0090471	0.008244
	Psyr_2279		hypothetical	192.871	116.611	0.726	**1.654**	4.359	**1.31E-05**	0.0003165	0.000287
	Psyr_2534		carboxymethylenebutenolidase	208.025	127.173	0.710	**1.636**	4.440	**9.00E-06**	0.0002244	0.000204
	Psyr_1336	272	tetrahydrodipicolinate succinylase, putative	164.279	100.561	0.708	**1.634**	3.936	**8.27E-05**	0.0015608	0.001422
	Psyr_0840		pentapeptide repeat-containing protein	127.808	78.490	0.704	**1.629**	3.452	**0.000556**	0.0087812	0.008002
	Psyr_1945		peptide synthase	991.631	610.181	0.701	**1.625**	9.586	**9.15E-22**	1.03E-19	9.40E-20
prfB	*Psyr_1310*	267	peptide chain release factor 2	173.264	107.042	0.695	**1.619**	3.976	**7.01E-05**	0.0013621	0.001241
	Psyr_1303	266	histidine kinase, HAMP region: chemotaxis sensory transducer	172.065	106.725	0.689	**1.612**	3.933	**8.38E-05**	0.0015751	0.001435
fliO	*Psyr_3445*	663	flagellar biosynthesis protein, FliO	123.467	76.669	0.688	**1.611**	3.325	**0.000884**	0.0132285	0.012054
flgG	*Psyr_3475*	668	flagellar basal body rod protein FlgG	515.672	320.390	0.687	**1.610**	6.790	**1.12E-11**	5.72E-10	5.21E-10

Table A-3. Continued.

Gene	Locus Tag	Op.	Function	RPKM *P.s.s.* B728a	RPKM *P.s.s.* B728a *ΔacsS*	log2 (Fold_change) normalized	Fold Change	z-score	p-value	q-value[1]	q-value[2]
	Psyr_1608		hypothetical; ice nucleation protein	754.261	471.556	0.678	**1.600**	8.118	**4.75E-16**	3.42E-14	3.12E-14
ptsN	*Psyr_4149*	809	PTS IIA-like nitrogen-regulatory protein PtsN; carbohydrate metabolism	241.374	151.279	0.674	**1.596**	4.569	**4.89E-06**	0.0001251	0.000114
gabD	*Psyr_2413*		succinate-semialdehyde dehydrogenase (NAD(P)+); GABA metabolism	172.041	108.412	0.666	**1.587**	3.818	**0.000134**	0.0024588	0.002241
	Psyr_1956		pyoverdine biosynthesis regulatory protein	5028.420	3169.053	0.666	**1.587**	20.701	**3.40E-95**	2.52E-92	2.29E-92
nadE	*Psyr_0594*	116	Coenzyme metabolism	129.906	81.943	0.665	**1.586**	3.311	**0.000929**	0.0138154	0.012589
	Psyr_4631		PrkA serine kinase	656.797	415.526	0.661	**1.581**	7.405	**1.31E-13**	7.63E-12	6.95E-12
	Psyr_4632	907	hypothetical	361.224	228.584	0.660	**1.581**	5.488	**4.06E-08**	1.39E-06	1.27E-06
pvdS	*Psyr_1943*		extracytoplasmic-function sigma-70 factor; regulation of pyoverdine biosynthesis	432.951	274.528	0.657	**1.577**	5.985	**2.16E-09**	9.11E-08	8.30E-08
	Psyr_4153	810	hypothetical	1401.972	894.250	0.649	**1.568**	10.653	**1.69E-26**	2.50E-24	2.28E-24
	Psyr_4374	851	TadE family protein; Flp pilus assemble protein TadG	243.574	156.090	0.642	**1.561**	4.396	**1.10E-05**	0.0002722	0.000248
gapdh	*Psyr_1108*		glyceraldehyde-3-phosphate dehydrogenase; gluconeogenesis	2006.597	1287.685	0.640	**1.559**	12.597	**2.19E-36**	4.54E-34	4.13E-34
fliG	*Psyr_3456*	664	flagellar motor switch protein G	153.062	98.696	0.633	**1.551**	3.442	**0.000578**	0.0089829	0.008186
lysS	*Psyr_1311*	267	lysyl-tRNA synthetase	171.356	110.616	0.632	**1.549**	3.633	**0.000279**	0.0047932	0.004368
	Psyr_1967		twin-arginine translocation pathway signal, TAT secretion	227.293	147.162	0.627	**1.545**	4.159	**3.19E-05**	0.0006903	0.000629
amrZ	*Psyr_3551*		Arc-like DNA binding , alginate and motility regulator	212.481	137.632	0.627	**1.544**	4.018	**5.88E-05**	0.0011678	0.001064
flgH	*Psyr_3474*	668	flagellar basal body L-ring protein	205.386	133.058	0.627	**1.544**	3.949	**7.86E-05**	0.0015038	0.00137
	Psyr_0205	41	MotA/TolQ/ExbB proton channel; TonB-system energizer ExbD	519.624	336.647	0.626	**1.544**	6.282	**3.35E-10**	1.58E-08	1.43E-08
talAB	*Psyr_1914*		transaldolase B; pentose phosphate pathway	314.008	203.633	0.625	**1.542**	4.873	**1.10E-06**	3.10E-05	2.83E-05
dat	*Psyr_1946*		diaminobutyrate--2-oxoglutarate aminotransferase; arginine biosynthesis	1945.280	1263.872	0.622	**1.539**	12.095	**1.13E-33**	2.09E-31	1.91E-31
	Psyr_1944		thioesterase; pyoverdine synthetase	1174.875	765.664	0.618	**1.535**	9.335	**1.01E-20**	1.05E-18	9.53E-19

Table A-3. Continued.

Gene	Locus Tag	Op.	Function	RPKM *P.s.s.* B728a	RPKM *P.s.s.* B728a *ΔacsS*	log2 (Fold_change) normalized	Fold Change	z-score	p-value	q-value[1]	q-value[2]
cheA 2	*Psyr_3434*	660	CheW-like protein:ATP-binding region, ATPase-like:Signal transducing histidine kinase, homodimeric:Hpt	202.524	133.673	0.600	**1.515**	3.770	**0.000163**	0.0029569	0.002694
flgK	*Psyr_3471*	668	flagellar hook-associated protein FlgK	240.038	158.509	0.599	**1.515**	4.101	**4.12E-05**	0.0008619	0.000785
	Psyr_1661		Peptidoglycan binding LysM, Tfp pilus assembly protein FimV; Type IV pillus	182.920	120.885	0.598	**1.513**	3.574	**0.000352**	0.0059135	0.005389
	Psyr_3717		ribonucleotide-diphosphate reductase subunit alpha; pyrimidine salvage	446.539	295.989	0.593	**1.509**	5.548	**2.89E-08**	1.01E-06	9.23E-07
fliC	*Psyr_3466*		flagellin	5379.918	3570.565	0.592	**1.507**	19.268	**1.00E-82**	5.76E-80	5.25E-80
flgD	*Psyr_3479*	669	flagellar basal body rod modification protein	860.042	570.915	0.591	**1.507**	7.677	**1.63E-14**	1.00E-12	9.16E-13
fliK	*Psyr_3449*		flagellar hook-length control protein	236.377	157.205	0.589	**1.504**	4.007	**6.16E-05**	0.0012196	0.001111
	Psyr_2668	521	helix-turn-helix, Fis-type	208.031	138.611	0.586	**1.501**	3.743	**0.000181**	0.0032496	0.002961
tkl	*Psyr_4792*	939	transketolase; involved in glycolysis	255.799	171.155	0.580	**1.495**	4.112	**3.91E-05**	0.0008288	0.000755
flgE	*Psyr_3478*	669	flagellar hook protein FlgE	575.465	385.597	0.578	**1.493**	6.150	**7.76E-10**	3.41E-08	3.11E-08
	Psyr_3614	699	methionine sulfoxide reductase B	181.362	121.673	0.576	**1.491**	3.442	**0.000577**	0.0090242	0.008186
	Psyr_4388		response regulator receiver	475.685	321.468	0.566	**1.480**	5.483	**4.17E-08**	1.42E-06	1.30E-06
argJ	*Psyr_4093*	799	bifunctional ornithine acetyltransferase/N-acetylglutamate synthase protein; arginine biosynthesis	182.517	123.396	0.565	**1.479**	3.393	**0.000691**	0.0105262	0.009592
yfiA	*Psyr_4148*	809	sigma 54 modulation protein/ribosomal protein S30EA	555.118	375.750	0.563	**1.478**	5.902	**3.59E-09**	1.45E-07	1.33E-07
flgL	*Psyr_3470*	668	flagellar hook-associated protein FlgL	226.890	154.081	0.559	**1.473**	3.744	**0.000181**	0.0032517	0.002961
flgF	*Psyr_3476*	668	flagellar basal body rod protein FlgF	266.875	181.290	0.558	**1.472**	4.058	**4.96E-05**	0.0009928	0.000905
	Psyr_2141		ferric uptake regulator family	543.140	370.499	0.552	**1.466**	5.733	**9.84E-09**	3.67E-07	3.35E-07
	Psyr_4151	809	phosphocarrier HPr protein	660.746	452.730	0.546	**1.460**	6.258	**3.90E-10**	1.81E-08	1.65E-08
algR3	*Psyr_0054*		alginate regulatory protein AlgR3	1012.150	693.995	0.545	**1.459**	7.734	**1.04E-14**	6.77E-13	6.17E-13
	Psyr_5080		Cyclopropane-fatty-acyl-phospholipid synthase	233.803	161.403	0.535	**1.449**	3.654	**0.000257**	0.0044573	0.004062

Table A-3. Continued.

Gene	Locus Tag	Op.	Function	RPKM *P.s.s.* B728a	RPKM *P.s.s.* B728a *ΔacsS*	log2 (Fold_change) normalized	Fold Change	z-score	p-value	q-value[1]	q-value[2]
	Psyr_4633	907	SpoVR family protein	327.953	227.742	0.526	**1.440**	4.266	**1.99E-05**	0.0004515	0.000411
flgC	*Psyr_3480*	669	flagellar basal body rod protein FlgC	640.062	445.433	0.523	**1.437**	5.929	**3.05E-09**	1.26E-07	1.15E-07
	Psyr_2140		hypothetical	635.390	443.833	0.518	**1.432**	5.852	**4.86E-09**	1.91E-07	1.74E-07
	Psyr_0937		mannose-1-phosphate guanylyltransferase/mannose-6-phosphate isomerase	258.596	181.770	0.509	**1.423**	3.673	**0.000239**	0.0042045	0.003831
	Psyr_0994		metal-dependent phosphohydrolase	226.794	159.854	0.505	**1.419**	3.415	**0.000637**	0.0097881	0.008919
	Psyr_1957	384	amino acid adenylation; pyoverdine sidechain peptide synthetase I, epsilon-Lys module	1146.385	809.861	0.502	**1.416**	7.637	**2.22E-14**	1.35E-12	1.23E-12
	Psyr_0203	41	TonB, C-terminal	324.653	230.969	0.491	**1.406**	3.987	**6.70E-05**	0.001311	0.001195
	Psyr_1476		hypothetical	372.183	265.235	0.489	**1.403**	4.249	**2.14E-05**	0.0004816	0.000439
	Psyr_3654	707	hypothetical	555.460	398.774	0.478	**1.393**	5.088	**3.61E-07**	1.08E-05	9.87E-06
	Psyr_1872		hypothetical	754.742	544.931	0.470	**1.385**	5.839	**5.26E-09**	2.05E-07	1.87E-07
clpA	*Psyr_3183*	617	putative AAA ATPase	456.630	330.499	0.467	**1.382**	4.509	**6.51E-06**	0.0001639	0.000149
fliS	*Psyr_3463*	666	flagellar protein FliS	276.229	200.542	0.462	**1.378**	3.476	**0.000508**	0.008145	0.007422
leuA	*Psyr_1257*		2-isopropylmalate synthase; leucine biosynthesis	299.360	217.458	0.461	**1.377**	3.613	**0.000302**	0.0051325	0.004677
	Psyr_1958	384	non-ribosomal peptide synthase:amino acid adenylation; pyoverdine sidechain peptide synthetase II, D-Asp-L-Thr component	782.943	569.145	0.460	**1.376**	5.833	**5.45E-09**	2.11E-07	1.92E-07
	Psyr_1959	384	amino acid adenylation; pyoverdine sidechain peptide synthetase III, L-Thr-L-Ser component	809.766	593.043	0.450	**1.366**	5.804	**6.46E-09**	2.45E-07	2.23E-07
modA	*Psyr_2756*	536	molybdenum ABC transporter periplasmic-binding protein	319.473	234.503	0.446	**1.363**	3.620	**0.000294**	0.0050098	0.004565
	Psyr_2433		hypothetical	381.893	280.616	0.445	**1.361**	3.946	**7.96E-05**	0.0015176	0.001383
	Psyr_1973		aromatic amino acid aminotransferase; leucine biosynthesis	310.323	228.120	0.444	**1.361**	3.552	**0.000381**	0.0063102	0.00575
	Psyr_1960	384	non-ribosomal peptide synthase:amino acid adenylation; pyoverdine sidechain peptide synthetase IV, D-Asp-L-Ser component	656.505	483.789	0.441	**1.357**	5.130	**2.90E-07**	8.80E-06	8.02E-06

Table A-3. Continued.

Gene	Locus Tag	Op.	Function	RPKM *P.s.s.* B728a	RPKM *P.s.s.* B728a *ΔacsS*	log2 (Fold_change) normalized	Fold Change	z-score	p-value	q-value[1]	q-value[2]
	Psyr_0133		helix-turn-helix, Fis-type	356.739	264.980	0.429	**1.347**	3.690	**0.000224**	0.0039599	0.003608
	Psyr_4291		hypothetical	330.850	245.932	0.428	**1.346**	3.545	**0.000392**	0.0064631	0.00589
	Psyr_2863		feruloyl esterase; tannase precursor	509.129	380.372	0.421	**1.339**	4.329	**1.50E-05**	0.0003567	0.000325
	Psyr_2107		ribosome modulation factor	5804.014	4345.777	0.418	**1.336**	14.568	**4.50E-48**	1.46E-45	1.33E-45
sodA	*Psyr_4152*	810	superoxide dismutase	974.295	729.576	0.418	**1.336**	5.946	**2.74E-09**	1.14E-07	1.04E-07
	Psyr_2145	424	hypothetical	309.444	232.489	0.413	**1.331**	3.314	**0.000919**	0.0137119	0.012495
fliD	*Psyr_3464*	667	flagellar hook-associated protein 2, N-terminal:flagellar hook-associated 2, C-terminal:flagellin hook IN	2177.497	1643.860	0.406	**1.325**	8.665	**4.50E-18**	3.83E-16	3.49E-16
	Psyr_2646		radical SAM family protein	415.402	316.454	0.393	**1.313**	3.667	**0.0002458**	0.0042651	0.003887
	Psyr_3845		extracellular ligand-binding receptor	549.911	425.465	0.370	**1.293**	3.994	**6.49E-05**	0.0012747	0.001162
map1	*Psyr_2146*	424	peptidase M24A	396.677	307.525	0.368	**1.290**	3.367	**0.000759**	0.0115144	0.010492
	Psyr_0799		fimbrial protein pilin, Type IV pilus	1415.710	1098.756	0.366	**1.289**	6.340	**2.30E-10**	1.11E-08	1.02E-08
	Psyr_1962		TonB-dependent siderophore receptor	1695.411	1384.836	0.292	**1.224**	5.612	**1.99E-08**	7.19E-07	6.55E-07
	Psyr_0457	88	hypothetical	1555.410	1278.035	0.284	**1.217**	5.226	**1.74E-07**	5.30E-06	4.83E-06
tssD	*Psyr_4965*		hypothetical; Hcp1 family type VI secretion system effector	3903.616	3241.573	0.268	**1.204**	7.868	**3.61E-15**	2.46E-13	2.24E-13
mucA	*Psyr_3957*	768	anti sigma-E protein RseA, N-terminal:anti sigma-E protein RseA, C-terminal	1419.828	1198.843	0.244	**1.185**	4.330	**1.49E-05**	0.0003566	0.000325
rpoS	*Psyr_1374*	280	RNA polymerase sigma factor RpoS	1405.768	1195.902	0.234	**1.176**	4.125	**3.70E-05**	0.0007866	0.000717
sucC	*Psyr_2012*	397	succinyl-CoA synthetase subunit beta; TCA cylce	1312.132	1540.080	-0.231	**-1.174**	-4.271	**1.95E-05**	0.0004431	0.000404
	Psyr_1117		carbohydrate-selective porin OprB	1093.614	1335.745	-0.288	**-1.221**	-4.917	**8.78E-07**	2.49E-05	2.27E-05
	Psyr_3074	597	hemolysin-type calcium-binding region:haemolysin-type calcium binding related	600.837	755.218	-0.330	**-1.257**	-4.196	**2.72E-05**	0.0005971	0.000544
atpD	*Psyr_5124*	1005	F0F1 ATP synthase subunit delta	497.956	638.218	-0.358	**-1.281**	-4.166	**3.11E-05**	0.0006742	0.000614
hfq	*Psyr_0572*	109	RNA-binding protein Hfq	357.721	468.908	-0.390	**-1.311**	-3.872	**0.000108**	0.0019939	0.001817
	Psyr_2005	395	succinate dehydrogenase, cytochrome b subunit	314.892	413.900	-0.394	**-1.314**	-3.672	**0.000240**	0.004205	0.003832

Table A-3. Continued.

Gene	Locus Tag	Op.	Function	RPKM *P.s.s.* B728a	RPKM *P.s.s.* B728a *ΔacsS*	log2 (Fold_change) normalized	Fold Change	z-score	p-value	q-value[1]	q-value[2]
	Psyr_3163		serralysin	2461.561	3273.277	-0.411	**-1.330**	-10.755	**5.60E-27**	8.55E-25	7.79E-25
	Psyr_4400	854	acetyl-CoA carboxylase biotin carboxyl carrier protein subunit	230.288	306.815	-0.414	**-1.332**	-3.306	**0.000944**	0.0140061	0.012763
	Psyr_3216		hypothetical	1805.100	2415.789	-0.420	**-1.338**	-9.427	**4.23E-21**	4.48E-19	4.08E-19
	Psyr_2006	395	succinate dehydrogenase, hydrophobic membrane anchor protein	518.719	702.690	-0.438	**-1.354**	-5.274	**1.34E-07**	4.23E-06	3.85E-06
atpB	*Psyr_5125*	1005	F0F1 ATP synthase subunit B	351.420	476.642	-0.439	**-1.356**	-4.359	**1.31E-05**	0.0003153	0.000287
fusA	*Psyr_4551*	883	elongation factor G	1773.082	2439.396	-0.460	**-1.376**	-10.300	**7.07E-25**	9.65E-23	8.79E-23
pvtK	*Psyr_4029*		pyruvate kinase	174.154	242.130	-0.475	**-1.390**	-3.338	**0.000844**	0.0126546	0.011531
	Psyr_2625	517	putative lipoprotein	203.912	284.110	-0.478	**-1.393**	-3.637	**0.000275**	0.0047314	0.004311
atpA	*Psyr_5123*	1005	F0F1 ATP synthase subunit alpha	264.965	375.652	-0.503	**-1.418**	-4.383	**1.17E-05**	0.0002876	0.000262
	Psyr_2013	397	succinyl-CoA synthetase subunit alpha; TCA cycle	490.651	699.452	-0.511	**-1.425**	-6.068	**1.29E-09**	5.59E-08	5.10E-08
	Psyr_2990		hypothetical	491.467	704.666	-0.520	**-1.434**	-6.181	**6.37E-10**	2.85E-08	2.60E-08
	Psyr_5027		histone-like DNA-binding protein	158.550	235.689	-0.572	**-1.486**	-3.896	**9.76E-05**	0.0018084	0.001648
	Psyr_0749		AMP-dependent synthetase and ligase	226.820	340.747	-0.587	**-1.502**	-4.797	**1.61E-06**	4.39E-05	4.00E-05
tig	*Psyr_1746*	357	trigger factor; protease	104.723	159.068	-0.603	**-1.519**	-3.357	**0.000788**	0.0118496	0.010798
tsf	*Psyr_1344*		elongation factor Ts	355.502	547.074	-0.622	**-1.539**	-6.401	**1.55E-10**	7.65E-09	6.97E-09
	Psyr_0583	113	hypothetical; predicted membrane protein	264.033	407.290	-0.625	**-1.542**	-5.550	**2.86E-08**	1.01E-06	9.21E-07
fabG-3	*Psyr_1647*	335	Lipid metabolism	225.165	353.290	-0.650	**-1.569**	-5.348	**8.87E-08**	2.93E-06	2.67E-06
	Psyr_0111	26	hypothetical	142.278	224.293	-0.656	**-1.576**	-4.301	**1.70E-05**	0.0003978	0.000362
tpiA	*Psyr_4184*	818	triosephosphate isomerase; gluconeogenesis	104.499	165.287	-0.661	**-1.581**	-3.716	**0.000202**	0.0035873	0.003269
atpC	*Psyr_5122*	1005	F0F1 ATP synthase subunit gamma	160.620	254.416	-0.663	**-1.584**	-4.623	**3.78E-06**	9.86E-05	8.99E-05
pyrH	*Psyr_1345*	274	uridylate kinase; pyrimidine biosynthesis	167.698	265.811	-0.664	**-1.585**	-4.732	**2.23E-06**	6.02E-05	5.48E-05
atpD	*Psyr_5121*	1005	F0F1 ATP synthase subunit beta	204.178	324.702	-0.669	**-1.590**	-5.263	**1.42E-07**	4.46E-06	4.05E-06

Table A-3. Continued.

Gene	Locus Tag	Op.	Function	RPKM *P.s.s.* B728a	RPKM *P.s.s.* B728a *ΔacsS*	log2 (Fold_change) normalized	Fold Change	z-score	p-value	q-value[1]	q-value[2]
	Psyr_4247		ornithine decarboxylase	211.504	337.714	-0.675	**-1.596**	-5.409	**6.35E-08**	2.14E-06	1.95E-06
aroQ	*Psyr_4399*	854	3-dehydroquinate dehydratase; phenylalanine/ tyrosine biosynthesis	116.879	186.845	-0.677	**-1.598**	-4.032	**5.54E-05**	0.0011049	0.001007
	Psyr_4987	976	hypothetical	146.727	235.365	-0.682	**-1.604**	-4.554	**5.26E-06**	0.0001337	0.000122
	Psyr_0038		hypothetical	127.679	205.740	-0.688	**-1.611**	-4.294	**1.76E-05**	0.0004067	0.000371
ppa-1	*Psyr_0624*		Energy production and conversion; TCA cycle	87.623	141.251	-0.689	**-1.612**	-3.560	**0.0003704**	0.006179	0.005631
	Psyr_0187		hypothetical	136.887	222.061	-0.698	**-1.622**	-4.516	**6.30E-06**	0.0001594	0.000145
gltA	*Psyr_2004*		type II citrate synthase; TCA cycle	190.068	310.474	-0.708	**-1.633**	-5.407	**6.40E-08**	2.14E-06	1.95E-06
atpC	*Psyr_5126*	1005	F0F1 ATP synthase subunit C	123.648	207.276	-0.745	**-1.676**	-4.621	**3.82E-06**	9.90E-05	9.02E-05
	Psyr_0188		hypothetical	158.789	266.692	-0.748	**-1.679**	-5.259	**1.45E-07**	4.50E-06	4.10E-06
acpP	Psyr_1648		Phospholipid and fatty acid metabolism	207.575	358.899	-0.790	**-1.729**	-6.396	**1.60E-10**	7.81E-09	7.12E-09
	Psyr_1375		4Fe-4S ferredoxin, iron-sulfur binding	55.158	98.752	-0.840	**-1.790**	-3.537	**0.0004046**	0.0066427	0.006053
	Psyr_4175		transport-associated protein	51.899	95.297	-0.876	**-1.836**	-3.603	**0.000314**	0.0053212	0.004849
	Psyr_2134		hypothetical; putative lipoprotein	137.329	256.502	-0.901	**-1.867**	-6.051	**1.44E-09**	6.16E-08	5.61E-08
minE	*Psyr_1611*	327	cell division topological specificity factor MinE	102.178	192.510	-0.914	**-1.884**	-5.304	**1.14E-07**	3.64E-06	3.30E-06
	Psyr_5135	1008	hypothetical	112.706	213.082	-0.919	**-1.890**	-5.606	**2.08E-08**	7.43E-07	6.77E-07
rnpA	*Psyr_5136*	1008	(Translation)	82.164	159.413	-0.956	**-1.940**	-5.013	**5.36E-07**	1.58E-05	1.44E-05
groEL	*Psyr_4072*	794	chaperonin GroEL	280.605	546.041	-0.960	**-1.946**	-9.314	**1.23E-20**	1.25E-18	1.14E-18
ddl	Psyr_3919	759	Cell wall / LPS / capsule	37.014	72.246	-0.965	**-1.952**	-3.400	**0.000674**	0.0102863	0.009373
syrG	*Psyr_2602*		LuxR regulatory protein; phytotoxin regulation	99.965	197.019	-0.979	**-1.971**	-5.683	**1.33E-08**	4.88E-07	4.45E-07
	Psyr_2228	441	hypothetical; nickel transport system substrate-binding protein	48.801	97.429	-0.997	**-1.996**	-4.059	**4.93E-05**	0.0009958	0.000905
	Psyr_0031		Alpha/beta hydrolase fold	211.561	423.674	-1.002	**-2.002**	-8.497	**1.95E-17**	1.56E-15	1.42E-15
	Psyr_2229	441	TonB-dependent siderophore receptor	51.008	102.178	-1.002	**-2.003**	-4.173	**3.00E-05**	0.0006547	0.000597
hrpZ1	*Psyr_1193*	242	type III helper protein HrpZ1	53.732	107.669	-1.003	**-2.003**	-4.286	**1.82E-05**	0.0004185	0.000381
	Psyr_0750	151	hypothetical; Ubiquinone biosynthesis	133.491	276.390	-1.050	**-2.070**	-7.132	**9.91E-13**	5.47E-11	4.99E-11

Table A-3. Continued.

Gene	Locus Tag	Op.	Function	RPKM *P.s.s.* B728a	RPKM *P.s.s.* B728a *ΔacsS*	log2 (Fold_change) normalized	Fold Change	z-score	p-value	q-value[1]	q-value[2]
syrF	*Psyr_2607*	512	regulatory protein, LuxR; phytotoxin regulation	31.354	65.354	-1.059	**-2.084**	-3.494	**0.000476**	0.00768	0.006998
rpppK	*Psyr_0944*	196	ribose-phosphate pyrophosphokinase; Histidine biosynthesis	72.518	151.440	-1.062	**-2.088**	-5.329	**9.85E-08**	3.24E-06	2.95E-06
	Psyr_2366	466	ABC transporter	30.408	65.818	-1.114	**-2.164**	-3.651	**0.000260**	0.0044964	0.004097
	Psyr_4652	912	colicin immunity protein/pyocin immunity protein	26.022	57.278	-1.138	**-2.201**	-3.466	**0.000528**	0.0084127	0.007666
	Psyr_1643	334	hypothetical	106.287	234.512	-1.141	**-2.206**	-7.030	**2.06E-12**	1.11E-10	1.01E-10
	Psyr_2497		putative lipoprotein	50.202	111.089	-1.146	**-2.212**	-4.853	**1.22E-06**	3.40E-05	3.09E-05
	Psyr_1592		hypothetical	41.514	91.963	-1.147	**-2.215**	-4.420	**9.87E-06**	0.000245	0.000223
	Psyr_4031		Fe-S type hydro-lyase tartrate/fumarate alpha region:Fe-S type hydro-lyase tartrate/fumarate beta region; TCA cycle	28.275	62.884	-1.153	**-2.224**	-3.669	**0.000243**	0.0042312	0.003856
	Psyr_3730	722		25.200	56.265	-1.159	**-2.232**	-3.485	**0.000492**	0.0079146	0.007212
groES	*Psyr_4073*	794	co-chaperonin GroES	149.979	335.233	-1.160	**-2.235**	-8.516	**1.65E-17**	1.34E-15	1.22E-15
	Psyr_1084		histone-like DNA-binding protein	105.425	240.062	-1.187	**-2.277**	-7.339	**2.16E-13**	1.24E-11	1.13E-11
	Psyr_3028		hypothetical	29.851	68.451	-1.197	**-2.293**	-3.945	**7.99E-05**	0.0015177	0.001383
hrpA2	*Psyr_1192*	242	type III helper protein HrpA2	31.668	72.864	-1.202	**-2.300**	-4.083	**4.44E-05**	0.0009112	0.00083
	Psyr_0260		hypothetical	107.422	249.223	-1.214	**-2.320**	-7.612	**2.71E-14**	1.63E-12	1.49E-12
	Psyr_5134	1008	putative inner membrane protein translocase component YidC	33.858	80.781	-1.254	**-2.385**	-4.446	**8.75E-06**	0.0002194	0.0002
	Psyr_1471		hypothetical	290.811	705.266	-1.278	**-2.425**	-13.333	**1.48E-40**	3.84E-38	3.50E-38
secG	*Psyr_4183*	818	preprotein translocase subunit SecG	46.030	111.772	-1.280	**-2.428**	-5.312	**1.08E-07**	3.49E-06	3.18E-06
	Psyr_2367	466	hypothetical; predicted ABC transporter	23.038	57.643	-1.323	**-2.502**	-3.914	**9.07E-05**	0.0016925	0.001538
	Psyr_0835		predicted RNA polymerase-binding protein DksA	124.225	313.707	-1.336	**-2.525**	-9.203	**3.47E-20**	3.40E-18	3.10E-18
	Psyr_0309	61	colicin immunity protein/pyocin immunity protein	41.603	105.563	-1.343	**-2.537**	-5.359	**8.36E-08**	2.78E-06	2.53E-06
	Psyr_2156	426	D-ribose pyranase	19.383	49.493	-1.352	**-2.553**	-3.688	**0.000225**	0.0039674	0.003615
syrB2	*Psyr_2610*	513	chlorinating enzyme; syringomycin biosynthesis	66.236	187.275	-1.499	**-2.827**	-7.756	**8.80E-15**	5.78E-13	5.27E-13

Table A-3. Continued.

Gene	Locus Tag	Op.	Function	RPKM *P.s.s.* B728a	RPKM *P.s.s.* B728a *ΔacsS*	log2 (Fold_change) normalized	Fold Change	z-score	p-value	q-value[1]	q-value[2]
minC	*Psyr_1613*		septum formation inhibitor	13.073	37.054	-1.503	**-2.834**	-3.456	**0.000549**	0.0086863	0.007915
	Psyr_5074	996	hypothetical	42.333	121.070	-1.516	**-2.859**	-6.286	**3.25E-10**	1.55E-08	1.41E-08
	Psyr_5102	1001	ABC transporter	12.205	35.977	-1.559	**-2.947**	-3.499	**0.000467**	0.0075584	0.006888
	Psyr_5103	1001	periplasmic binding protein	11.591	35.076	-1.597	**-3.025**	-3.515	**0.000439**	0.0071455	0.006511
	Psyr_2270	449	hexapaptide repeat-containing transferase	62.224	188.762	-1.601	**-3.033**	-8.169	**3.12E-16**	2.35E-14	2.14E-14
	Psyr_2269	449	putative GTP cyclohydrolase	30.418	93.506	-1.620	**-3.074**	-5.798	**6.70E-09**	2.52E-07	2.29E-07
	Psyr_3633		threonine/serine transporter	30.581	94.046	-1.620	**-3.075**	-5.817	**6.01E-09**	2.29E-07	2.09E-07
syrD	*Psyr_2613*	514	cyclic peptide transporter; phytotoxin transport	29.064	93.249	-1.682	**-3.208**	-5.947	**2.73E-09**	1.14E-07	1.04E-07
syrB1	*Psyr_2611*	513	amino acid adenylation; syringomycin biosynthesis	76.948	253.075	-1.717	**-3.288**	-9.945	**2.66E-23**	3.37E-21	3.07E-21
	Psyr_5075	996	cobalamin synthesis protein/P47K:cobalamin synthesis protein/P47K	58.437	195.136	-1.739	**-3.339**	-8.810	**1.25E-18**	1.14E-16	1.04E-16
	Psyr_1470		hypothetical	113.971	389.551	-1.773	**-3.417**	-12.616	**1.73E-36**	3.75E-34	3.41E-34
	Psyr_2368	466	periplasmic solute binding protein, cation ABC transporter	60.329	217.474	-1.850	**-3.604**	-9.704	**2.91E-22**	3.43E-20	3.13E-20
syrP	*Psyr_2612*	514	syringomycin synthesis and transport	25.163	94.087	-1.902	**-3.738**	-6.504	**7.80E-11**	3.89E-09	3.55E-09
	Psyr_1469	299	hypothetical	71.956	271.399	-1.915	**-3.771**	-11.097	**1.30E-28**	2.18E-26	1.99E-26
	Psyr_2271		hypothetical	15.886	64.945	-2.031	**-4.087**	-5.642	**1.68E-08**	6.08E-07	5.54E-07
	Psyr_1466		hypothetical	5.726	23.628	-2.045	**-4.125**	-3.418	**0.000631**	0.0097194	0.008857
	Psyr_1468	299	hypothetical	34.969	166.491	-2.251	**-4.760**	-9.638	**5.52E-22**	6.36E-20	5.80E-20
	Psyr_0768		hypothetical	3.212	18.425	-2.520	**-5.735**	-3.426	**0.000613**	0.0094709	0.00863
avrPto1	*Psyr_4919*		type III effector protein AvrPto1	5.092	32.131	-2.657	**-6.309**	-4.658	**3.19E-06**	8.40E-05	7.65E-05

TABLE A-4. Expression of genes in a peptide synthesis rich region of *P.s.s.* B728a differentially expressed between deletion mutants of GacS and/or SalA compared to wild type *P.s.s.* B728a.

Gene	Locus Tag	Op.	Function	Basal		NaCl		H2O2		Low Fe		Low N		Epiphytic		Apoplastic	
				GacS	SalA	GacS	SalA	GacS	SalA	GacS	SalA	GacS	SalA	GacS	SalA	GacS	SalA
	Psyr_2634		histidine kinase, HAMP region: chemotaxis sensory transducer	**1**	**1**	**1**	**1**	**1**	**-3.17**	**1**	**1**	**-2.30**	**1**	**-2.96**	**1**	**1**	**1**
	Psyr_3351		histidine kinase, HAMP region: chemotaxis sensory transducer	**1**	**1**	**1**	**1**	**1**	**1**	**1**	**3.10**	**1**	**1**	**1**	**1**	**1**	**1**
	Psyr_3427	660	hypothetical protein	**1**	**1**	**1**	**1**	**1**	**1**	**1**	**1**	**1**	**-1.74**	**1**	**1**	**1**	**1**
cheW-2	*Psyr_3428*	660	CheW-like protein	**1**	**1**	**1**	**1**	**1**	**1**	**1**	**1**	**1**	**1**	**1**	**1**	**1**	**1**
	Psyr_3429	660	CheW-like protein	**1**	**1**	**1**	**1**	**1**	**1**	**1**	**1**	**1**	**1**	**1**	**1**	**1**	**1**
	Psyr_3430	660	Cobyrinic acid a,c-diamide synthase (cobB homolog)	**1**	**1**	**2.60**	**1**	**1**	**1**	**1**	**1**	**1**	**1**	**1**	**1**	**1**	**1**
motD	*Psyr_3431*	660	flagellar motor protein MotD	**1**	**1**	**2.71**	**1**	**1**	**1**	**1**	**1**	**1**	**1**	**1**	**1**	**1**	**1**
motC	*Psyr_3432*	660	flagellar motor protein MotC	**1**	**1**	**3.77**	**1**	**1**	**1**	**1**	**1**	**1**	**1**	**1**	**1**	**1**	**1**
cheB-2	*Psyr_3433*	660	chemotaxis-specific methylesterase	**1**	**1**	**2.21**	**1**	**1.92**	**1**	**1**	**1**	**1.73**	**1**	**1**	**1**	**1**	**1**
cheA-2	*Psyr_3434*	660	CheW-like protein	**1**	**1**	**1**	**1**	**1**	**1**	**1**	**1**	**1**	**-3.65**	**1**	**1**	**1**	**1**
cheZ	*Psyr_3435*	660	Chemotaxis phosphatase	**1**	**1**	**1**	**1**	**1**	**1**	**1**	**1**	**1**	**-1.99**	**1**	**1**	**1**	**1**
cheY-2	*Psyr_3436*	660	Response regulator receiver	**1**	**1**	**1**	**1**	**1**	**1**	**1**	**1**	**1**	**-2.41**	**1**	**1**	**1**	**1**
cheR-2	*Psyr_3485*	671	Chemotaxis protein methyltransferase CheR	**1**	**1**	**1**	**1**	**1**	**-1.89**	**1**	**1**	**-1.88**	**-2.04**	**-1.86**	**1**	**1**	**1**
cheV-3	*Psyr_3486*	671	Response regulator receiver:CheW-like protein	**1**	**1**	**1**	**1**	**1**	**-2.39**	**1**	**1**	**-1.81**	**-2.19**	**1**	**1**	**1**	**1**
	Psyr_3534		histidine kinase, HAMP region:Cache: chemotaxis sensory transducer	**-3.36**	**-6.25**	**1**	**1**	**-4.95**	**-4.56**	**1**	**1**	**1**	**1**	**-4.57**	**-5.30**	**1**	**1**
	Psyr_4218		histidine kinase, HAMP region: chemotaxis sensory transducer	**1**	**1**	**1**	**1**	**1**	**1**	**1**	**1**	**1**	**-2.81**	**-2.45**	**1**	**1**	**1**
	Psyr_5004		chemotaxis sensory transducer	**1**	**1**	**1**	**1**	**1**	**1**	**1**	**1**	**1**	**1**	**-1.73**	**-1.87**	**1**	**1**

VITA

Name: Jessica Williams Greenwald

Address: Department of Plant Pathology & Microbiology
c/o Dr. Dennis C. Gross
Texas A&M University
College Station, TX 77843-2132

Email Address: jwgreenwald13@gmail.com

Education: B.S., Biology, The College of William & Mary, 2005